# UNIVERSITÀ DEGLI STUDI DI PADOVA

**Dipartimento di Fisica e Astronomia "Galileo Galilei"**

**Master Degree in Physics**

**Final Dissertation**

## Di-Higgs production in effective field theories

**Thesis supervisor**                    **Candidate**

**Prof. Ramona Gröber**                    **Lorenzo Tiberi**

**Academic Year 2023/2024**

# Contents

**7 Conclusions**          **87**

# Introduction

The greatest recent result in particle physics was the discovery of the Higgs boson in 2012 by the ATLAS and CMS collaborations [1, 2]. With the discovery of the Higgs boson the last missing ingredient of the Standard Model (SM) of particle physics has been found. It remains to show that the Higgs boson is indeed the one predicted within the SM. So far the experimental results strongly indicate so [3, 4].

Despite its ability to describe almost all up-to-date experimental results in particle physics, the SM is far from being the ultimate theory of physics as it lacks different aspects to be complete. Some of the problems we have not yet answered to are:

- The matter-anti-matter asymmetry: in the early stages of our Universe there must have been a mechanism that has favoured baryons over antibaryons, this mechanism is not described in the SM. The Shakarov conditions to successful generate this asymmetry require cannot be fully satisfied by the SM.

- Naturalness problem: The Higgs boson mass receives quantum corrections that are highly sensitive to any UV scale and requires a fine-tuning in order to match the expression to the observed value of $m_h = 125$GeV.

- Dark matter (DM): Dark Matter represents 27 of the energy content of our Universe. The SM lacks a suitable candidate for it.

- Smallness of neutrino mass: experiments have shown that the masses of neutrinos are considerably smaller than the masses of the other particles such as quarks or leptons. The SM cannot explain tis hierarchy of masses and strictly speaking does not provide any mass at all to the neutrinos. This in turn raises also the question of the nature of neutrino masses, namely whether they are Dirac o Majorana particles.

- EWSB: according to the Higgs mechanism when the scalar field assumes a vacuum expectation value (v.e.v) then the so called electroweak symmetry of SM $SU(2)_L \otimes U(1)_Y$ breaks into a smaller subgroup $U(1)_{\text{e.m.}}$. This leads to the acquisition of mass by the $W$ and $Z$ bosons leaving the photon massless. While the Higgs mechanism successfully explains this symmetry breaking, it does not provide a deeper understanding of why this breaking occurs or why the Higgs field takes the particular form observed experimentally.

Research on the Higgs Sector could allow us to proceed further in all the mentioned directions. Solving some of the above problems necessarily requires the addition of new physics (NP) in terms of new particles. Going beyond Standard Model (BSM) is a natural way to improve our understanding on the open questions we have.

Since so far no striking new signals of new physics has been discovered it is imperative to assume that there is a mass gap between Electroweak scale $\Lambda_{EW} \sim 246$ GeV and the new physics scale.

When facing large separation of scales we can exploit the model independent approach of Effective Field Theory (EFT). The latter holds when $E < \Lambda_{\rm UV}$, where $E$ is a generic energy of the process while $\Lambda_{\rm UV}$ is a cutoff scale beyond which EFT description is no more valid.

Unless we find the ultimate theory valid up to arbitrary high energy scales, we can think about iterating the above process where after an observation of a new particle we write down a theory that is valid up to $\Lambda'_{\rm UV} > \Lambda_{\rm UV}$. In this way we end up with an hierarchy of scales where different descriptions are suitable for a specific energy domain. These EFTs have a common feature: the SM will be their low-energy limit as they must reproduce what we observe up to now.

This way of proceeding is called Bottom-Up approach. In this work we try to go the other way around and start assuming a very concrete UV completion of the SM (Top-Down approach). We proceed by matching this model to two IR theories that are commonly used in Higgs physics: Standard Model Effective Field Theory (SMEFT) and Higgs Effective Field Theory (HEFT).

They differ both in the power counting and on the the assumptions made on the Higgs field. Standard Model Effective Field Theory is commonly used when the UV theory is weakly coupled, while HEFT usually is needed if a strongly coupled UV scenario is assumed. In SMEFT, the Higgs field transforms as in the SM in an SU(2) doublet. All new physics effects are parameterised by higher dimensional operators suppressed by a new physics scale $\Lambda$. The dominant effects in Higgs physics stem from dimension-six operators. The basic idea of HEFT stems from the chiral Lagrangian, hence a strongly interacting theory. In this case, the Higgs boson no longer transforms together with the Goldstone boson in an SU(2) doublet, but instead the Goldstones and the Higgs boson get seperated: the Higgs boson now transforms as a singlet. Typically a counting of canonical dimensions is adopted [5–7], in which the Higgs boson does not count-up the dimensions. Higgs interactions with one or $n$ Higgs bosons hence arise at the same order in the counting of the canonical dimension. Hence processes with a di-higgs final state are particularly convenient to make differences between SMEFT and HEFT evident.

Our aim is to identify concrete models where SMEFT does not describe well the UV model and consequently HEFT must be used. The opposite is not possible since SMEFT can be thought of as an HEFT subcase.

In Ref. [8] potential particles that need HEFT instead of SMEFT have been identified and called Loryon particles. Those acquire more than a half of their mass from EWSB. [8, 9]

As pointed out above, the SM electroweak sector undergoes a spontaneous symmetry breaking: the gauge symmetry group leaves the SM lagrangian invariant under $SU(2)_L \otimes U(1)_{\rm Y}$, however when Higgs field acquires a v.e.v. the lagrangian is only invariant under $U(1)_{\rm e.m.}$ and the $W$ and $Z$ bosons

become massive. Understanding whethere HEFT or SMEFT is the right effective description might go hand in hand with understanding whether the pattern we are assuming in the SM, namely $SU(2)_L \otimes U(1)_Y \to U(1)_{e.m.}$ could be an effective description of another more fundamental dynamics. To give a flavour of this aspect we recover an historical example from Ginzburg-Landau effective model for superconductivity.

There the action functional is:

$$LG(s) = \int_{Re^3} dv^3 \left[ \frac{1}{2} |(\nabla - 2ieA)\Phi|^2 + \frac{\gamma}{2} (|\Phi|^2 - a^2) \right] \tag{1}$$

where $(\nabla - ieA)$ is the covariant derivative for a non relativistic system reflecting $U(1)$ invariance and $\Phi = |\Phi|e^{i\theta}$ is the order parameter, a macroscopic wave function representing the condensate of Cooper pairs.

The minimum of the action is for $|s| = a$ and $(\nabla - 2ieA)\Phi = 0$ (and $\gamma > 0$).

The action of the SM Higgs is extremely similar to the latter:

$$S_H = \int d^4x \left( |D_\mu H|^2 - \lambda (H^\dagger H - \frac{v^2}{2})^2 \right) \tag{2}$$

where $H$ is the Higgs doublet and $D_\mu$ is the covariant derivative of the $SU(2)_L \otimes U(1)_Y$. This theory has a minimum at $\langle H^\dagger H \rangle = v^2/2$. The expansion around this minimum leads to massive $W^+, W^-, Z$ bosons.

However Landau-Ginzburg is the effective description of a more fundamental theory (BCS). In analogy to Landau-Ginzburg, one would expect a shorter distance completion/origin of the Higgs mechanism. The appearence of a Mexican hat with a minimum at $v = 246$ GeV may be the low energy effective parametrization of a shorter distance dynamics, leading to an effective $SU(2)_L \otimes U(1)_Y$. In this sense SMEFT and HEFT provides two possible parametrizations of the same, yet unknown UV sector, leading to the observed massive gauge bosons.

The outline of this work is as follows: in Chapter 1 we revise the basics of SM and of EFT that we consider, namely SMEFT and HEFT, in this way we set down the notation and appreciate the first structural differences of the the two EFTs. Chapter 2 is about the scalar singlet model as a first UV model chosen for the analysis, here we provide a phenomenological study to restrict the parameter space. In chapter 3 we focus on matching the UV model to SMEFT and to HEFT using mainly a diagrammatic approach, here first differences at the level of coupling correlations show up.

Chapter 4 shows the theoretical motivation behind our choice of the UV models. In chapter 5 we perform a numerical evaluation of the scalar singlet model at the level of squared amplitudes and check where HEFT and where SMEFT is needed. In chapter 6 we present a UV model with a colored scalar suitable to show the differences between HEFT and SMEFET. We conclude in chapter 7 with final comments on the relevance of this work in the interpretation of the upcoming HL-LHC data.

# Chapter 1

# Effective Field Theories for the Higgs boson

Once the Higgs boson existence was confirmed the SM was finally complete. The latest discovery of scalar field interacting as the predicted Higgs boson stands as a confirmation of the theoretical stage set down in the $60's$ [10–12].

The SM has an inherit symmetry group that is gauged and it is given by a direct product of $3$ Lie groups:

$$\mathcal{G}_{\text{SM}} = SU(3)_C \otimes SU(2)_L \otimes U(1)_Y \, . \tag{1.1}$$

Strong interactions mediated by gluons are described by the $SU(3)_C$ gauge group. Gluons have colour charge which is the charge associated to strong force. The electroweak sector is denoted by $SU(2)_L \otimes U(1)_Y$ where the first is associated with weak isospin force while the second is called hypercharge. Besides the symmetry it is also crucial to specify a possible spontaneous symmetry breaking (SSB) of the group $\mathcal{G}_{SM}$ into a smaller subgroup $\mathcal{G}_{SM}^{SSB}$.

In the SM we observe exactly a SSB of the electroweak sector (EW), namely:

$$\mathcal{G}_{SM} \xrightarrow{\text{SSB}} \mathcal{G}_{SM}^{SSB} = SU(3)_C \otimes U(1)_{e.m.} \tag{1.2}$$

In this pattern the strong force is left unaltered while EW sector breaks into two different interactions: weak and electromagnetic.

The weak force is mediated by three vector bosons $(W^+, W^-, Z)$ while the electromagnetic force is mediated by massless photons $(\gamma)$. There are different reasons why EW sector has to be broken. In nature we observe 3 different massive particles $W^\pm$, $Z$ with masses $M_W \sim 80.4$ GeV and $M_z \sim 90$ GeV, however the inclusion of an explicit mass term for the gauge bosons lead to a violation of $SU(2)_L \otimes U(1)_Y$ local symmetry. This problem is indeed solved by the Higgs mechanism [13, 14]. Due to its "Mexican-hat" shape when the scalar field corresponding to Higgs field goes into its vacuum configuration it acquires a vacuum expectation value (v.e.v.) different from $0$. This means that the ground state is no more invariant under $\mathcal{G}_{SM}$ but only under $\mathcal{G}_{SM}^{SSB}$. From the Goldstone theorem we have that the number of Goldstone bosons is equivalent to the number of broken generators. In the SM we have 3 broken generators that corresponds to the longitudinal polarization of $W^\pm$, $Z$. Thus the latter become massive. Analogous reasoning holds for fermions such as electrons and quarks that are

kept with no mass in the SM lagrangian and acquire mass only when EW sector is broken.
Another fact pointing towards SSB is that EW theory considers weak and electromagnetic force as indistinguishable at high energy, however experimental evidences such as parity violation tell us these interactions behave differently at low energies.[1]

## 1.1 The Standard Model of particle physics

We report a brief summary of the SM as it will make it easier to follow the notation used. The SM lagrangian can be written in compact form as:

$$\mathcal{L}_{\text{SM}} = \mathcal{L}_{kin}^{g.b.} + \mathcal{L}_{f}^{kin} + \mathcal{L}_{H} + \mathcal{L}_{Y} + \mathcal{L}_{kin}^{g.b.d.} . \tag{1.3}$$

The main sectors in $\mathcal{L}_{SM}$ are given by:

- The bosonic sector: It includes both gauge both kinetic terms of gauge bosons and the Higgs sector. Terms describing duals of field strength tensors are also included for the sake of completeness:

$$\mathcal{L}_{kin}^{g.b.} = \mathcal{L}_{kin}^{g.b.} + \mathcal{L}_{kin}^{g.b.d.} + \mathcal{L}_{H} = -\frac{1}{4}G_{\mu\nu}^{A}G^{A\mu\nu} - \frac{1}{4}W_{\mu\nu}^{I}W^{I\mu\nu} - \frac{1}{4}B_{\mu\nu}B^{\mu\nu} + (D_{\mu}H)^{\dagger}(D^{\mu}H)$$

$$- V(H^{\dagger}H) - \frac{\theta_3 g_3^2}{32\pi^2}G_{\mu\nu}^{A}\tilde{G}^{A\mu\nu} - \frac{\theta_2 g_2^2}{32\pi^2}W_{\mu\nu}^{I}\tilde{W}^{I\mu\nu} - \frac{\theta_1 g_1^2}{32\pi^2}B_{\mu\nu}\tilde{B}^{\mu\nu}, \tag{1.4}$$

where the gauge coupling associated to gauge $SU(3)_C$, $SU(2)_L$ and $U(1)_Y$ are $g_3$, $g_2$, $g_1$. The field strength tensors are given by :

$$G_{\mu\nu}^{A} = \partial_{\mu}G_{\nu}^{A} - \partial_{\nu}G_{\mu}^{A} + g_3 f^{ABC}G_{\mu}^{B}G_{\nu}^{C},$$
$$W_{\mu\nu}^{I} = \partial_{\mu}W_{\nu}^{I} - \partial_{\nu}W_{\mu}^{I} + g_2 \epsilon^{IJK}W_{\mu}^{J}W_{\nu}^{K},$$
$$B_{\mu\nu}^{I} = \partial_{\mu}B_{\nu} - \partial_{\nu}B_{\mu},$$

with $f^{ABC}$ and $\epsilon^{IJK}$ the structure constants of $SU(3)$ and $SU(2)$ respectively. In the second line we have the dual field-strength tensors defined as $\tilde{F}^{\mu\nu} = \frac{1}{2}\epsilon_{\mu\nu\rho\sigma}F^{\rho\sigma}$.
However the $\theta F\tilde{F}$ terms can be rewritten as a total derivatives, they will contribute only via topological effects that we are going to ignore in the following.[2] In the SM the Higgs field transforms as a doublet under $SU(2)_L$ (more on this later). It can be written as :

$$H = \frac{1}{\sqrt{2}}\exp\left(i\frac{\vec{\pi}(x)\vec{\sigma}}{v}\right)\begin{pmatrix} 0 \\ v + h(x) \end{pmatrix} \tag{1.5}$$

---

[1]The SM is also renormalizabile, and every theory beyond standard model (BSM) should reproduce such a characteristic.

[2]While contributions from abelian gauge field never matters, it is possible to have an effect in perturbation theory from non abelian gauge fields due to istanton configurations associated with those fields. Ignoring those terms implies istanton configurations are not considered and that the only source of CP violation comes from phase of the CKM matrix $V_{CKM}$.

where $\vec{\pi}$ is a vector of the Goldstone bosons and in the unitary gauge it reduces to :

$$H_{u.g.} = U(\pi)H = \frac{1}{\sqrt{2}} \begin{pmatrix} 0 \\ v + h(x) \end{pmatrix}. \tag{1.6}$$

The covariant derivative acting on $H$ is:

$$D_\mu H = \left( \partial_\mu - ig_2 \frac{\sigma^I}{2} W_\mu^I - ig_1 Y B_\mu \right) H, \tag{1.7}$$

where $\sigma^I$ are the Pauli matrices and hence the generators of the fundamental representation of $SU(2)_L$ while $Y = Q - T_3$ is the hypercharge. The scalar potential for the Higgs field reads:

$$V(H) = -\mu^2(H^\dagger H) + \lambda(H^\dagger H)^2. \tag{1.8}$$

After electroweak-symmetry breaking (EWSB) the electroweak (EW) vector bosons become massive:

$$\mathcal{L}_{bos}^{SSB} = -\frac{1}{4} G_{\mu\nu}^A G^{A\mu\nu} - \frac{1}{4} W_{\mu\nu}^I W^{I\mu\nu} - \frac{1}{4} B_{\mu\nu} B^{\mu\nu} + \frac{1}{2}(\partial h)^2 - \frac{1}{2} m_h^2 h^2$$
$$+ \frac{(v+h)^2 g_2^2}{4} W_\mu^+ W^{-\mu} + \frac{(v+h)^2 (g_2^2 + g_1^2)}{8} Z_\mu Z^\mu - \lambda v h^3 - \frac{\lambda}{4} h^4 \tag{1.9}$$

where the physical gauge bosons are written in terms of the Weinberg angle $\theta_W$:

$$W_\mu^\pm = \frac{W_\mu^1 \pm i W_\mu^2}{\sqrt{2}},$$
$$Z_\mu = c_W W_\mu^3 - s_W B_\mu,$$
$$A_\mu = c_W B_\mu + s_W W_\mu^3,$$

having set $c_W = \cos(\theta_W)$ and $s_W = \sin(\theta_W)$. The gauge boson masses are given by:

$$M_{W^\pm}^2 = \frac{g_2^2 v^2}{4}, \qquad M_Z^2 = \frac{(g_2^2 + g_1^2)v^2}{8}. \tag{1.10}$$

- the fermionic sector: This part contains kinetic terms for the fermions as well as interactions of the fermions with gauge bosons. The most general covariant derivative acting on a fermion field is:

$$D_\mu \psi = \left( \partial_\mu - ig_3 \frac{\lambda^A}{2} G_\mu^A - ig_2 \frac{\sigma^I}{2} W_\mu^I - ig_1 Y_f B_\mu \right) \psi \tag{1.11}$$

with $T^A = \frac{\lambda^A}{2}$ and $\tau^I = \frac{\sigma^I}{2}$ are the generators of the fundamental representation of $SU(3)_C$ and $SU(2)_L$ while the $U(1)_Y$ generator is denoted by $Y$. Fermions $\psi$ will couple to some or all the gauge boson present in $D_\mu$ accordingly with their quantum numbers. All the charges under $\mathcal{G}_{SM}$ are summarized in 1.1 Note that we have introduced a convenient notation for left handed

| | $\ell$ | $e$ | $q$ | $u$ | $d$ | $H$ | $G$ | $W$ | $B$ |
|---|---|---|---|---|---|---|---|---|---|
| $SU(3)_c$ representation | 1 | 1 | 3 | 3 | 3 | 1 | 8 | 1 | 1 |
| $SU(2)_L$ representation | 2 | 1 | 2 | 1 | 1 | 2 | 1 | 3 | 1 |
| $U(1)_Y$ charge | $-\frac{1}{2}$ | $-1$ | $\frac{1}{6}$ | $\frac{2}{3}$ | $-\frac{1}{3}$ | $\frac{1}{2}$ | 0 | 0 | 0 |

Table 1.1: Charges of the SM fermions, gauge bosons and H, under the SM gauge group.

quarks and leptons that are doublets under $SU(2)_L$, while right-handed components are singlet under $SU(2)_L$:

$$q_L^i = \begin{pmatrix} u_L^i \\ d_L^i \end{pmatrix} \qquad\qquad l_L^i = \begin{pmatrix} \nu_L^i \\ e_L^i \end{pmatrix} \qquad\qquad (1.12)$$

where $i = 1, 2, 3$ runs over the three generations. In the unitary gauge, this part of the Lagrangian is:

$$\mathcal{L}_f^{SM\,u.g.} = \sum_f \bar{f}_L i\slashed{\partial} f_L + \sum_f \bar{f}_R i\slashed{\partial} f_R - \frac{g_2}{\sqrt{2}}(W_\mu^+ J^{-\mu} + W_\mu^- J^{+\mu}) - \frac{g_2}{c_W} Z_\mu J_Z^\mu \qquad (1.13)$$

$$- eA_\mu J_{em}^\mu - g_3 G_\mu^A J^{A,\mu} . \qquad (1.14)$$

$$J^{+\mu} = \bar{d}_L \gamma^\mu u_L + \bar{e}_L \gamma_\mu \nu_L , \qquad J^{-\mu} = \bar{u}_L \gamma^\mu d_L + \bar{\nu}_L \gamma^\mu e_L , \qquad (1.15)$$

$$J^{A\mu} = \sum_q \bar{q}\gamma^\mu T^A q , \qquad J_Z^\mu = \sum_f \bar{f}_L \gamma^\mu T^3 f_L + \sum_f Q_f \bar{f}\gamma^\mu f , \qquad (1.16)$$

$$J_{em}^\mu = \sum_f Q_f \bar{f}\gamma^\mu f . \qquad (1.17)$$

It contains kinetic terms for fermions as well as interactions between gauge bosons $W^\pm, Z, G$ and matter fermions embedded in $J$'s. The kinetic terms of the fermions have a $SU(n_f)_L \otimes SU(n_f)_R$ symmetry, that is explicitly broken by the interactions with gauge bosons down to SM gauge group.

- Yukawa lagrangian: $\mathcal{L}_Y$ stands for the Yukawa terms, it describes interactions between the Higgs field with fermions. In order to preserve gauge invariance we have to introduce a slight modification of the $H$ field, i.e. $\tilde{H} = i\sigma_2 H^*$ that has quantum numbers $(1, 2, -1/2)$.

$$-\mathcal{L}_Y = [Y_e]_{i,j}\bar{l}_i H e_j + [Y_u]_{i,j}\bar{q}_i \tilde{H} u_j + [Y_d]_{i,j}\bar{q}_i H d_j + \text{h.c.} \qquad (1.18)$$

The indices $\{i, j\} = 1, 2, 3$, stand for the generation of the fermions hence

$$u_{L/R} = \begin{pmatrix} u \\ c \\ t \end{pmatrix}_{L/R} , \qquad d_{L/R} = \begin{pmatrix} d \\ s \\ b \end{pmatrix}_{L/R} , \qquad e_{L/R} = \begin{pmatrix} e \\ \mu \\ \tau \end{pmatrix}_{L/R} , \qquad \nu_L = \begin{pmatrix} \nu_e \\ \nu_\mu \\ \nu_\tau \end{pmatrix} . \qquad (1.19)$$

After SSB $\mathcal{L}_Y$ contains both mass terms for fermions as well as Yukawa interactions with the

physical Higgs boson $h$:

$$\mathcal{L}_Y = \frac{-(v + h(x))}{\sqrt{2}} (\bar{u}_L^i Y_u^{ij} u_R^j + \bar{d}_L^i Y_d^{ij} d_R^j + \bar{e}_L^i Y_u^{ij} e_R^j + h.c.) \,. \tag{1.20}$$

In principle $Y_{e,u,d}$ are $3 \times 3$ complex matrices representing the only source of flavour violation in the SM. When we want to compute physical observable for the fermions it is necessary to go to the so called mass eigenbasis or physical basis.

This requires obtaining a diagonal form for the Yukawa matrix $y$ which is achieved by a unitary transformations acting differently on right-handed and left-handed matter fields:

$$\begin{cases} u_L^{'} = L_u u_L \\ d_L^{'} = L_d d_L \\ e_L^{'} = L_e e_L \end{cases} \qquad \begin{cases} u_R^{'} = R_u u_R \\ d_R^{'} = R_d d_R \\ e_R^{'} = R_e e_R \end{cases} , \tag{1.21}$$

where rotation matrices are all unitary

$$LL^\dagger = L^\dagger L = \mathbb{I} \qquad\qquad RR^\dagger = R^\dagger R = \mathbb{I}. \tag{1.22}$$

Thus Yukawa matrices can be diagonalised by means of a bi-unitary transformation:

$$\hat{Y}_f = L_f Y_f R_f^\dagger = \begin{pmatrix} \hat{Y}_{f1} & 0 & 0 \\ 0 & \hat{Y}_{f2} & 0 \\ 0 & 0 & \hat{Y}_{f3} \end{pmatrix} . \tag{1.23}$$

This change of basis where we act with matrices $L, R$ on fields affects other sectors of the SM lagrangian. While the kinetic sector, the electromagnetic and the weak neutral interactions are still flavor diagonal in the mass basis, the weak charged interactions are modified as

$$\mathcal{L}_{CC} = -\frac{g_2}{\sqrt{2}} \{ \bar{u}_L^{'} (L_u L_d^\dagger) W^+ d_L + \bar{\nu}_L^{'} (L_\nu L_e^\dagger) e_L^{'} \} \,, \tag{1.24}$$

where $L_u L_d^\dagger$ is called Cabibbo-Kobayashi-Maskawa ($V_{CKM}$) matrix, while the analogous for leptons is called Pontecorvo-Maki-Sakata-Nakagawa ($U_{PMNS}$) matrix. These are unitary matrices with flavor mixing properties, note that as long as we keep neutrinos as massless particles we have to choose $U_{PMSN} = \mathbb{I}$.

## 1.2 Doublet or singlet

In this work we use two different effective field theories: SMEFT and HEFT. Both can be used in the description of low energy processes involving the Higgs boson.

In SMEFT the Higgs boson transforms as a part of a complete SU(2) doublet while in HEFT it

transforms as a singlet under the SM chiral group $SU(2)_L \otimes SU(2)_R$.

A way of presenting this is based on symmetry arguments [15]: SMEFT follows from a linear realization of EWSB while HEFT is a consequence of a non-linear realization.[3] We recall that in the SM the Higgs sector has the following Lagrangian:

$$\mathcal{L}_H = (D_\mu H)^\dagger (D^\mu H) - V(H) \,, \tag{1.25}$$

where $H$ transforms as a doublet under the SM gauge group, written in terms of 4 real components $\phi_i$:

$$H = \frac{1}{\sqrt{2}} \begin{pmatrix} \phi_2 + i\phi_1 \\ \phi_4 - i\phi_3 \end{pmatrix} \,. \tag{1.26}$$

In the limit of $g_1 \to 0$ and $y_u = y_d$ it is possible to rewrite the Lagrangian in such a way to make the global $O(4)$ symmetry explicit. For the sake of simplicity consider $D_\mu \to \partial_\mu$ just in the following steps:

$$\mathcal{L}_\phi = \frac{1}{2}(\partial_\mu \vec{\phi})(\partial^\mu \vec{\phi}) + \frac{m^2}{2} \vec{\phi} \cdot \vec{\phi} - \frac{\lambda_1}{8} (\vec{\phi} \cdot \vec{\phi})^2 \,. \tag{1.27}$$

The real fields $\phi_i$ are arranged into $\vec{\phi}$ as follows:

$$\vec{\phi} = \begin{pmatrix} \phi_1 \\ \phi_2 \\ \phi_3 \\ \phi_4 \end{pmatrix} = \begin{pmatrix} \phi_1 \\ \phi_2 \\ \phi_3 \\ v + h \end{pmatrix} \,, \tag{1.28}$$

where $\phi_i$ are the Goldstone bosons of EWSB and $h$ is the physical Higgs boson. The field $\vec{\phi}$ transforms linearly under $O(4)$ as $\vec{\phi} \to O\vec{\phi}$ and in this sense custodial symmetry $O(4)$ is an exact symmetry of the pure Higgs sector of the SM.

EWSB induces a non vanishing v.e.v. $\langle \phi_4 \rangle \neq 0$ and the $O(4)$ global symmetry is spontaneously broken, the vacuum state is invariant only under the $O(3)$ subgroup. In geometrical terms the vacuum state is an $\mathcal{S}^3$ sphere with radius $v$:

$$\langle \vec{\phi}^{\mathrm{T}} \cdot \vec{\phi} \rangle = \phi_1^2 + \phi_2^2 + \phi_3^2 + \phi_4^2 = v^2 \,. \tag{1.29}$$

The 3 Goldstone bosons are associated to the longitudinal polarization of the massive vector bosons. Recalling a local isomorphism from group theory we know:

$$O(4) \simeq SU(2)_L \times SU(2)_R / \mathbb{Z}_2 \,. \tag{1.30}$$

To see how the $SU(2)_L \otimes SU(2)_R$ act on $H$, we can combine it with its conjugate $\tilde{H} = i\sigma_2 H^*$ to form the $2 \times 2$ matrix field $\Sigma \equiv \left( \tilde{H}, H \right)$ transforming as $\Sigma \to L\Sigma R^\dagger$ where $L(R) \in SU(2)_{L/R}$. It

---

[3]This point is formalized in the CCWZ [16, 17] framework that describes Goldstone Bosons under a generic SSB pattern

is convenient to decompose the $\Sigma$ matrix field as:

$$\Sigma = \frac{1}{\sqrt{2}}(v+h)U, \qquad \text{with} \qquad U = e^{i\frac{\pi_i \sigma_i}{v}}, \qquad (1.31)$$

where $\sigma_i$ are the Pauli matrices providing a basis in the SU(2). The relation $Tr[\Sigma^\dagger \Sigma] = 2H^\dagger H = (\vec{\phi})^T \vec{\phi}$ allows to rewrite $\mathcal{L}_H$ in terms of $U$:

$$\mathcal{L}_U = \frac{1}{2}(\partial h)^2 + \frac{1}{2}(v+h)^2 \text{tr}\big[(\partial_\mu U)^\dagger (\partial^\mu U)\big] + \frac{m^2}{2}\text{tr}[(v+h)^2 \mathbb{I}] - \frac{\lambda}{8}(\text{tr}\big[(v+h)^2 \mathbb{I}\big])^2. \qquad (1.32)$$

The latter Lagrangian is also know as Electroweak Chiral Lagrangian and invariant under the chiral group $SU(2)_L \times SU(2)_R/\mathbb{Z}_2$ which is isomorphic to $O(4)$. The Goldstone bosons are coupled only derivatively.

The different components of $H$ transform under chiral group $SU(2)_L \otimes SU(2)_R$ as follows:

$$h \to h, \qquad U \to LUR^\dagger. \qquad (1.33)$$

The Higgs boson $h$ indeed transforms as a singlet under $SU(2)_L \otimes SU(2)_R$, and hence also under the EW gauge symmetry. Following [15–17] we say that the electroweak symmetry is non-linearly realised. Equation (1.32) is indeed an expression of the scalar sector of HEFT at LO.

HEFT contains SMEFT (and the SM) as a special case where a non-linear field redefinition can be found to map the scalar components ($h$ and $\pi_i$) into a single $SU(2)_L$ doublet $H$. The $O(4)$ invariants of the SM Higgs Sector can indeed be rewritten in each of these different languages:

$$|\partial H|^2 = \frac{1}{2}(\partial \vec{\phi}^{\mathsf{T}}) \cdot (\partial \vec{\phi}) = \frac{1}{2}(\partial h)^2 + \frac{1}{2}(v+h)^2 (\partial U)^2, \qquad (1.34)$$

$$(\partial |H|^2)^2 = (\vec{\phi} \cdot \vec{\phi})^2 = (v+h)^2 (\partial h)^2. \qquad (1.35)$$

It is therefore possible to express the so called linear $\sigma$ model in a non-linear realization exploiting a change of basis.

The aim of this thesis is to find physical processes where it is not possible to recover a SMEFT limit (linear $\sigma$) from an HEFT formulation (non-linear $\sigma$ model), hence the case in which the effective field theory does not admit a linear realisation.

## 1.3   Standard Model Effective Field Theory

An increasing number of experimental facts suggests that the SM is the right theory to describe physics up to a few hundreds of GeV. The absence of any direct or indirect signal of New Physics suggests that new degrees of freedom if they are there might live much above the electroweak scale. Whenever we face a scale separation, the use of an EFT is appropriate. In fact a way to think about SM is by considering it as a low-energy theory of some UV model.

This means that, if we want to treat the SM as an EFT we need to address the following points:

- select the low-energy degrees of freedom: assuming that the SM is the correct theory at scales $E \ll \Lambda$ means the low-energy degrees of freedom are the same ones as in the SM.

- symmetries of the theory: SMEFT needs to respect the same symmetries as the SM, meaning that the operators are invariant under $\mathcal{G}_{SM} = SU(3) \otimes SU(2) \otimes U(1)$ gauge group.

- the vacuum preserves $SU(3) \otimes U(1)$ symmetry after the SSB. This follows from the fact that SMEFT has the same particle content as the SM, hence a scalar transforming as $(1, 2)_{1/2}$ field that acquires a non vanishing non zero vacuum expectation value.

- a power counting scheme: In case of SMEFT the canonical dimension of the operator is counted. The operator itself is suppressed by $\Lambda^{4-d}$ where $d$ indicated the canonical dimension of the operator.

Strictly speaking SMEFT is not renormalizable as it contains infinite number of terms with a consequent infinite number of divergences that would require an infinite number of counterterms to be absorbed. However if we work at a specific order of accuracy, SMEFT is a truthfully renormalizable QFT. If we take indeed only the above points as guiding principles in the construction of SMEFT, we could write an infinite number of terms. Thanks to the power counting (PC) we can organize systematically the terms in an expansion in $1/\Lambda_{SMEFT}$ :

$$\mathcal{L}_{SMEFT} = \mathcal{L}_{SM} + \sum_i \frac{c_i^{(5)}}{\Lambda_{SMEFT}} \mathcal{O}_i^{d=5} + \sum_i \frac{c_i^{(6)}}{\Lambda_{SMEFT}^2} \mathcal{O}_i^{d=6} + \sum_i \frac{c_i^{(7)}}{\Lambda_{SMEFT}^3} \mathcal{O}_i^{d=7} + .... \quad (1.36)$$

Even though the series is well written it still has an infinite number of terms, we have to fix an order of accuracy at which we stop the expansion. The order can be cut if one can assume that any order higher gives contributions smaller than experimental accuracy of the problem:

$$\mathcal{L}_{SMEFT} = \mathcal{L}_{SM} + \sum_i \frac{c_i^{(d)}}{\Lambda_{SMEFT}^{d-4}} \mathcal{O}_i^d + \mathcal{O}\left(\frac{1}{\Lambda^{d+1}}\right). \quad (1.37)$$

In the expressions above $\mathcal{O}_i^d$ are gauge invariant operator of dimension $d$ while $c_i$ are called Wilson coefficients. These coefficients are crucial in the search new physics (NP) as they encode information about UV theory. A well known example is the Fermi Theory where the Fermi constant $G_F$ is related to parameters of the UV theory, namely $\frac{G_F}{\sqrt{2}} = \frac{g^2}{2M_W^2}$.

The natural question to answer should be the meaning of $\Lambda_{SMEFT}$. If we consider accidental symmetries (Baryon number, Lepton number) of SM we find they are broken around $\Lambda_{LNV}, \Lambda_{BNV} \sim 10^{16} GeV$. It is clear that, if $\Lambda_{SMEFT} = \Lambda_{BNV,LNV}$ then we could not observe any signal from new physics at collider experiments.

On the other hand the naturalness problem seems to suggest a lower value for $\Lambda_{SMEFT}$: the quadratic sensitivity of the 1-loop corrections $\delta m_H^2$ to the Higgs mass would require a $\Lambda_{SMEFT}$ close to 1 TeV

in order to avoid a fine-tuning of the UV parameters. The usual assumption allows for different scales in the problem, in particular a selection rule on the energy scales $\Lambda \ll \Lambda_{LNV,BNV}$ is taken. The SMEFT expansion is rewritten as:[4]

$$\mathcal{L}_{SMEFT} = \mathcal{L}_{SM} + \frac{c^{(5)}}{\Lambda_{LNV}}\mathcal{O}_5 + \sum_i \frac{c_i^{(d=6)}}{\Lambda_{SMEFT}^{d-4}}\mathcal{O}_i^d. \tag{1.38}$$

From now on we deal only with a cutoff energy scale much below the scale where Lepton and Baryon number are violated, therefore we assume $\Lambda_{SMEFT} = \Lambda \ll 10^{16}$ GeV. For the purpose of this thesis, we will focus on the part involving the Higgs doublet $H$. In particular, the rest of the thesis will focus on di-Higgs production. In this case the relevant operators are:

$$\begin{aligned}
\mathcal{L}_{SMEFT} \supset \mathcal{L}_{SM} &+ \frac{C_{\Box H}}{\Lambda^2}(H^\dagger H)\Box(H^\dagger H) + \frac{C_H}{\Lambda^2}(H^\dagger H)^3 + \frac{C_{HD}}{\Lambda^2}(H^\dagger D_\mu H)^*(H^\dagger D^\mu H) \\
&+ \frac{C_{uH}}{\Lambda^2}(H^\dagger H)\bar{q}\tilde{H}u + \text{h.c.} + \frac{C_{dH}}{\Lambda^2}(H^\dagger H)\bar{q}Hd + \text{h.c.} + \frac{C_{eH}}{\Lambda^2}(H^\dagger H)\bar{l}He + \text{h.c.} \\
&+ \frac{C_{HW}}{\Lambda^2}(H^\dagger H)W_{\mu\nu}^I W^{I\mu\nu} + \frac{C_{HG}}{\Lambda^2}(H^\dagger H)G_{\mu\nu}^A G^{A\mu\nu} + \frac{C_{HB}}{\Lambda^2}H^\dagger H B_{\mu\nu}B^{\mu\nu} + \mathcal{O}(\frac{1}{\Lambda^4}).
\end{aligned} \tag{1.39}$$

SMEFT is usually written in the unbroken phase even though, when it comes to make comparison with HEFT, we have to bring it in the broken phase. It is important to note how SSB is altered in the SMEFT framework, where higher dimensional operators modify the relations we know from SM. Importantly enough, this implies doing a redefinition of the v.e.v. which receives now contributions from dimension-6 operators:

$$V(H^\dagger H) = \lambda\left(H^\dagger H - \frac{v^2}{2}\right)^2 - \frac{C_H}{\Lambda^2}\left(H^\dagger H\right)^3, \tag{1.40}$$

therefore the new minimum will be:

$$\langle H^\dagger H\rangle = \frac{v_T^2}{2} = \frac{v^2}{2}\left(1 + \frac{3C_H v^2}{4\lambda}\right). \tag{1.41}$$

Beside the scalar potential part of $\mathcal{L}_{SMEFT}$, we have to perform a shift in the $h$ field to ensure canonically normalized kinetic term. In unitary gauge we have:

$$H = \frac{1}{\sqrt{2}}\begin{pmatrix} 0 \\ (1+c_{H,kin})h + v_T \end{pmatrix}, \quad \text{where} \quad c_{H,kin} = \left(C_{\Box H} - \frac{C_{HD}}{4}\right)\frac{v^2}{\Lambda^2}. \tag{1.42}$$

These shifts, due to higher dimensional operators, affect all parameters of the model that include the Higgs boson: gauge couplings, mass of gauge bosons as well as yukawa couplings. It is important to note that the above $h$ field redefinition introduces additional self couplings as $h(\partial h)^2$ or $h^2(\partial h)^2$.

---

[4]In SMEFT we have only one five dimensional operator, the so-called Weinberg operator that violates Lepton Number. A high value of $\Lambda_{LNV}$ may explain why neutrino masses are so small.

There is yet another another redefinition of the $h$ field that does not present such derivative couplings (at least at order $1/\Lambda^2$) is:

$$h \rightarrow h + \frac{v^2}{\Lambda^2}\left(C_{H\square} - \frac{C_{HD}}{4}\right)\left(h + \frac{h^2}{v} + \frac{h^3}{3v^2}\right). \tag{1.43}$$

In this way we get a canonically normalized kinetic term for $h$ as well as no derivative self interactions for the Higgs field. The Wilson coefficients $C_{H\square}$ and $C_{HD}$ become a universal factor in every Higgs coupling, this holds independently from the $h$ field redefinition chosen. Importantly enough the non linear redefinition of the $h$ field 1.43 is not gauge invariant as we are shifting only one real component out of the four that enters the Higgs doublet. For a gauge invariant shift we should shift the Goldstone bosons as reported in [18]. We now comment on how dimension 6 operators modify the different parts of the SM. The SM Yukawa sector is modified by gauge invariant dimension 6 operator as reported in 1.39. In the broken phase the Yukawa matrices receive a correction of the order $\mathcal{O}\left(\frac{v^2}{\Lambda^2}\right)$ while the interactions with $h$ field are additionally shifted by a $c_{H,kin}$ term. The broken phase lagrangian reads [19]:

$$\mathcal{L}_{Yukawa} = -[\mathcal{M}_f]^{p,r}\,(\bar{f}_L^p f_R^r) - [\mathcal{Y}_{f,h}]^{p,r}\,h(\bar{f}_L^p f_R^r) + \text{h.c.}\,,$$
$$[\mathcal{M}_f]^{p,r} = \frac{v_T}{\sqrt{2}}\left([Y]^{p,r} - \frac{1}{2}\frac{v^2}{\Lambda^2}\,[C_{fH}]^{p,r}\right),$$
$$[\mathcal{Y}_{f,h}]^{p,r} = \frac{1}{\sqrt{2}}\left((1 + c_{H,kin})Y^{p,r} - \frac{3}{2}\frac{v^2}{\Lambda^2}\,[C_{f,H}]^{p,r}\right), \tag{1.44}$$

where $p,r$ are flavor indeces while $f = \{u,d,e,\nu\}$. The Yukawa matrices $\mathcal{Y}_{f,h}$ are no longer proportional to the mass matrices $\mathcal{M}_f$. The crucial consequence is that once we move to the mass basis we can set $\mathcal{M}_f$ to get a diagonal form so that the mass of the particles is well defined by the SM contribution plus a term proportional to $\frac{v^2 C_{fH}}{\Lambda^2}$. This means that the interaction between the $h$ boson and other fermions can become flavor violating starting at $\mathcal{O}(1/\Lambda^2)$.

In the broken phase these operators give corrections to the kinetic terms of the gauge fields. In order to recover the right normalization a redefinition of the gauge field and gauge couplings is needed: From eq.(1.39) we notice how the field strength tensors are modified by dimension-6 operators.

$$\bar{W}_\mu^I = Z_g W_\mu^I\,, \qquad \bar{g}_2 = Z_{g_2}^{-1} g_2\,, \qquad Z_g = 1 - C_{HW}\frac{v^2}{\Lambda^2}\,,$$
$$\bar{B}_\mu^I = Z_{g'} B_\mu^I\,, \qquad \bar{g}_1 = Z_{g_1}^{-1} g_1\,, \qquad Z_g = 1 - C_{HB}\frac{v^2}{\Lambda^2}\,,$$
$$\bar{G}_\mu^A = Z_g G_\mu^A\,, \qquad \bar{g}_3 = Z_{g_3}^{-1} g_3\,, \qquad Z_g = 1 - C_{HG}\frac{v^2}{\Lambda^2}\,.$$

It's possible to rewrite the gauge sector in terms of $\bar{W}_\mu^I$, $\bar{B}_\mu^I$ and $\bar{G}_\mu^A$ [5]. Note that in this way the

---

[5]More precisely this redefinition canonically normalize the kinetic term for gluons since the weak gauge bosons still present a mixing terms proportional to $C_{HWB}$ operator, however if we assume it to vanish then the terms are already

covariant derivative form $D_\mu = \partial_\mu - ig_i A^i = \partial_\mu - i\bar{g}_i \bar{A}^i$ is preserved and consequently the sector describing the gauge fermion interactions does not change.

These corrections affect also the definition of the $W$ boson mass:

$$M_W = \frac{\bar{g}_2 v_T}{2}, \qquad \text{where} \qquad Z_g = 1 - C_{HW} \frac{v^2}{\Lambda^2}.$$

Before matching to some UV theory, the Warsaw basis is a model independent ensemble of operators that we use to parametrize small deviations from the SM due to new physics signals. By doing a naive dimensional analysis one can obtain an idea of the relative size of the effective operators. We show this for the subset of operators that will be relevant in the following.

In principle we consider only a subset of those operators depending on the process we are interested in. In the following we mainly deal with $C_{H\square}$, $C_{uH}$, $C_H$ and $C_{HG}$ Wilson coefficients.

While considering only the canonical dimension of this operators non difference between their relative size is evident, the $\hbar$ counting leads to differences [20]. Let us assume that we can express all the couplings and the masses of the EFT in terms of reference coupling (mass) $g_*$ ($m_*$) belonging to the UV theory. From the path integral formulation we know that the action $S$ must bring a dimension of $\hbar$ such that the factor $e^{i\frac{S}{\hbar}}$ has the right dimensions. Considering this counting in $\hbar$ leads to $[g_*] = \frac{1}{\sqrt{\hbar}}$ and the Lagrangian is expressed in terms of these reference quantities of the UV model as $\mathcal{L} = \frac{m_*^4}{g_*^2}\hat{\mathcal{L}}$ where $\hat{\mathcal{L}}\left(\frac{g_* H}{m_*}, \frac{\partial}{m_*}\right)$ is a dimensionless quantity.

The relevant operators would have an $\hbar$ counting as:

$$\mathcal{O}_{H\square} = \frac{C_{\square H}}{\Lambda^2}(H^\dagger H)\square(H^\dagger H), \qquad\qquad C_{H\square} \sim g_*^2, \qquad\qquad (1.45)$$

$$\mathcal{O}_H = \frac{C_H}{\Lambda^2}(H^\dagger H)^3, \qquad\qquad C_H \sim g_*^4, \qquad\qquad (1.46)$$

$$\mathcal{O}_{uH} = \frac{C_{uH}}{\Lambda^2}(H^\dagger H)(\bar{q}\tilde{H}u), \qquad\qquad C_{uH} \sim g_*^3, \qquad\qquad (1.47)$$

therefore for strongly coupled UV theories $C_H$ will dominate while weakly interacting UV theories will be mainly described by $C_{H\square}$.

This apparently unrelated comment may be useful in the following as SMEFT will be shown to have an "heavy" dependence on $C_{H\square}$. SMEFT shows its limits exactly when the UV theory becomes strongly interacting and in this sense $C_{H\square}$ may not be enough to parametrize new physics effects. Then HEFT is supposed to take its place as more appropriate IR limit. A naive dimensional analysis (NDA) allows us to organize the effective operators allowed in SMEFT showing also how a refined $\hbar$ counting can give us additional information about operators with the same canonical dimension having different weights in a top down approach. The higher dimensional part of the SMEFT lagrangian can be seen as an object living in an $n$ dimensional space $\mathcal{L} \supset \sum_n C_n \mathcal{O}_n$ where $n$ is the number of operators at dimension 6, then $O_n$ are the elements of the vector basis that should contain only independent objects. We would like to find a non redundant basis for this object.

---

canonically normalized

| | $X^3$ | | $\phi^6$ and $\phi^4 D^2$ | | $\psi^2\phi^3$ |
|---|---|---|---|---|---|
| $Q_G$ | $f^{ABC}G_\mu^{A\nu}G_\nu^{B\rho}G_\rho^{C\mu}$ | $Q_\phi$ | $(\phi^\dagger\phi)^3$ | $Q_{e\phi}$ | $(\phi^\dagger\phi)(\bar{L}_p e_r \phi)$ |
| $Q_{\tilde{G}}$ | $f^{ABC}\tilde{G}_\mu^{A\nu}G_\nu^{B\rho}G_\rho^{C\mu}$ | $Q_{\phi\Box}$ | $(\phi^\dagger\phi)\Box(\phi^\dagger\phi)$ | $Q_{u\phi}$ | $(\phi^\dagger\phi)(\bar{Q}_p u_r \tilde{\phi})$ |
| $Q_W$ | $\epsilon^{IJK}W_\mu^{I\nu}W_\nu^{J\rho}W_\rho^{K\mu}$ | $Q_{\phi D}$ | $(\phi^\dagger D^\mu\phi)^*(\phi^\dagger D_\mu\phi)$ | $Q_{d\phi}$ | $(\phi^\dagger\phi)(\bar{Q}_p d_r \phi)$ |
| $Q_{\tilde{W}}$ | $\epsilon^{IJK}\tilde{W}_\mu^{I\nu}W_\nu^{J\rho}W_\rho^{K\mu}$ | | | | |
| | $X^2\phi^2$ | | $\psi^2 X\phi$ | | $\psi^2\phi^2 D$ |
| $Q_{\phi G}$ | $\phi^\dagger\phi\, G_{\mu\nu}^A G^{A\mu\nu}$ | $Q_{eW}$ | $(\bar{L}_p\sigma^{\mu\nu}e_r)\sigma^I\phi W_{\mu\nu}^I$ | $Q_{\phi l}^{(1)}$ | $(\phi^\dagger i\overleftrightarrow{D}_\mu\phi)(\bar{L}_p\gamma^\mu L_r)$ |
| $Q_{\phi\tilde{G}}$ | $\phi^\dagger\phi\,\tilde{G}_{\mu\nu}^A G^{A\mu\nu}$ | $Q_{eB}$ | $(\bar{L}_p\sigma^{\mu\nu}e_r)\phi B_{\mu\nu}$ | $Q_{\phi l}^{(3)}$ | $(\phi^\dagger i\overleftrightarrow{D}_\mu^I\phi)(\bar{L}_p\sigma^I\gamma^\mu L_r)$ |
| $Q_{\phi W}$ | $\phi^\dagger\phi\, W_{\mu\nu}^I W^{I\mu\nu}$ | $Q_{uG}$ | $(\bar{Q}_p\sigma^{\mu\nu}u_r)T^A\tilde{\phi}G_{\mu\nu}^A$ | $Q_{\phi e}$ | $(\phi^\dagger i\overleftrightarrow{D}_\mu\phi)(\bar{e}_p\gamma^\mu e_r)$ |
| $Q_{\phi\tilde{W}}$ | $\phi^\dagger\phi\,\tilde{W}_{\mu\nu}^I W^{I\mu\nu}$ | $Q_{uW}$ | $(\bar{Q}_p\sigma^{\mu\nu}u_r)\sigma^I\tilde{\phi}W_{\mu\nu}^I$ | $Q_{\phi q}^{(1)}$ | $(\phi^\dagger i\overleftrightarrow{D}_\mu\phi)(\bar{Q}_p\gamma^\mu Q_r)$ |
| $Q_{\phi B}$ | $\phi^\dagger\phi\, B_{\mu\nu}B^{\mu\nu}$ | $Q_{uB}$ | $(\bar{Q}_p\sigma^{\mu\nu}u_r)\tilde{\phi}B_{\mu\nu}$ | $Q_{\phi q}^{(3)}$ | $(\phi^\dagger i\overleftrightarrow{D}_\mu^I\phi)(\bar{Q}_p\sigma^I\gamma^\mu Q_r)$ |
| $Q_{\phi\tilde{B}}$ | $\phi^\dagger\phi\,\tilde{B}_{\mu\nu}B^{\mu\nu}$ | $Q_{dG}$ | $(\bar{Q}_p\sigma^{\mu\nu}d_r)T^A\phi G_{\mu\nu}^A$ | $Q_{\phi u}$ | $(\phi^\dagger i\overleftrightarrow{D}_\mu\phi)(\bar{u}_p\gamma^\mu u_r)$ |
| $Q_{\phi WB}$ | $\phi^\dagger\sigma^I\phi\, W_{\mu\nu}^I B^{\mu\nu}$ | $Q_{dW}$ | $(\bar{Q}_p\sigma^{\mu\nu}d_r)\sigma^I\phi W_{\mu\nu}^I$ | $Q_{\phi d}$ | $(\phi^\dagger i\overleftrightarrow{D}_\mu\phi)(\bar{d}_p\gamma^\mu d_r)$ |
| $Q_{\phi\tilde{W}B}$ | $\phi^\dagger\sigma^I\phi\,\tilde{W}_{\mu\nu}^I B^{\mu\nu}$ | $Q_{dB}$ | $(\bar{Q}_p\sigma^{\mu\nu}d_r)\phi B_{\mu\nu}$ | $Q_{\phi ud}$ | $(\tilde{\phi}^\dagger i\overleftrightarrow{D}_\mu\phi)(\bar{u}_p\gamma^\mu d_r)$ |

Figure 1.1: Dimension 6 operators of the Warsaw basis. The upper part of the table contains the purely bosonic operators which will be the main object of this thesis.

In particular possible redundancies may be due to:

1. **Integration by parts**: assuming all fields vanish at infinity i.e. total derivatives do no contribute to $S = \int d^4x\mathcal{L}$ .

2. **Field redefinition**: A deep result in QFT, known as $\hat{S}$ matrix equivalence theorem, tells us that fields are not fundamental objects. In fact particles are more fundamental objects. The $S$ matrix remains equivalent under field redefinition. In practise, this is often implemented making use of equations of motions relations.

3. **Fierz Identities:** these identities follow from a completeness relation on certain matrix space especially when operators have internal symmetry, typically any $SU(N)$ is provided with a Fierz Identity.

Finding a non redundant basis is non trivial task that was accomplished in [21]. The so called "Warsaw basis" up to dimension 6, considering all flavors, contains 2499 operators. The Warsaw basis is non-redundant and as such neither of the basis elements can be mapped onto the others by field redefinition, Fierz identities or Integration by parts i.e. they are independent. The subset of Warsaw basis at dimension six is presented in fig.1.1 leaving though out the four fermion interactions, which will not be relevant for the rest of the thesis.

## 1.4 HEFT

As it was pointed out in the previous section, HEFT is an EFT where the physical Higgs boson appears as a gauge singlet under $\mathcal{G}_{SM}$ and as a singlet under the chiral group $SU(2)_L\otimes SU(2)_R$ [22]. As pointed

out above a change of variables allows us to express the Higgs sector in terms of $\Sigma = \frac{v+h}{\sqrt{2}}U$ where $h$ is the physical Higgs boson while the $U$ matrix contains the Goldstone bosons.

The Higgs boson lagrangian reads:

$$(D_\mu H)^\dagger D^\mu H - V(H) \rightarrow \frac{1}{2}(\partial h)^2 + \frac{v^2}{4}\text{Tr}\left[D_{(\mu}U)^\dagger D^\mu U\right] - V(h)\,.$$

We note also the scalar potential does not depend on $U$, in other words Goldstone modes are only derivatively coupled. Since we are going to comment on the Yukawa sector as well, we rewrite it using the polar parametrization of $H$:

$$-Y_u\bar{q}_L\tilde{H}u_R - Y_e\bar{l}_L He_r + \text{h.c.} \rightarrow -\frac{v+h}{\sqrt{2}}\left(\bar{q}_L U Y_Q q_R + \bar{l}_L U l_R + \text{h.c.}\right),$$

where $Y_Q = \text{Diag}(Y_u, Y_d)$, $Y_l = \text{Diag}(0, Y_e)$ and the right handed doublets for single generation are given by:

$$q_R = \begin{bmatrix} u_R \\ d_R \end{bmatrix}, \quad l_R = \begin{bmatrix} 0 \\ e_R \end{bmatrix}. \tag{1.48}$$

The transformations under the chiral group are:

$$h \rightarrow h, \qquad U \rightarrow LUR^\dagger\,.$$

The global custodial symmetry is then broken explicitly by the gauge coupling $g_1$ and the Yukawa sector. For instance the covariant derivative in the scalar sector transforms as follows:

$$D_\mu U = \partial_\mu U - ig_2\frac{\sigma^I}{2}W_\mu^I U + ig_1 B_\mu U\frac{\sigma_3}{2} \rightarrow L(\partial_\mu U)R^\dagger - ig_2\frac{\sigma^I}{2}W_\mu^I LUR^\dagger + ig_1 B_\mu LUR^\dagger\frac{\sigma_3}{2}, \tag{1.49}$$

where $L/R$ are unitary matrices belonging to $SU(2)_{L/R}$. Clearly in the last term $R$ commutes with $\sigma_3$ only if we take the diagonal subgroup of $SU(2)_R$, so the last terms breaks explicitly the chiral group. Even in the $g_1 \rightarrow 0$ limit we still have a breaking of the chiral group due to the Yukawa term. Take for instance the quark bilinear:

$$-\frac{v+h}{\sqrt{2}}\left(\bar{q}_L U Y_Q q_R\right) \rightarrow -\frac{v+h}{\sqrt{2}}\left(\bar{q}_L L^\dagger L U R^\dagger Y_Q R q_R\right), \tag{1.50}$$

since $Y_Q$ is diagonal the only way to have an invariance under $SU(2)_L \otimes SU(2)_R$ is by restricting the element $R \in SU(2)_R$ to its diagonal subgroup $U(1)_Y$, in this way $[R^\dagger, Y_Q] = 0$.[6] In this way we have

---

[6]Another way to see the breaking of the chiral group is by exploiting a spurion trick where $\hat{W}_\mu$ and $\hat{B}_\mu$ are $2 \times 2$ matrix spurion fields. They act as gauge bosons of the chiral group and therefore transform in the adjoint representation:

$$\hat{W}_\mu \rightarrow V_L\hat{W}_\mu V_L^\dagger + iV_L(\partial_\mu V_L)^\dagger\,, \tag{1.51}$$

$$\hat{B}_\mu \rightarrow V_R\hat{B}_\mu V_R^\dagger + iV_R(\partial_\mu V_R)^\dagger\,, \tag{1.52}$$

where $V_{L/R} \in SU(2)_{L/R}$. In this way the global custodial symmetry is promoted to a local one. If (1.51) and (1.52) hold the SM lagrangian is invariant under the chiral gauge group. When we reduce this to the SM case we fix the spurion fields

checked that the chiral symmetry is explicitly broken by $g_1$ and by $Y_u \neq Y_d$ also in the formulation where $H$ has been rewritten seperating $h$ from the Goldstone bosons.

Once the quantities above have been defined the lagrangian in terms of the explicit Goldstone bosons matrix is:

$$
\mathcal{L}_{SM} = -\frac{1}{4}G^A_{\mu\nu}G^{A\mu\nu}\left(\frac{h}{v}\right) - \frac{1}{4}W^I_{\mu\nu}W^{I\mu\nu} - \frac{1}{4}B_{\mu\nu}B^{\mu\nu}
$$
$$
+ \sum_\psi \bar{\psi}_L i\slashed{D}\psi_L + + \sum_\psi \bar{\psi}_R i\slashed{D}\psi_R + \frac{1}{2}\partial_\mu h\partial^\mu h + \frac{v^2}{4}\mathrm{tr}\left[(D_\mu U)^\dagger D^\mu U\right] - V(h)
$$
$$
- \frac{v}{\sqrt{2}}(\bar{q}_L U Y_Q q_R + \bar{l}_L U Y_Q l_R + h.c.)\,. \tag{1.54}
$$

When we gauge the symmetry every element of $L$ and of $R$ acquires a dependence from the spacetime coordinate such that $L \to L(x)$ and $R \to R(x)$, since $g_1 \neq 0$ and $Y_u \neq Y_d$ the above lagrangian is only invariant under the subgroup $SU(2)_L \otimes U(1)_Y$ which coincides with 1.1. Under the SM gauge group $\mathcal{G}_{SM}$ we have $(D_\mu U)_\mathcal{G} = L(D_\mu U)e^{i\sigma_3\alpha(x)Y}$ where $Y$ stands for the hypercharge and the Yukawa sector respects this gauge symmetry of course as well.

Thus the lagrangian of eq. (1.54) is invariant under the SM gauge group $SU(3)_c \otimes SU(2)_L \otimes U(1)_Y$. The HEFT is based on the same gauge symmetry as the SMEFT and contains the same degrees of freedom but the Higgs doublet $H$ is replaced by the scalar singlet $h$ and the matrix $U$ describing the Goldstone bosons. The HEFT lagrangian is obtained from eq. 1.54 above by adding different Taylor series terms to each gauge invariant block. These series have the gauge singlet $\frac{h}{v}$ quantity as expansion parameter with unknown coefficients in front of them up to order infinity. The HEFT Lagrangian reads [22–28]:

$$
\mathcal{L}_{HEFT} \supset -\frac{1}{4}G^A_{\mu\nu}G^{A\mu\nu}\mathcal{F}_G\left(\frac{h}{v}\right) + \sum_\psi \bar{\psi}_L i\slashed{D}\psi_L + + \sum_\psi \bar{\psi}_R i\slashed{D}\psi_R + \frac{1}{2}\partial h\partial h
$$
$$
+ \frac{v^2}{4}\mathrm{tr}\left[(D_\mu U)^\dagger D^\mu U\right]\mathcal{F}_U\left(\frac{h}{v}\right) - V(h) - \frac{v}{\sqrt{2}}(\bar{q}_L U Y_Q q_R + \bar{l}_L U Y_Q l_R + h.c.)\mathcal{G}\left(\frac{h}{v}\right)\,. \tag{1.55}
$$

In particular when we consider an expansion around the EW vacuum we obtain $\langle U \rangle = 1$ and we recover the SM expressions both for fermion masses in the Yukawa sector as well as the expressions for the masses of the massive vector bosons:

$$
\frac{v^2}{4}\mathrm{tr}\left[(D_\mu U)^\dagger D^\mu U\right]\mathcal{F}_U\left(\frac{h}{v}\right) = M_W^2 W_\mu^+ W^{-\mu}\mathcal{F}_U\left(\frac{h}{v}\right) + \frac{M_Z^2}{2}Z_\mu Z^\mu\mathcal{F}_U\left(\frac{h}{v}\right),
$$

to their vecuum expectation value:

$$
\hat{W}_\mu \to g_2\frac{\sigma^I}{2}W^I_\mu, \qquad \hat{B}_\mu \to g_1\frac{\sigma^3}{2}B^I_\mu, \tag{1.53}
$$

and as a consequence the SM lagrangian is invariant only under $SU(2)_L \otimes U(1)_Y$ that is exactly the gauge group of the SM.

$U$ contains an infinite number of interactions of the EW Goldstone bosons:

$$U \sim 1 + 2i\frac{\pi^a \sigma^a}{v} - 2\frac{(\pi^a \sigma^a)(\pi^b \sigma^b)}{v^2} + \mathcal{O}\left(\frac{\pi^3}{v^3}\right), \quad a, b = 1, 2, 3, \tag{1.56}$$

and a summation over repeated indices is understood. Since the Pauli matrices are traceless the kinetic term of $U$ keeps only even powers of $\pi$ so the imaginary part disappears. In the high energy regime, thanks to the Goldstone Boson Equivalence theorem, these $\pi$'s can be viewed as the longitudinally polarized massive gauge bosons $W^+, W^-$ and $Z$.

In particular the quantities $\mathcal{F}_{G,U}, Y_Q, V(h), \mathcal{G}$ appear as power series in $\frac{h}{v}$:

$$\mathcal{F}_G(h) = 1 + a_{g1}\frac{h}{v} + a_{g2}\left(\frac{h}{v}\right)^2 + a_{3g}\left(\frac{h}{v}\right)^3 + a_{g4}\left(\frac{h}{v}\right)^4 + \dots, \tag{1.57}$$

$$V(h) = v^4\left[b_1\left(\frac{h}{v}\right)^3 + b_2\left(\frac{h}{v}\right)^4 + \dots\right], \tag{1.58}$$

$$\mathcal{F}_U(h) = 1 + a_1\frac{h}{v} + a_2\left(\frac{h}{v}\right)^2 + a_3\left(\frac{h}{v}\right)^3 + a_4\left(\frac{h}{v}\right)^4 + \dots, \tag{1.59}$$

$$\mathcal{G}(h) = 1 + c_1\frac{h}{v} + c_2\left(\frac{h}{v}\right)^2 + c_3\left(\frac{h}{v}\right)^3 + c_4\left(\frac{h}{v}\right)^4 + \dots. \tag{1.60}$$

This framework is particularly useful in the analysis of processes involving multiple Higgs bosons as it offers an immediate parametrization for interactions involving several $h$ (see for instance [29]).

The expansion in $\frac{h}{v}$ suggests that HEFT has a cutoff scale strictly related to the Higgs v.e.v. Given also that the $h$ and the Goldstone bosons do not come together in the same multiplet the Higgs boson no longer unitarises longitudinal gauge boson scattering. In fact one finds that for energies greater than $4\pi v$ HEFT ceases to be valid.

Let us consider the amplitude $\mathcal{M}(WW \to hh)$ that is a relevant subprocess for the vector boson fusion (VBF) production channel. In the limit of $s \gg m_W^2, m^2$ where $m_W$ is the vector boson mass while $m$ is the Higgs mass, the polarization vector has a dominant longitudinal part growing with the energy. This allows to express the scattering amplitude as:

$$\mathcal{M}_{HEFT}(WW \to hh) \sim \frac{s}{m_W^2}(a_2 - 2a_1). \tag{1.61}$$

In the SM we have a precise relation $a_2 = 2a_1$ such that this amplitude does not grow with energy and perturbative unitarity is preserved. This happens due to the Higgs doublet structure. Indeed, the the $SU(2)_L$ symmetry protects the process from divergence, namely the Standard Model Higgs boson "unitarizes" the scattering amplitudes.

However in HEFT the relation between $a_1$ and $a_2$ is not fixed, leading to a growth of the scattering amplitude with energy which will lead to a violation of perturbative unitarity when $\sqrt{s}_{\text{max}} \sim 4\pi v \sim$ 3 TeV.

This statement might make it seem that the validity range of HEFT does not cover LHC energies, however we recall that the energy usually involved in the partonic center of mass at colliders is smaller than 3 TeV, therefore HEFT is a valuable tool to describe low energy effects of NP scenarios at the

LHC.

Similar to SMEFT we need to organize the terms in HEFT by establishing a power counting (PC) rule. Since HEFT is a mixture of SMEFT and chiral perturbation theory ($\chi$-PT) the PC rule becomes more complicated as in SMEFT. Here we adopt the convention used in [30] where terms are organized in loop counting $d_\chi = 2L + 2$ where $L$ is the loop number. In the following we will mainly deal with $d_\chi = 2$ terms (especially for singlet model) but we also treat $d_\chi = 4$ later in the project.

It is worth to recall that due to the Higgs boson being a gauge singlet the coefficients $a, b, c$ are uncorrelated, while in the SM limit they are taken to be for instance $b_1 = b_2$ (more on this point later).

Because of this property, the HEFT parametrization is usually considered to describe large deviations from the SM. HEFT provides a more general framework where SMEFT and SM are contained as particular limit in its parameter space. This framework is still invariant under the gauge group $SU(3)_C \times U(1)_{e.m.}$ while the pure scalar sector has an additional invariance under the chiral group $SU(2)_L \times SU(2)_R$.

While the Higgs boson is a singlet both under chiral transformation and under EW gauge symmetry, the $\pi^a$ Goldstone boson transforms non-linearly under EW chiral transformation. This indeed is a consequence of the specific SSB pattern and can be formalized by the CCWZ formalism [16, 17].

## 1.5 SMEFT vs HEFT

One can now ask when one should use HEFT instead of SMEFT. This has been discussed in various approaches in the literature. For instance in [31] it was found that HEFT is required when non analytic terms in the electroweak doublet $H$ appear in the expressions. Instead in [9] a geometric approach was adopted. Defining some geometric invariant quantities in the scalar field space that are not affected by field redefinition problem, these quantities tend to diverge when HEFT is the right low energy theory to use [9]. According to the latter the scalar fields (here $\pi^i$ and $h$) are treated as coordinates over a Riemannian manifold $\mathcal{M}$. As we know, change of coordinates should not change the physics. The latter statement naturally implies that in the field space we can build geometric like quantities that are invariant under the Lagrangian basis that is used.

In general terms, a kinetic term with a field dependent metric is written as:

$$\mathcal{L} = \frac{1}{2} g_{i,j}(\Phi) \partial_\mu \Phi^i \partial^\mu \Phi^j \,, \tag{1.62}$$

where $i, j$ are indices running over components of the scalar fields that are multiplets in general. With the metric in this field space defined we are able to obtain the Christoffel symbols and Riemann curvature tensor. In practice we discern whether a model can be parametrized by SMEFT or HEFT only computing some geometrical quantities such as Ricci scalar curvature of $\mathcal{M}$ and see whether it is finite or infinite at the putative $O(4)$ invariant point where electroweak symmetry is restored. Topological consideration will make the differences between SMEFT, HEFT and SM clear:

- The SM has a flat scalar manifold with an $O(4)$ fixed point in it. In this point the custodial symmetry group $SU(2)_L \times SU(2)_R$ is restored. When $\langle H^\dagger H \rangle = v^2/2$ only a subgroup $SU(2)_{L+R}$ is unbroken. It is possible to perform a local linear transformation of $\mathcal{M}$ coordinates, which results in the SM assumption of $H$ as a linear multiplet (doublet).

- SMEFT has a curved scalar manifold. This is due to the additional derivative Higgs operators $C_{H\Box}, C_{HD}$.

  SMEFT has an $O(4)$ fixed point, since the $H$ multiplet transforms in a linear way. The curvature is crucial in SMEFT and cannot be completely removed by a gauge invariant field redefintion, i.e. it has some physical effects. In the geometric formulation of the SMEFT, the SM limit is recovered for:
  $$g_{i,j}^{SMEFT} \xrightarrow{\Lambda \to \infty} \delta_{i,j} = g_{i,j}^{SM}$$

- HEFT has a curved scalar manifold and in general does not contain an $O(4)$ fixed point. Only when the HEFT manifold contains an $O(4)$ invariant point a mapping to SMEFT is possible and the linear transformation under the EW group is restored.

For a detailed treatment on the geometry of the field space see [24, 32] based on the two-derivative terms. These arguments can be generalised to higher-derivatives making use of jet bundles [33].

The path we are going to take here in order to highlight possible differences between these EFTs is a more phenomenological one. We want to see how correlations among couplings arising in SMEFT do not hold anymore in HEFT. These relations are induced by the assumption of having $H$ as a doublet, which is not assumed in the HEFT context. This point may be clearly seen when we focus on the couplings of the Higgs boson to SM particles. Let us consider for instance the coupling between gluons and Higgs doublet $H$ in both SMEFT and HEFT:

$$\mathcal{L}_{SMEFT} \supset \frac{C_{HG}}{\Lambda^2} G_{\mu\nu}^A G^{A\mu\nu} H^\dagger H \xrightarrow{SSB} \frac{C_{HG}}{2\Lambda^2}(v^2 + 2hv + h^2)G_{\mu\nu}^A G^{A\mu\nu}, \qquad (1.63)$$

$$\mathcal{L}_{HEFT} \supset -\frac{1}{4}G_{\mu\nu}^A G^{A\mu\nu} \mathcal{F}_G\left(\frac{h}{v}\right) = -\frac{1}{4}G_{\mu\nu}^A G^{A\mu\nu}\left(1 + a_1\frac{h}{v} + a_2\left(\frac{h}{v}\right)^2\right). \qquad (1.64)$$

$$(1.65)$$

As long as the Higgs boson is part of the doublet we see a correlation among single Higgs boson and double Higgs production. This does not need to hold true in HEFT. There the coefficients of one Higgs boson to gluons and two Higgs bosons to gluons are uncorrelated.

We could then exploit the relation $h = \sqrt{2H^\dagger H} - v$ to reconstruct the doublet, namely:

$$\mathcal{L}_{HEFT} \supset -\frac{1}{4}G_{\mu\nu}^A G^{A\mu\nu}\left[1 + a_1\frac{\sqrt{2H^\dagger H}}{v} - a_1 + a_2\left(\frac{\sqrt{2H^\dagger H} - v}{v}\right)^2\right] =$$

$$= -\frac{1}{4}G_{\mu\nu}^A G^{A\mu\nu}\left[1 + (a_1 - 2a_2)\frac{\sqrt{2H^\dagger H}}{v} + \frac{2H^\dagger H}{v^2}a_2\right]. \qquad (1.66)$$

This shape of $\mathcal{L}_{HEFT}$ introduce the second way to differentiate HEFT from SMEFT cited above, i.e. non-analyticities in $H^\dagger H$ at the Lagrangian level. Crucially this non-analyticity cannot be removed by field redefinition and it's placed in $|H|^2 = 0$ which is the point where EW symmetry is restored. It's interesting to note the way we delete non-analytic terms is by considering $a_1 = 2a_2$ that is precisely the SMEFT relation. In that specific case $\mathcal{L}_{SMEFT} = \mathcal{L}_{HEFT}$, therefore at the lagrangian level the SMEFT case is a particular case of the HEFT one where coefficient are correlated by expression such as the one above.

We note that adding higher terms in the SMEFT expansion also decorrelates $a_1$ and $a_2$. The statement that we hence obtain by performing such an analysis is a statement on the convergence of the HEFT/SMEFT series rather than an answer whether SMEFT can indeed not describe the model.

The presence of such non-analytic terms indicates that low energy physics must be described in terms of HEFT. This was first pointed out in the article by Falkowski and Rattazzi [31].

## 1.6 Loryon particles

A particularly interesting scenario for SMEFT/HEFT comparison deals with particles called Loryons [8]. Loryons are particles that get most of their mass from EWSB, hence all the SM particles are Loryons. New particles are Loryons if their physical mass is at least given by 50% from electroweak symmetry breaking. Suppose to deal with a scalar particle as a NP candidate, its total (field dependent) mass is:

$$m_{NP}^2(H^\dagger H) = m_{\text{ex}}^2 + \lambda_{\Phi h} H^\dagger H \,. \tag{1.67}$$

In (1.67) $m_{\text{ex}}^2$ is the explicit mass which is a free parameter and can be taken arbitrarily high, whereas the other contribution is fixed by Higgs expectation value $\langle H^\dagger H \rangle = 0$ and requiring $\lambda_{\Phi h} < 4\pi$ for validity of perturbation theory limits the mass of the Loryon particles. In this sense Loryons can be considered as non decoupling particles.

Consider for instance a generic scalar field $\Phi$ with quantum numbers $[L, R]$ representing charges under chiral group. Then $\Phi$ transform as $\Phi \to U_L \Phi U_R^\dagger$ where $U_{R/L} \in SU(2)_{L/R}$. The mass terms of such a scalar read:

$$\mathcal{L}_{NP} \supset -\frac{m_{ex}^2}{2\rho}\text{tr}(\Phi^\dagger\Phi) - \frac{\lambda_{\Phi h}}{2\rho}\text{tr}(\Phi^\dagger\Phi)\frac{1}{2}\text{tr}(H^\dagger H) \,, \tag{1.68}$$

where $\rho = 0(1)$ for a complex (real) representation. Here $\lambda_{ex} = 2m_{ex}^2/v^2$ , in this way $m_{ex}^2 = \frac{\lambda_{ex}v^2}{2}$ is independent from the v.e.v. while the second term represents the Higgs portal interaction.

In the broken phase the latter term provides a mass for all the components of $\Phi$ together with interaction terms between $\Phi$ and $h$. A useful quantity for the following is the ratio:

$$f = \frac{\lambda_{\Phi h}}{\lambda_{ex} + \lambda_{\Phi h}} \,, \tag{1.69}$$

which provides an indication of how much mass new particles get their mass from EWSB. As found in [34] when $f > 0.5$ no SMEFT description exists and we are forced to use HEFT to describe the low
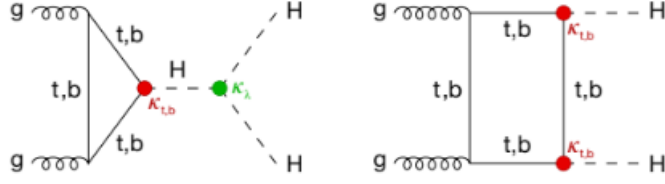
Figure 1.2: Higgs pair production in ggF, the main contribution come from top and bottom quark since the Yuakawa interaction is proportional to the mass of the quark. [3]

energy description of a specific UV model. Even though in this work we'll restrict ourselves to scalar Loryons it is natural to extend the above considerations to the fermionic case. We define a $L \times R$ matrix $\Psi$ transforming as $[L, R]_Y$ under custodial irrepresentation (irreducible representaion). In that case the explicit mass terms would be:

$$\mathcal{L} \supset -M_{ex}\text{tr}\Big(\bar{\Psi}\Psi\Big)y_{12} - \bar{\Psi}_1 H \Psi_2 + h.c.. \tag{1.70}$$

We can define as before a $y_{ex} = \sqrt{2}M_{ex}/v$ as coming from an explicit mass term, while the second term in (1.70) leads to a mass term stemming from EWSB.

In the following we refer to "Loryon limit" or "extreme Loryon" in the case $f \to 1$. Another case, that requires HEFT instead of SMEFT is the presence of new sources of electroweak symmetry breaking that remain in the limit $v \to 0$ [32].

## 1.7 Higgs pair production at LHC

As already stated above, we are interested in finding a concrete UV realisation that needs to be described by HEFT rather than SMEFT and that shows phenomenological difference that can be measured at the LHC. For this reason a discussion of the major Higgs pair production channel at colliders is in order here. For an hadronic collider such as LHC with (hadronic) centre of mass energy $\sqrt{S} = 13$TeV the largest contribution to Higgs pair production comes from gluon gluon fusion (ggF) $\sigma_{\text{ggF}} = 31.7$fb (at next-to-next-to leading order in the strong coupling constant) [4] whose diagrams are shown in fig. 1.2. The second biggest channel is given by vector boson fusion (VBF) with $\sigma_{\text{vbf}} = 1.73$ fb at next-to-next-to-next-to leading order (N$^3$LO) [35] whose relative diagrams are shown in fig.1.3. In the following we focus on the EW sector of the SM that can be tested through the VBF process. VBF is a $2 \to 4$ process where two protons collide giving two jets and two Higgs particles in the final state. The initial state particle that really interacts with $W^{\pm}$ is a quark. At the LHC the diagrams contributing to the process at LO are given in fig.1.3. Despite its cross section being 10 times lower than ggF, VBF has other interesting properties that will be evident in higher luminosity machines:

**high $p_T$ distribution:** $p_T$ measures the momentum of the particles perpendicular to the beam axis, in this case we refer to Higgs bosons $p_T$ distribution meaning the number of events that are detected at a specific $p_T$. While ggF has a maximum for $p_{T,max}^{ggF} \sim 30$ GeV VBF offers higher
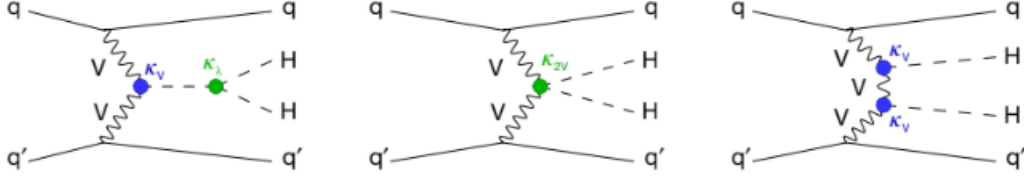
Figure 1.3: From left to right we display the Feynman diagrams according to SM: the $s$ channel, the contact diagram and the $s$ channel, the missing $u$ channel is equivalent to $t$ channel with two Higgs bosons in the final state exchanged.[3]

peak values $p_{T,max}^{VBF} \sim 80$ GeV. High $p_T$ is a distinctive feature of VBF and can be used to separate signal from background.

**Distinctive signature:** Rapidity measure relative velocity of a particles along beams axis, VBF has 2 high-energy jets with a large rapidity gap between them, i.e. they are emitted in opposite directions along beam axis. This feature allows to better isolate events signatures coming from VBF with respect to the background signal. In other words background events can be rejected with higher efficiency and signal to noise ratio is enhanced significantly.

**theory uncertainty:** The VBF process is generically under much better control on what regards the theory uncertainties with respect to the ggF process. Gluon fusion processes have usually very large higher order corrections (for instance they increase the LO cross section by nearly a factor two at NLO [36]). The VBF process instead can be seen as a color singlet exchange between two quarks, namely $\hat{\sigma}$ is $\alpha_S$ independent. More precisely, due to color conservation the NLO QCD corrections affect only the external quark lines, so that there is no color exchange between the two incoming quarks. This does though not hold at higher orders [37]. when we compute cross section at LHC we rely on the parton model theory thinking about quarks and gluons as the proton constituents which we call parton [38]. In a generic cross section computation we make use of the so called "LHC master formula" where the partonic distribution function and partonic cross section are convoluted:

$$\sigma(pp \to X) = \sum_{ab} \int_0^1 dx_1 dx_2 f_a(x_1, \mu_F^2) f_b(x_2, \mu_F^2) \times \hat{\sigma}_{ab \to X}(x_1, x_2, \alpha_S(\mu_R^2), \frac{Q^2}{\mu_F^2}, \frac{Q^2}{\mu_R^2}) \, . \tag{1.71}$$

$f_i(x_i, \mu_F), i = q, g$ are the parton distribution functions (PDFs), these scale dependent object quantify the probability to find a parton with a momentum $p_i = x_i P$ where P is proton momentum, while $\hat{\sigma}$ is the partonic cross section. Strictly speaking the parton distribution function refer to quarks and gluons. By $\mu_F$ and $\mu_R$ we refer to the factorization and the renormalization scales. The former is a crucial quantity in collider physics, it 's an energy scale establishing the border between perturbative and non perturbative regime. The latter is a parameter from renormalization prescription in since quantum field theory parameters usually run with energy scale.

VBF at LO (in QCD) can be seen as a color singlet exchange between two quarks, namely $\hat{\sigma}$ is

$\alpha_S$ independent, leading to more precise theoretical predictions.

More precisely, due to color conservation also QCD NLO correction affects only external gluon, so that there's no color exchange between the two incoming quarks, this does not hold at higher orders [37].

**EWSB nature:**  VBF is particularly sensible to EWSB patterns since it directly involves weak gauge bosons and only contains EW interactions at LO. This means it is a preferred channel if we want to test whether EWSB is linearly (SMEFT) or non linearly (HEFT) realized.

# Chapter 2

# Scalar Singlet

As an exemplatory case to outline the differences between the two EFTs we chose an extension of the SM with a scalar singlet field for which we perform a matching both to the SMEFT and to the HEFT. The reason why we chose the real scalar singlet (RSS) model can be summarized as follows:

- It appears in the list of Loryon particles with large parameter space compared to other candidates.[8]

- It gives a contribution to a specific Wilson Coefficient, namely ($C_{H\Box}$) at tree level. $C_{H\Box}$ generates a deviation to the Higgs couplings to vector bosons and fermions when performing a field redefintion to canconically normalise the Higgs kinetic term. This means the operator generates deviations in the Higgs couplings both relevant for VBF and ggF.

- The simplicity of the model.

Introducing a scalar singlet is a quite popular choice studied in great detail in literature in various context. For instance if the singlet field is stable it is a possible candidate for Dark Matter and it could explain matter-antimatter asymmetry of the Universe [39, 40].

We note though that the addition of a scalar singlet does not fix the hierarchy problem as mass of the Higgs is quadratically sensitive to the new physics scale.

In the first part of the chapter we define the parameters entering the model, after that we perform a phenomenological analysis in order to constrain the parameter space, both theoretical and experimental constraints are taken into account. The UV model introduces a real scalar singlet $\Phi$ with SM gauge group couplings equal to:

| Field | $(C, L)_Y$ | $[L, R]_Y$ |
|-------|------------|------------|
| $\Phi$ | $(1, 1)_0$ | $[1, 1]_0$ |

where in the second column we have charges under SM gauge group while the last column shows the charges under the chiral group. The Lagrangian of the scalar singlet model is given by

$$\mathcal{L}_{UV} = \mathcal{L}_{SM} + (D_\mu H)^\dagger (D^\mu H) + \frac{1}{2}\partial_\mu \Phi \partial^\mu \Phi - \mu_1^2 H^\dagger H$$
$$-\frac{\mu_2^2}{2}\Phi^2 - \lambda_1 (H^\dagger H)^2 - \frac{\lambda_2}{4}\Phi^4 - \frac{\lambda_3}{2}\Phi^2 (H^\dagger H) - A H^\dagger H \Phi - \frac{\mu}{3}\Phi^3 .$$

(2.1)

The model is clearly invariant under the SM gauge group since $\Phi$ is a singlet. Often a $\mathbb{Z}_2$ symmetry for $\Phi$ is introduced. In that case, $A = 0$ and $\mu = 0$. The fields and their vacuum expectation values are defined as follows:

$$H = \frac{v + h}{\sqrt{2}} U(\pi) \begin{pmatrix} 0 \\ 1 \end{pmatrix}, \qquad \Phi = v_s + S, \tag{2.2}$$

$$\langle 0 | H | 0 \rangle = \frac{v}{\sqrt{2}} \begin{pmatrix} 0 \\ 1 \end{pmatrix}, \qquad \langle 0 | \Phi | 0 \rangle = v_s. \tag{2.3}$$

Here the $U$ matrix contains the Goldstone bosons associated to SSB:

$$U(\pi) = e^{i \frac{\pi^a \sigma^a}{v}}, \qquad a = 1, 2, 3. $$

As stated in the first chapter, this formulation naturally leads to a chiral version of the SM lagrangian. Here we are going to write the Lagrangian for our BSM in the broken phase, where similarities with Chiral lagrangian and HEFT basis are clear. As a first step we try to know the spectrum of the theory, and consider minimum of the potential :

$$\left. \frac{\partial V(H, \Phi)}{\partial H} \right|_{\langle H \rangle, \langle \Phi \rangle} = 0, \qquad \left. \frac{\partial V(H, \Phi)}{\partial \Phi} \right|_{\langle H \rangle, \langle \Phi \rangle} = 0. \tag{2.4}$$

$$\tag{2.5}$$

We require a theory free from tadpoles obtaining the following conditions:

$$-A v_s - \frac{\lambda_3 v_s^2}{2} - \mu_1^2 - \lambda_1 v^2 = 0, \tag{2.6}$$

$$-\frac{A v^2}{2} - \frac{1}{2} \lambda_3 v^2 v_s - \mu_2^2 v_s - \lambda_2 v_s^3 - \mu v_s^2 = 0. \tag{2.7}$$

In order to pass to the physical basis we should rotate the mass sector by means of a special orthogonal matrix $R$, such that $R^T R = I$. We have introduced a new parameter $\chi$ which we call mixing angle. Its sine and cosine will link unphysical fields $h$ and $S$ to the physical ones $h_1$ and $h_2$.
The mass matrix in the interaction basis correspond to:

$$M_{int} = \begin{pmatrix} m_{11} & m_{12} \\ m_{21} & m_{22} \end{pmatrix} = \begin{pmatrix} m_{11} & m_{12} \\ m_{12} & m_{22} \end{pmatrix} = R M_D R^T, \tag{2.8}$$

where in the last step we've expressed $M_{int}$ in terms of a diagonal matrix whose elements are exactly the values in the mass basis. More explicitly:

$$M_{int} = \begin{pmatrix} \cos(\chi) & \sin(\chi) \\ -\sin(\chi) & \cos(\chi) \end{pmatrix} \begin{pmatrix} m & 0 \\ 0 & M \end{pmatrix} \begin{pmatrix} \cos(\chi) & -\sin(\chi) \\ \sin(\chi) & \cos(\chi) \end{pmatrix}. \tag{2.9}$$

The relation between physical and unphysical fields reads as follows:

$$\begin{pmatrix} \cos(\chi) & -\sin(\chi) \\ \sin(\chi) & \cos(\chi) \end{pmatrix} \begin{pmatrix} h \\ S \end{pmatrix} = \begin{pmatrix} h_1 \\ h_2 \end{pmatrix}. \tag{2.10}$$

Note that we have just rotate the field variables by quantities proportional to $\chi$, however, the combination $h^2 + S^2 = h_1^2 + h_2^2$ is invariant. Hence we could think of the above transformation as a rotation in the space of field basis.

The Higgs boson $h_1$ appears as a linear combination of $h$ and $S$ rescaled by a proper trigonometric function. The eigenvalues of the mass matrix corresponds to physical masses and are given by:

$$\begin{aligned} m_{1,2}^2 &= \frac{1}{2}\left( m_{11} + m_{22} \mp \sqrt{4m_{12}^2 + (m_{11} - m_{22})^2} \right) \\ &= \frac{1}{2}\left( m_{11} + m_{22} \pm (m_{11} - m_{22})\frac{1}{\cos(2\chi)} \right). \end{aligned} \tag{2.11}$$

Substituting back the expression obtained from tadpole conditions I get the physical masses formulas:

$$m^2 = \tfrac{1}{2}\Big[2\lambda_1 v^2 + \mu_2^2 + \tfrac{1}{2}(\lambda_3 v^2 + 6v_s^2\lambda_2 + 4v_s\mu) - \sqrt{4v^2(\lambda_3 v_s + A)^2 + (2\lambda_1 v^2 - \mu_2^2 - \tfrac{1}{2}(\lambda_3 v^2 + 6v_s^2\lambda_2 + 4v_s\mu))^2}\Big], \tag{2.12}$$

$$M^2 = \tfrac{1}{2}\Big[2\lambda_1 v^2 + \mu_2^2 + \tfrac{1}{2}(\lambda_3 v^2 + 6v_s^2\lambda_2 + 4v_s\mu) + \sqrt{4v^2(\lambda_3 v_s + A)^2 + (2\lambda_1 v^2 - \mu_2^2 - \tfrac{1}{2}(\lambda_3 v^2 + 6v_s^2\lambda_2 + 4v_s\mu))^2}\Big], \tag{2.13}$$

where we have identified $m_1^2 \to m^2 (\mathrm{GeV})^2$ and $m_2^2 \to M^2(\mathrm{GeV})^2$. In the following we assume the former to be the scalar particle observed at LHC with $m = 125$ GeV. We can link the mixing angle to the other parameters:

$$\tan(2\chi) = \frac{2m_{12}}{m_{22} - m_{11}} = \frac{2(\lambda_3 v v_s + Av)}{\mu_2^2 + \frac{1}{2}\left(\lambda_3 v^2 + 6v_s^2\lambda_2 + 4v_s\mu\right) - 2\lambda_1 v^2}. \tag{2.14}$$

Note that it's possible to express the $\lambda$'s couplings in terms of other parameters of the model, using (2.12) and (2.14) we have:

$$\lambda_3 = \frac{(M^2 - m^2)\sin(2\chi) - \sqrt{2}Av}{2vv_s}, \tag{2.15}$$

$$\lambda_1 = \frac{\cos(2\chi)(m^2 - M^2) + m^2 + M^2}{4v^2}, \tag{2.16}$$

$$\lambda_2 = \frac{m^2 + (M^2 - m^2)\cos^2(\chi) - \sqrt{2}\mu v_s}{4v_s^2}. \tag{2.17}$$

In the following we will assume that $m$ is the mass of the light Higgs observed at LHC $m = 125$ GeV, while $M$ will describe the physical mass of heavy d.o.f., in other words our hierarchy of masses is

$m \ll M$.

The UV parameters of the model can be expressed in terms of the masses, the v.e.v.s and the mixing angle as follows:

$$\lambda_1 = \frac{\cos(2\chi)(m^2 - M^2) + m^2 + M^2}{4v^2} \,, \tag{2.18}$$

$$A = \frac{\sin(2\chi)(M^2 - m^2) - 2\lambda_3 v v_s}{2v} \,, \tag{2.19}$$

$$\mu_1^2 = -\frac{1}{4}\left[\left(-2\lambda_3 v_s^2 + m^2 + M^2\right) + \cos(2\chi)(m^2 - M^2) - 2\frac{v_s}{v}\sin(2\chi)(m^2 - M^2)\right] \,, \tag{2.20}$$

$$\mu_2^2 = \frac{1}{2}\left[\left(\lambda_3 v^2 - m^2 - M^2 + 2\lambda_2 v_s^2\right) + \frac{v}{v_s}\sin(2\chi)(m^2 - M^2) + \cos(2\chi)(m^2 - M^2)\right] \,, \tag{2.21}$$

$$\mu = \frac{1}{2v_s}\left[m^2 + M^2 - \lambda_3 v^2 - 4\lambda_2 v_s^2 - \frac{1}{4}\frac{v}{v_s}\sin(2\chi)(m^2 - M^2) - \cos(2\chi)(m^2 - M^2)\right] \,. \tag{2.22}$$

The choice of the input parameters is quite arbitrary and other choices are possible. A comment is in order. The scalar singlet with an explicit breaking of a $Z_2$ symmetry can be also written elsewise. As shown in [41–43] if one adds a tadpole term to the Lagrangian the singlet v.e.v. can be absorbed, leading to a dramatic simplification in the expressions of the Wilson coefficients for the effective field theory analysis. Instead of the v.e.v one than has as input parameter one of the potential parameters, i.e. for instance $\mu$.

We can rewrite (2.1) in the broken phase once the mass sector has been rotated:

$$\begin{aligned}
\mathcal{L}_{UV} = & -\frac{1}{4}G_{\mu\nu}^a G^{a\mu\nu} - \frac{1}{4}W_{\mu\nu}^I W^{I\mu\nu} - \frac{1}{4}B_{\mu\nu}B^{\mu\nu} - V(h,S) + \frac{v^2}{4}\text{Tr}\left[(D_\mu U)^\dagger D^\mu U\right] \\
& \left[1 + 2\cos(\chi)\frac{h_1}{v} + 2\sin(\chi)\frac{h_2}{v} + \cos(\chi)^2\left(\frac{h_1}{v}\right)^2 + \sin(\chi)^2\left(\frac{h_2}{v}\right)^2 + 2\cos(\chi)\sin(\chi)\frac{h_1 h_2}{v^2}\right] \\
& + \frac{1}{2}(\partial_\mu h_1)(\partial^\mu h_1) + \frac{1}{2}(\partial_\mu h_2)(\partial^\mu h_2) + i\sum_{j=l,q,e,\nu,d,u}\bar{\Psi}_j \slashed{D}\Psi_j \\
& -\frac{v}{\sqrt{2}}\left(Y_Q\bar{q}_L U q_R + Y_l \bar{l}_L U l_R + \text{h.c.}\right)\left[1 + \cos(\chi)\frac{h_1}{v} + \sin(\chi)\frac{h_2}{v}\right] \,, \tag{2.23}
\end{aligned}$$

where $Y_Q = \text{diag}(Y_u, Y_d)$, $Y_l = \text{diag}(0, Y_e)$ and the right handed doublets for single generation are given by:

$$q_R = \begin{bmatrix} u_R \\ d_R \end{bmatrix} \,, \quad l_R = \begin{bmatrix} 0 \\ e_R \end{bmatrix} \,. \tag{2.24}$$

Note that while in the unbroken phase the singlet field $\Phi$ couples only to the Higgs doublet $H$, this is no longer true for $h_2$ as it couples to $W^\pm$, $Z$ gauge bosons as well as to fermions. This happens only through mixing between $H$ and $\Phi$. In agreement with the last statement we note that the typical interaction strength of $S$ with SM particles is proportional to $\sin(\chi)$ while $h$ Higgs boson couples with a $\cos(\chi)$. The SM limit is recovered for $\sin(\chi) \xrightarrow{\text{SM}} 0$ and $\cos(\chi) \xrightarrow{\text{SM}} 1$. An additional note is that terms proportional to $A$ and $\mu$ only enters in the scalar potential therefore the complementary part of broken phase lagrangian is the same irrespectively of $A, \mu$ .

The scalar potential contains all non derivative interactions between the two scalar fields and has the following form:

$$V(h, S) = \frac{m^2}{2}h_1^2 + \frac{M^2}{2}h_2^2 + d_1 h_1^3 + d_2 h_1^2 h_2 + d_3 h_1 h_2^2 + d_4 h_2^3 + z_1 h_1^4$$
$$+ z_2 h_1^3 h_2 + z_3 h_1^2 h_2^2 + z_4 h_1 h_2^3 + z_5 h_2^4 \,. \tag{2.25}$$

The explicit expressions for the coefficients are collected where the shorthand notation $c = \cos(\chi)$ and $s = \sin(\chi)$ was adopted:

$$d_1 = \frac{Ac^2 s}{2} + c^3 \lambda_1 v - \frac{1}{2}c^2 \lambda_3 s v_s + \frac{1}{2}c\lambda_3 s^2 v - \frac{\mu s^3}{3} + \lambda_2 s^3 v_s \,, \tag{2.26}$$

$$d_2 = \frac{Ac^3}{2} - Acs^2 + \frac{1}{2}c^3 \lambda_3 v_s - 3c^2 \lambda_1 sv + c^2 \lambda_3 sv + c\mu s^2 + 3c\lambda_2 s^2 v_s - c\lambda_3 s^2 v_s - \frac{1}{2}\lambda_3 s^3 v \,, \tag{2.27}$$

$$d_3 = \frac{1}{2}\lambda_3 vc^3 + c^2 s(-\lambda_3 v_s + 3\lambda_2 v_s + \mu - 2A) + cs^2(3v\lambda_1 - \lambda_3 v) + s^3(\lambda_3 v_s + \frac{A}{2}) \,, \tag{2.28}$$

$$d_4 = \frac{Acs^2}{2} + \frac{c^3 \mu}{3} + c^3 \lambda_2 v_s - \frac{1}{2}c^2 \lambda_3 sv + \frac{1}{2}c\lambda_3 s^2 v_s - \lambda_1 s^3 v \,, \tag{2.29}$$

$$z_1 = \frac{1}{4}c^4 \lambda_1 + \frac{1}{4}c^2 s^2 \lambda_3 + \frac{1}{4}\lambda_2 s^4 \,, \tag{2.30}$$

$$z_2 = -c^3 s\lambda_1 + \frac{1}{2}c^3 \lambda_3 s + c\lambda_2 s^3 - \frac{1}{2}c\lambda_3 s^3 \tag{2.31}$$

$$z_3 = \frac{\lambda_3}{4}c^4 + c^2 s^2(-\lambda_3 + \frac{3}{2}\lambda_1 + \frac{3}{2}\lambda_2) + \frac{1}{4}s^4 \lambda_3 \,, \tag{2.32}$$

$$z_4 = c^3 s\lambda_2 - \frac{1}{2}\lambda_3 sc^3 - cs^3 \lambda_1 + \frac{1}{2}s^3 c\lambda_3 \,, \tag{2.33}$$

$$z_5 = \frac{1}{4}c^4 \lambda_2 + \frac{1}{4}c^2 s^2 \lambda_3 + \frac{1}{4}s^4 \lambda_2 \,. \tag{2.34}$$

# 2.1 Phenomenology

In this section, I will discuss phenomenological and theoretical constrains on the singlet model. This will allow to restrict the parameters of the model. In particular we address the following points :

**Theory:**

- Perturbative Unitarity.

- Vacuum Stability.

- Perturbativity and 1-loop RGE.

**Experiments:**

- EW precision tests (EWPO).

- Higgs signal strength.

Since the scalar singlet is well studied in the literature [44–46] most of the results we need were already
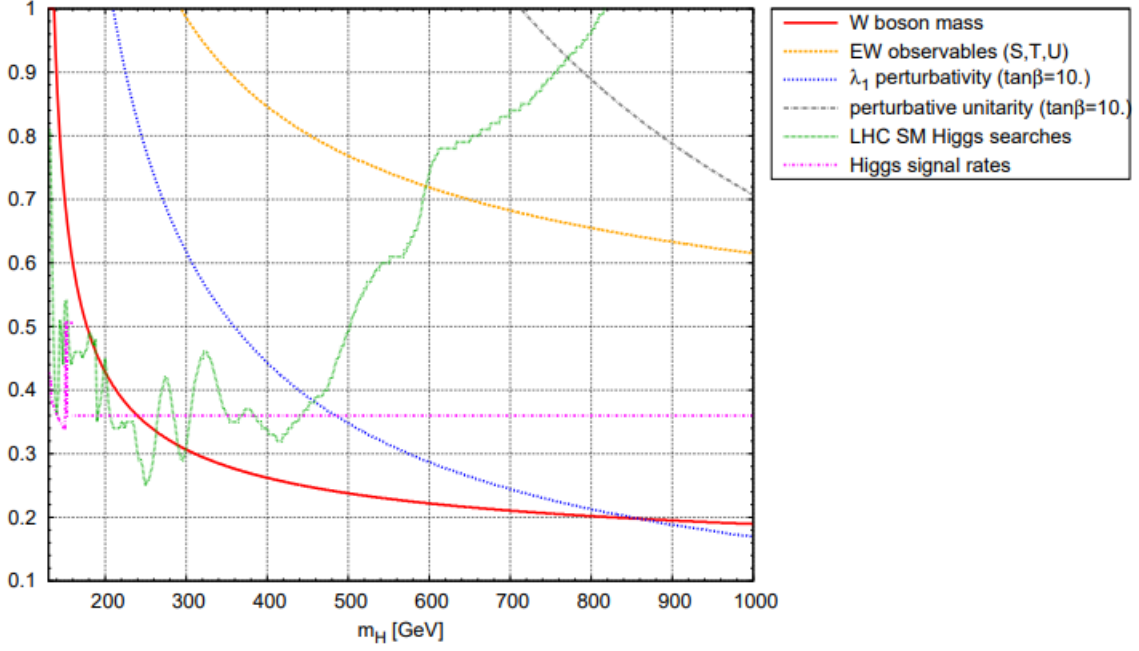
Figure 2.1: Upper bounds on $\sin(\chi)$ with respect to the heavy particle mass, i.e. the eigenvalue in the mass basis. The figure is taken from ref. [45].

presented elsewhere.

For instance, in fig. 2.1 taken from ref. [45] the limits on the sine of the mixing angle from various constrains are collected.

## 2.1.1 Perturbative Unitarity

Perurbative unitarity is a fundamental feature of any field theory we deal with and is used to obtain bounds on the parameters of the model. A relevant historical example is given in [47] where authors could set an upper bound on the Higgs mass before its discovery. They found a condition $m^2 \leq \frac{4\pi\sqrt{2}}{G_F}$ imposing perurbative unitarity on the Winberg-Salam model. Also for HEFT/SMEFT one always employs perturbation theory to obtain unitarity bounds, in that case one usually find a critical energy scale where EFT description breaks down.

In our case we impose perturbatitve unitarity to check whether some combinations of parameters yielding a too large scattering amplitude, if we find those combination we can restrict even more the parameter space of the scalar singlet model, in this sense perturbative unitarity can give information on the allowed parameters.

The fundamental quantity we take into account is the partial wave amplitude for a generic $2 \to 2$ scattering [48]:

$$a_{fi}^{J} = \frac{\beta_f^{1/4}(s, m_{f1}^2, m_{f2}^2)\beta_i^{1/4}(s, m_{i1}^2, m_{i2}^2)}{32\pi s} \int_{-1}^{1} d(\cos(\theta)) d_{\mu_i,\mu_f}^{J}(\theta) \mathcal{T}_{fi}(\sqrt{s}, \cos(\theta)), \qquad (2.35)$$

where $\beta_{i/f}$ are some kinematical factor depending on the mass of the particle in the initial or in the final state and $\mathcal{T}_{fi}$ is the scattering matrix element. We especially look at 0-th order partial wave with total spin equal 0 in the initial and in the final state for a $2 \rightarrow 2$ scattering. In this case the Wigner matrix $d^J(\theta)$ reduces to $P^J(\cos(\theta))$. Unitarity constraint leads to the well know formula:

$$\left| \operatorname{Re}(a^0(s)) \right| \le \frac{1}{2} \quad , \qquad \operatorname{Im}(a^0(s)) \le 1 \,. \tag{2.36}$$

In this case we focus on all possible $2 \rightarrow 2$ processes involving $h_1, h_2$ and later impose the above constraints on every eigenvalue of the zero partial wave matrix.

$$a^0_{fi} = \begin{pmatrix} a^0_{h_1h_1 \rightarrow h_1h_1} & a^0_{h_2h_2 \rightarrow h_1h_1} & a^0_{h_1h_2 \rightarrow h_1h_1} \\ a^0_{h_1h_1 \rightarrow h_2h_2} & a^0_{h_2h_2 \rightarrow h_2h_2} & a^0_{h_1h_2 \rightarrow h_2h_2} \\ a^0_{h_1h_1 \rightarrow h_1h_2} & a^0_{h_2h_2 \rightarrow h_1h_2} & a^0_{h_1h_2 \rightarrow h_1h_2} \end{pmatrix} \,. \tag{2.37}$$

We start by writing down some of the amplitudes relative to different $2 \rightarrow 2$ scattering channels:

$$\mathcal{M}_{h_1h_1h_1h_1}(s, \theta) = -d_1^2 \left[ \frac{1}{t(s, m, \cos(\theta)) - m^2} + \frac{1}{u(s, m, \cos(\theta)) - m^2} + \frac{1}{s - m^2} \right]$$
$$- d_2^2 \left[ \frac{1}{t(s, m, \cos(\theta)) - M^2} + \frac{1}{u(s, m, \cos(\theta)) - M^2} + \frac{1}{s - M^2} \right] - z_1 \,, \quad \text{(2.38)}$$

$$\mathcal{M}_{h_2h_2h_2h_2}(s, \theta) = -d_3^2 \left[ \frac{1}{t(s, M, \cos(\theta)) - m^2} + \frac{1}{u(s, M, \cos(\theta)) - m^2} + \frac{1}{s - m^2} \right]$$
$$- d_4^2 \left[ \frac{1}{t(s, M, \cos(\theta)) - M^2} + \frac{1}{u(s, M, \cos(\theta)) - M^2} + \frac{1}{s - M^2} \right] - z_5 \,, \quad \text{(2.39)}$$

$$\mathcal{M}_{h_1h_2h_1h_2}(s, \theta) = -d_3d_1 \left[ \frac{1}{t(s, m, M, \cos(\theta)) - m^2} + \frac{1}{u(s, m, M, \cos(\theta)) - m^2} \right]$$
$$- \frac{d_2^2}{s - m^2} - \frac{d_3^2}{s - M^2} - z_3 \,. \tag{2.40}$$

We note that for a tree level evaluation we only obtain real amplitudes. In very general terms we expect that contact interactions dominate for high energies while relevant operators such as $d_i$ become important at low energy. In the vicinity of the poles scattering amplitudes diverge as an indication that higher order corrections are needed. Since we are neglecting the width effects in this tree level analysis we should not trust the results in the vicinity of the poles and we apply a kinematic cut to avoid those divergences (following [49]). In particular we neglect regions where:

$$\left| 1 - \frac{s}{m^2} \right| > 0.25 \tag{2.41}$$

The remaining $t$ and $u$ channel amplitudes may lead to divergences as well, again depending only on $s$ since we integrate over the scattering angle. In particular logarithmic expression that can diverge under certain limits appear [49]. The above kinematic cut is sufficient to avoid those divergences from $t$ and $u$ channel under the assumption $m < M$.

## 2.1.2 Vacuum Stability

We demand that the scalar potential $V(H, \Phi)$ is bounded from below, i.e. it has at least one stable minimum at $V(v, v_s)$ such that:

$$V(v, v_s) \leq V(H, \Phi) \,.$$

We report the expression for $V$:

$$V(H, \Phi) = = V_H(H, \Phi) + V_\phi(H, \phi) + V_{H,\phi}(H, \phi)$$
$$V_H(H, \Phi) = \mu_1^2 H^\dagger H + \lambda_1 (H^\dagger H)^2 \,,$$
$$V_\Phi(H, \Phi) = \frac{1}{2}\mu_2^2 \Phi^2 + \frac{\mu}{3}\Phi^3 + \frac{\lambda_2}{4}\Phi^4 \,,$$
$$V_{H,\Phi}(H, \Phi) = A H^\dagger H \Phi + \frac{\lambda_3}{2}(H^\dagger H)\Phi^2 \,. \tag{2.42}$$

A stable minimum requires $V_H$ and $V_\Phi$ to be bounded from below that is equivalent to $\lambda_1 > 0$ and $\lambda_2 > 0$ ensuring no instabilities along the $\Phi = 0$ and $H = 0$ directions.

Additional conditions have to be derived to ensure no instabilities in $V(H, \Phi)$ as well. We have already encountered the condition of stability for low field values, namely we identify the mass matrix with the hessian of the scalar potential for small oscillation around $V(v, v_s)$.

Substituting eq. (2.7) to $\mu_2^2$ we get the following mass matrix:

$$M = \begin{pmatrix} m_{11} & m_{12} \\ m_{12} & m_{22} \end{pmatrix} = \begin{pmatrix} 2\lambda_1 v^2 & \lambda_3 v v_s + A v \\ \lambda_3 v v_s + A v & 2\lambda_2 v_s^2 + \mu v_s - \frac{v^2 A}{2 v_s} \end{pmatrix} \,. \tag{2.43}$$

We have a stability condition valid at the electroweak scale when the fields are placed in their vacuum $\langle \Phi \rangle = \frac{v_s}{\sqrt{2}}$ and $\langle H \rangle = \frac{v}{\sqrt{2}}$. In other words we check $V(v, v_s)$ is indeed a minimum if the mass matrix is positive definite[41]:

$$\det M \Big|_{\langle \Phi \rangle, \langle H \rangle} > 0$$
$$\left(2\lambda_1 v^2\right)\left(2\lambda_2 v_s^2 + \mu v_s - \frac{v^2 A}{2 v_s}\right) > \left(\lambda_3 v^2 v_s^2 + 2A^2 v^2 + 2\sqrt{2}A v^2 v_s\right) \,. \tag{2.44}$$

Note that in the $\mathcal{Z}_2$ symmetric limit this reduces to $4\lambda_1\lambda_2 > \lambda_3^2$ [50]. At this stage we cannot say whether $V(v, v_s)$ is a global minimum or just a local one. Thus we need to check the behaviour of $V(H, \Phi)$ also for large field values to avoid any unboundedness from below.

For large fields, it is enough to consider terms quartic in the scalar fields as they dominate over quadratic or triple power of fields:

$$V_4(\Phi, H) = \left(\sqrt{\lambda_1} H^\dagger H\right)^2 + \left(\frac{\sqrt{\lambda_2}}{2}\Phi^2\right)^2 + \frac{\lambda_3}{2}\Phi^2 H^\dagger H \,. \tag{2.45}$$

We also recall canonically relevant couplings, i.e. associated to relevant operators, usually vanish under RG flow, so we can safely neglect $A$ and $\mu$.

In the end the scalar potential is reduced to:

$$V_4(H, \Phi) = \left( \sqrt{\lambda_1} H^\dagger H - \frac{\sqrt{\lambda_2}}{2} \Phi^2 \right)^2 + \left( \frac{\lambda_3}{2} + \sqrt{\lambda_1 \lambda_2} \right) H^\dagger H \Phi^2 \,. \tag{2.46}$$

We see two different scenarios, in the first case $\lambda_3 > 0$ we have that both terms are positive and for any large field value I only need to impose :

$$\lambda_1(\Lambda) > 0, \qquad \lambda_2(\Lambda) > 0,$$

where $\Lambda$ is some arbitrary energy scale.

In the case that $\lambda_3$ has negative values the first term remains positive while the second one may lead to instabilities for large field values.

The potential is bounded from below in any direction only when an additional constraint is added:

$$4\lambda_1 \lambda_2 - \lambda_3^2 > 0 \,. \tag{2.47}$$

This must be satisfied at all energy scales and is a relevant constraint especially in the evaluation of the 1-loop RGE.

The sign of $\lambda_3$ is a crucial information for the stability of scalar potential and it's worth considering how couplings evolve with the energy scale through 1-loop RGE running.

### 2.1.3 Coupling perturbativity and 1-loop RGE

We study the running of the couplings of the UV model with a twofold objective: 1.) to check if the conditions for stability of $V(H, \Phi)$ is safe up to Planck scale $\Lambda_{\text{Planck}} \sim 10^{19}$ GeV and 2.) to verify that the couplings do not exceed $4\pi$ value even at high scale values to remain within the applicability of perturbation theory up to $\Lambda_{\text{Planck}}$.

In order to see how couplings evolve with energy we should consider the RG flow including one loop corrections of the most relevant couplings of the model.

We impose the following condition on the couplings:

$$|\lambda_i(\Lambda)| < 4\pi \,, \qquad i = 1, 2, 3, \qquad \Lambda < \Lambda_{\text{Planck}} \,. \tag{2.48}$$

In the Appendix A we show in A.1 the results of a numerical analysis for the RGE evolution with a specific choice of the initial values for the parameters of the model showing accordance with fig. 2.1. From the SM it is well known that $\lambda_1$ turns to negative values for energies around $\Lambda \sim 10^8$ GeV making the EW vacuum metastable [51, 52]. This issue can be indeed solved in the scalar singlet model: consider the $\mathbb{Z}_2$ symmetric model with $v_s \gg v$ then from eq. (2.12) we get $m^2 \simeq 2\lambda_1 v^2 \left( 1 - \frac{\lambda_3^2}{4\lambda_2 \lambda_1} \right)$, i.e. $\lambda_1$ receives a shift at the EW scale due to its interaction with the singlet.

For the sake of completeness we collect the one loop equations considered in the numerical analysis [50]:

$$\lambda'_1(t) = \frac{1}{16\pi^2}\left[\frac{1}{2}\left(24\lambda_1(t)^2 - 6y_t(t)^2 + \frac{3}{8}\left(2g_2(t)^4 + (g_2(t)^2 + g_1(t)^2)^2\right)\right.\right. \tag{2.49}$$

$$\left.\left. + (-9g_2(t)^2 - 3g_1(t)^2 + 12y_t(t)^2)\lambda_1(t) + \frac{1}{2}\lambda_3(t)^2\right)\right], \tag{2.50}$$

$$\lambda'_3(t) = \frac{1}{16\pi^2}\left[4\lambda_3(t)^2 + 12\lambda_1(t)\lambda_3(t) - \frac{3}{2}(3g_2(t)^2 + g_1(t)^2)\lambda_3(t)\right. \tag{2.51}$$

$$\left. + 6y_t(t)^2\lambda_3(t) + 6\lambda_2(t)\lambda_3(t)\right], \tag{2.52}$$

$$\lambda'_2(t) = \frac{1}{16\pi^2}\left[2\lambda_3(t)^2 + 18\lambda_2(t)^2\right], \tag{2.53}$$

$$g'_1(t) = \frac{1}{16\pi^2}(-b_{01})g_1(t)^3, \tag{2.54}$$

$$g'_3(t) = \frac{1}{16\pi^2}(-b_{03})g_3(t)^3, \tag{2.55}$$

$$g'_2(t) = \frac{1}{16\pi^2}(-b_{02})g_2(t)^3, \tag{2.56}$$

$$y'_t(t) = \frac{1}{16\pi^2}y_t(t)\left[\frac{9}{2}y_t(t)^2 - \frac{9}{4}g_2(t)^2 - \frac{17}{12}g_1(t)^2 - 8g_3(t)^2\right], \tag{2.57}$$

$$\lambda_1(0) = \lambda_{1,0}, \quad \lambda_3(0) = \lambda_{3,0}, \quad \lambda_2(0) = \lambda_{2,0}, \tag{2.58}$$

$$g_1(0) = g_{1,0}, \quad g_3(0) = g_{3,0}, \quad g_2(0) = g_{2,0}, \quad y_t(0) = y_{t0}, \tag{2.59}$$

$$b_{01} = -\frac{41}{6}, \quad b_{02} = \frac{19}{6}, \quad b_{03} = 7. \tag{2.60}$$

$$\tag{2.61}$$

A few remarks are in order before proceeding :

- by $\lambda'$ we mean $\lambda' = \frac{d\lambda(t)}{dt}$ where t is a combination of parameters including scale of RG evolution $t = log\left(\frac{\mu_{run}^2}{v^2}\right)$. Note that by $t = 0$ we mean EW scale while the Planck scale leads to $t \sim 20$.

- $\lambda'_h$ receives an additional contribution with respect to its SM RG, this term is crucial in the stabilization of EW vacuum. In the scalar singlet extension EW vacuum turns from a metastable (as in SM) to a fully stable minimum. In this scenario we say that the EW vacuum is stabilized.

- even though the gauge couplings $g_2, g_1$ do not vary much over the different energy scales (this doesn't hold for $g_3$) we consider their contribution. This means we have a system of 7 coupled differential equations that will be solved numerically by means of `Mathematica 13.3`.

- We have not included the running of the $A$ and $\mu$ parameters of the UV model. Being super-renormalizable operators they are significant at low energies and become less important at higher $t$.

Performing a numerical evaluation in fig. 2.2a and 2.2b for the SM and the scalar singlet model respectively we can infer that the EW vacuum becomes stabilized in the scalar singlet model.
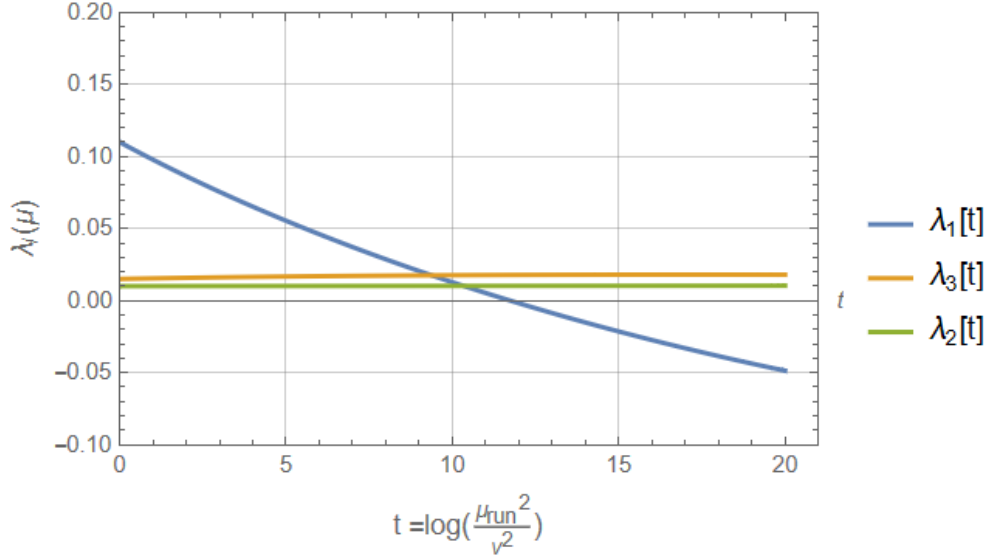
(a) SM case where $\lambda_1(t = 0) = 0.13$ and $V(h)$ changes sign at $\mu \sim 10^{10}$ GeV, this means we could enter an unstable phase at sufficiently high energies.
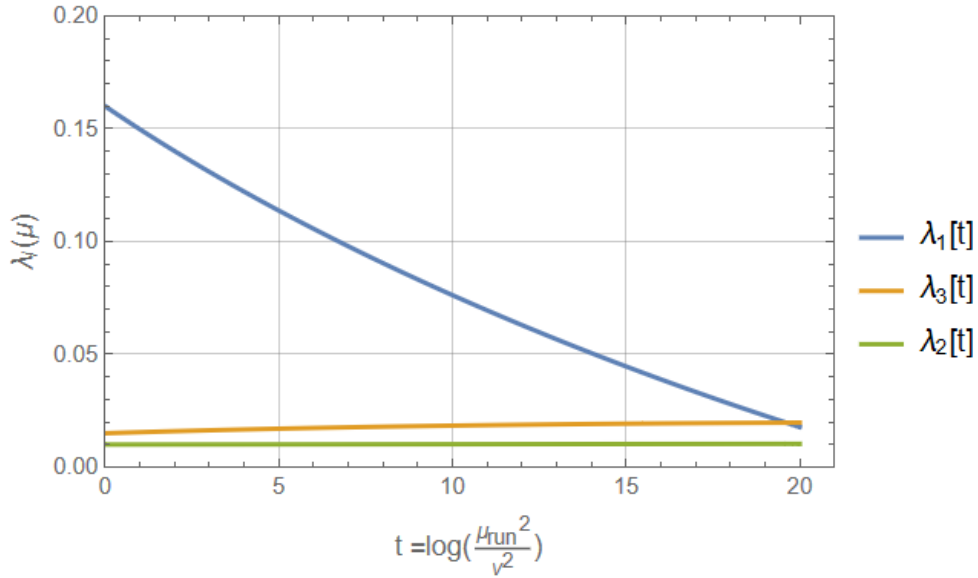


(b) If we consider that the scalar singlet shifts $\lambda_1$ at the EW scale we can end up with $\lambda_1(t = 0) = 0.16$, in this way the quartic coupling stays positive up to the Planck scale.

Figure 2.2: Evolution of $\lambda_i$ ($i = 1, 2, 3$) from the EW to the Planck scale. The labels are difficult to read.

Fine tuning the ratio $\frac{\lambda_3^2}{4\lambda_2}$ can let $\lambda_1$ stay positive up to Planck scale. Note that singlet quartic coupling $\lambda_2$ and the mixed coupling $\lambda_3$ also remain positive if they are set to positive values at low energy scales.

### 2.1.4 EWPO

Further constrains on the UV model come from the computation of different quantities connected with the EW sector. As far as EW observables are concerned it is well known that the most relevant contribution beyond tree level come from oblique corrections that are flavour independent. In general we write a scattering amplitude involving an exchange of gauge bosons as $\mathcal{M} \sim J_\mu \Pi^{\mu,\nu} J_\nu$ where the $J$'s denote a fermionic weak current.

The most general vacuum polarization rank-2 tensor respecting Lorentz invariance is written as:

$$\Pi^{\mu\nu}(p^2) = \Pi(p^2)\eta^{\mu\nu} + \Delta(p^2)p^\mu p^\nu, \tag{2.62}$$

however the second term is usually neglected as we usually contract it with massless fermionic currents $\mathcal{J}^\mu = \bar{q}\gamma^\mu q$.

For this reason in the following we will consider corrections to EW vacuum polarization in the form $\Pi^{\mu,\nu} = \Pi\eta^{\mu\nu}$. Computing the vacuum polarisations the strongest bound on the mixing angle is provided by $W$ mass measurement [53].[1]

Instead we use Peskin-Takeuchi parameters [56] to set a limit on the mixing angle. They provide a shortcut to test our NP model through evaluation of the three different quantities:

$$T \equiv \frac{1}{\alpha}\left(\frac{\Pi_{\text{new}}^{WW}(0)}{M_W^2} - \frac{\Pi_{\text{new}}^{ZZ}(0)}{M_Z^2}\right),$$

$$S \equiv 4c^2 s^2 \alpha \left(\frac{\Pi_{\text{new}}^{ZZ}(M_Z^2) - \Pi_{\text{new}}^{ZZ}(M_Z^2)}{M_Z^2} - c^2 - s^2 cs\frac{\Pi_{\text{new}}^{Z\gamma}(M_Z^2)}{M_Z^2} - \frac{\Pi_{\text{new}}^{\gamma\gamma}(M_Z^2)}{M_Z^2}\right),$$

$$U \equiv 4s^2 \alpha \left(\frac{\Pi_{\text{new}}^{WW}(M_W^2) - \Pi_{\text{new}}^{WW}(M_Z^2)}{M_Z^2} - cs\frac{\Pi_{\text{new}}^{Z\gamma}(M_Z^2)}{M_Z^2} - \frac{\Pi_{\text{new}}^{\gamma\gamma}(M_Z^2)}{M_Z^2}\right) - S,$$

where $\alpha = \alpha(M_Z) = \frac{e(M_Z)^2}{4\pi} \sim \frac{1}{127}$, $c = \cos(\theta_W), s = \sin(\theta_W)$ and $\Pi_{VV}^{\text{new}} = \Pi_{VV}^{\text{tot}} + \Pi_{VV}^{\text{SM}}$ quantifies the contributions from BSM. Note that the electroweak sector considers also the vacuum polarization correction from the photonic field $\Pi^{\gamma\gamma}$ together with the mixed contribution $\Pi^{Z\gamma}$.

The corresponding interval where these quantities vary are:

$$0.02 \leq S \leq 0.04, \qquad -0.07 \leq T \leq 0.17, \qquad -0.07 \leq U \leq 0.13. \tag{2.63}$$

---

[1]Noting though that we will refrain from applying this bound, due to the discrepancies between various measurements of the $W$ boson mass [54, 55].

New physics (NP) extension of the standard model can be tested to respect these bounds, in particular for the scalar singlet model we get a quite accurate bounds on the mixing angle. Contributions from NP come with two basic effects:

- new Feynman diagrams not present in the Standard model.

- rescaling of the Standard model interaction by some factor. In the singlet model, the Higgs boson interactions are usually multiplied by $\cos(\chi)$.

In this case we have two new Feynman diagrams coming from interactions with the new scalar singlet:

$$i\Pi_{WW} = \quad W^- \;\text{〰〰}\; W^- \quad + \quad W^- \;\text{〰〰}\; W^- \quad = i\Pi_{WW}^{(1)} + i\Pi_{WW}^{(2)}. \qquad (2.64)$$

An analogous equation holds also for the $Z$ boson. We can explicitly write the expression for the corrections to the EW vacuum due to scalar singlet interactions exploiting a dimensional regularization scheme shifting the number of dimensions to $d = 4 - \epsilon$.

The first diagram in dimensional regularization reads:

$$i\Pi_{WW}^{(1,\text{UV})\mu\nu} = \sin(\chi)^2 \Big(\frac{2iM_W^2}{v}\Big)^2 \mu^\epsilon \int \frac{d^dk}{(2\pi^d)} \frac{i}{k^2 - M_W^2} \Big(-\eta^{\mu\nu} + \frac{k^\mu k^\nu}{M_W^2}\Big) \frac{i}{(p+k)^2 - M^2} \qquad (2.65)$$

$$= \sin(\chi)^2 \Big(\frac{2iM_W^2}{v}\Big)^2 \mu^\epsilon \int_0^1 dx \int \frac{d^dk}{(2\pi^d)} \frac{i}{((k+px)^2 - C)^2} \Big(-\eta^{\mu\nu} + \frac{k^\mu k^\nu}{M_W^2}\Big) \qquad (2.66)$$

$$= \sin(\chi)^2 \Big(\frac{2iM_W^2}{v}\Big)^2 \mu^\epsilon \int_0^1 dx \int \frac{d^dk}{(2\pi^d)} \frac{i}{(k^2 - C)^2} \eta^{\mu\nu} \Big[-1 + \frac{1}{4M_W^2}(1 + \frac{\epsilon}{4})k^2\Big] \qquad (2.67)$$

$$= \sin(\chi)^2 \Big(\frac{2iM_W^2}{v}\Big)^2 \eta^{\mu\nu} \int_0^1 dx \Big(-I_{0,2} + (1 + \frac{\epsilon}{4})\frac{1}{4M_W^2} I_{1,2}\Big) \qquad (2.68)$$

$$= \sin(\chi)^2 \Big(\frac{2iM_W^2}{v}\Big)^2 \frac{i\eta^{\mu\nu}}{(4\pi)^2} \int_0^1 dx \Big[-\Delta_\epsilon + \log\Big(\frac{\mu^2}{C}\Big) + \frac{C}{2M_W^2}\Big(\Delta_\epsilon + 1 + \log\Big(\frac{\mu^2}{C}\Big)\Big)\Big]. \qquad (2.69)$$

The main steps are as follows: the first line shows the loop integral of the first diagram in (2.64) for which we wrote the loop integral over the virtual momentum and the Feynman rules of the UV model. In the second line Feynman parametrization is adopted assuming $C = -xp^2(1-x) + M_W^2(1-x) + xM^2$ and reducing the integrand to a unique denominator. In the third line we shift $k \to k - px$, note that $p$ is an external momentum. We decompose the tensor structure isolating the scalar integral that can be solved with the master formula [57]:

$$I_{r,m} = \int \frac{d^dk_E}{(2\pi)^d} \frac{(k_E^2)^r}{(k_E^2 - C)^m} = i(-1)^{r-m} \frac{1}{(4\pi)^{\frac{d}{2}} C^{m-r-\frac{d}{2}}} \frac{\Gamma(r + \frac{d}{2})\Gamma(m - r - \frac{d}{2})}{\Gamma(m)\Gamma(\frac{d}{2})}. \qquad (2.70)$$

In the last step we have included all the divergent quantities in $\Delta_\epsilon$. Note that up to this point we have

made no approximation. Formally we apply a renormalization procedure known as modified minimal subtraction scheme ($\overline{\text{MS}}$) where we get rid of divergent quantities up to constant factors. This step introduces a scheme dependence of the final result.

For $\Pi_{WW}^{(2)}$ we can proceed in an analogous way:

$$i\Pi_{WW}^{(2,\text{UV})\mu\nu} = \frac{1}{2}\sin(\chi)^2\Big(\frac{2iM_W^2}{v}\Big)\eta^{\mu\nu}\int\frac{d^dk}{(2\pi)^d}\frac{i}{k^2-M^2}\,, \tag{2.71}$$

$$= \sin(\chi)^2\frac{-M_W^2\eta^{\mu\nu}}{v^2}\int\frac{d^d(p+k)}{(2\pi)^d}\frac{1}{(p+k)^2-M^2}\frac{k^2-M_W^2}{k^2-M_W^2}\,, \tag{2.72}$$

$$= \sin(\chi)^2\frac{-M_W^2\eta^{\mu\nu}}{v^2}\int_0^1 dx\int\frac{d^d(k}{(2\pi)^d)}\frac{k^2+(1-x)^2q^2-M_W^2}{[k^2-C]^2}\,, \tag{2.73}$$

$$= \sin(\chi)\frac{-iM_W^2}{(4\pi)^2v^2)}\eta^{\mu\nu}\int_0^1 dx\Big[\Big(2C+(1-x)^2p^2-M_W^2\Big)\Delta_\epsilon \tag{2.74}$$

$$+ (2C+(1-x)^2q^2-M_W^2)\log\Big(\frac{\mu^2}{C}\Big)+C\Big]\,. \tag{2.75}$$

Our approximation consists in $M^2\gg M_W^2, p^2$ which implies $C\sim xM^2$ and consequently $\log\Big(\frac{\mu^2}{C}\Big)\sim -\log\Big(\frac{M^2}{\mu^2}\Big)$. Fixing then the renormalization scale to $\mu=M_Z$ we get the following expressions for the scalar part of EW vacuum polarization:

$$\Pi_{WW}(p)\simeq\sin(\chi)^2\frac{M_W^2}{(4\pi)^2v^2}\Big[\frac{M^2}{2}+\Big(3M_W^2+\frac{p^2}{3}\Big)\log\Big(\frac{M^2}{M_Z^2}\Big)\Big] \tag{2.76}$$

$$\Pi_{ZZ}(p)\simeq\sin(\chi)^2\frac{M_Z^2}{(4\pi)^2v^2}\Big[\frac{M^2}{2}+\Big(3M_Z^2+\frac{p^2}{3}\Big)\log\Big(\frac{M^2}{M_Z^2}\Big)\Big] \tag{2.77}$$

Beyond these completely new contributions, we have that the SM contributions including the Higgs boson couplings are suppressed by a factor of $\cos^2(\chi)$. It is possible to rewrite the full polarization tensor in a convenient form:

$$\Pi^{tot} = \Pi_{f,W}^{(SM)} + \Pi_h' + \Pi_S', \tag{2.78}$$

where the first term includes corrections from fermions and gauge bosons which remains the same as in the SM. The second term stands for the Higgs boson corrections, while the last terms describes the contribution from the scalar singlet.

The explicit dependence on the mixing angle is written as an overall rescaling of the scalar integrals:

$$\Pi^{tot} = \Pi_{f,W,h}^{(SM)} + (\cos(\chi)^2-1)\Pi_h + \sin(\chi)^2\Pi_S = \Pi_{f,W,h}^{(SM)} + \sin(\chi)^2\left(\Pi_h - \Pi_S\right)\,. \tag{2.79}$$

We note that the scalar tensors are simply related by $\Pi_h = \Pi_S(M^2\to m^2)$. It's possible to explicitly write the expression for $T$ parameter as:

$$T = \sin(\chi)^2\frac{1}{16\pi^2v^2\alpha(M_Z)}\Big[3(M_Z^2-M_W^2)\log\frac{m^2}{M_Z^2}+3(M_W^2-M_Z^2)\log\frac{M^2}{M_Z^2}\Big]\,. \tag{2.80}$$

The upper bound shown in fig. 2.1 is well reproduced by the above expression, we can substitute different values of $M$ obtaining a correspondent upper bound for $\sin(\chi)$.

### 2.1.5 Higgs signal strength

Recent experimental results from CMS collaboration [3] constrain the $a_1 = a = \kappa_V$ coefficient in a range that is about 5 times smaller than range at the discovery. At $2\sigma$ confidence we have:

$$\kappa_V = \cos(\chi)^2 \, . \tag{2.81}$$

As reported in [3] for an $s = 13$ TeV machine with an integrated luminosity $\mathcal{L}$ of $138$ fb$^{-1}$:

$$\kappa_V \in [0.86, 1.18] \, .$$

This means:

$$1 - \sin(\chi)^2 \leq 0.86 \qquad \rightarrow \qquad \sin(\chi) \leq 0.3741 \, . \tag{2.82}$$

Note that this result is completely independent from $M$ and hence corresponds to a line parallel to the $x$ axis in the Fig. 2.1. In the following numerical analysis we are going to adopt the latter condition as the upper bound on the mixing angle.

# Chapter 3

# Matching

Effective Field theories are predictive in a specific and limited energy range. The reasons why EFTs break down may be differ from case to case: either new degrees of freedom enter into the dynamics (as Fermi theory with massive vector bosons $W^{\pm}, Z$ that require the full electroweak theory) or the UV theory becomes strongly coupled (such as the Chiral Lagrangian with respect to UV theory, i.e. QCD ). However, the EFT should reproduce the full UV theory in specific subsets of the parameter space.

In this chapter we match our UV model both to SMEFT and HEFT. SMEFT and HEFT can't be directly compared as they have different power counting and consequently different domains of validity:

- SMEFT is the proper EFT description as long as the dimensionless parameter $\frac{E}{\Lambda}$ remains small, where $E$ is an energy scale of the problem while $\Lambda$ is a reference scale for NP. More precisely we deal with two different expansions in SMEFT: $\frac{v}{\Lambda}$ is the ratio between electroweak scale and new physics scale, and $\frac{p^2}{\Lambda^2}$ where $p^2$ is some kinematic Lorentz invariant. The latter is related to the derivative expansion while the former, in a geometric language is related to the curvature of the scalar manifold [24].

- HEFT has a different power counting, we classify operators in the number of derivative also called chiral counting $d_{\chi} = 2l + 2$ where $l$ is the loop number. Hence HEFT basically counts the loop order[5]. This EFT happens to be valid up to scale $4\pi v$, this limit was briefly derived above from an argument on the unitarity violation. Recalling a similarity with the chiral lagrangian that ceases to be valid at $4\pi f_{\pi}$, where $f_{\pi}$ is the pion decay constant, HEFT has an analogous limit where $f_{\pi}$ is replace by v.

A complete EFT program usually involves runnning of the EFT parameters after matching as we are interesting in using EFT parameters at an energy scale lower than the matching one [1].

Once we get an expression for coefficients of the effective theory in terms of the UV parameters we let parameters evolve through RGE down to the desired scale. In this case we are also able to resum large logarithms that usually arise in QFT.

---

[1]The matching scale is usually identified with the scale of NP .

In this chapter we will restrict ourselves to tree-level accuracy, hence we match at tree-level and do not preform the running of the Wilson coefficients since tree level matching is valid at every scale.

## 3.1  Integrating out

As said EFTs should reproduce the same prediction as the UV model within a specific energy range. We can check whether this is true or not by looking at physical observables. In QFT every observable is computed from the scattering amplitude that in turn are related to the partition function through the Green functions. Formally we impose an equality between generating functionals of the UV model and the EFT one:

$$Z_{\text{UV}}[J] = \int \mathcal{D}H \int \mathcal{D}\Phi \ \ e^{iS_{UV}[H,\Phi]+i\int JH} = Z_{\text{EFT}}[J] = \int \mathcal{D}\phi \ \ e^{iS_{EFT}[\phi]+i\int J\phi} \,. \tag{3.1}$$

This is the usual way we write a path integral coupling an external current $J$ to every field. From the low energy prospective the heavy field is non dynamical so we just solve the E.O.M. for heavy field and find the classical expression of $\Phi$ in terms of $H$. Then we substitute back into the original Lagrangian:

$$\frac{\delta S_{UV}[\Phi,H]}{\delta \Phi}\bigg|_{\Phi^C} = 0 \,, \qquad \frac{\partial \mathcal{L}_{UV}}{\partial \Phi} - \partial_\mu \frac{\partial \mathcal{L}_{UV}}{\partial(\partial_\mu \Phi)} = 0 \,. \tag{3.2}$$

We say that the heavy degree of freedom has been integrated out.

After this replacement the lagrangian assumes a non-local form

$$\int \mathcal{D}\Phi e^{iS_{UV}[H,\Phi_C[H]]} = e^{iS_{NL}[H]} \neq e^{iS_{EFT}[H]} \,. \tag{3.3}$$

To obtain a proper EFT Lagrangian, and being interested in dynamics at $E \ll M$, we could expand the non local interaction arising from the above substitution $H^\dagger H \frac{1}{\Box+M^2}(H^\dagger H)^2$ in series of $\frac{1}{M^2}\big(1 - \frac{\Box}{M^2} + ..\big)$.

Once we get an expression where the only dynamical field is the light one, i.e. $H$ we can compare with low energy model independent theory.

In particular we are going to match correlation functions computed in the UV theory with those computed in the IR (EFT) since these quantities should describe the same physics in the IR limit:

$$Z_{\text{UV}}[J] = Z_{\text{EFT}}[J] \,. \tag{3.4}$$

However note that imposing an equality at the Green's function level may be too stringent since correlators may change under field redefinition while the matching at the level of $\hat{S}$ matrix element (diagrammatic approach) relaxes this point.

Even though the diagrammatic approach is quite intuitive for EFT users, it could become tedious

especially at higher loop analysis where the number of diagrams grows exponentially with the loop order.

The diagrammatic approach is equivalent to the functional matching method. The matching criterion is built on the 1 light particle irreducible effective action (1LPI), where only light degrees of freedom occupy external legs.

In particular we compute it both in the EFT and in the UV theory and equate them at RG scale $\mu = M$:

$$\Gamma_{L,EFT}[\Phi](\mu = M) = \Gamma_{L,UV}[\Phi](\mu = M) \,. \tag{3.5}$$

If we consider Feynman diagrams in terms of their path integral formulation where Green functions are written in terms of functional derivatives of the partition function then the equivalence between functional and diagrammatic method is clear. In particular dealing with scalar fields:

$$\langle \phi(x_1)...\phi(x_n) \rangle = \frac{\int \mathcal{D}\phi e^{iS[\phi]} \phi(x_1)...\phi(x_n)}{\int \mathcal{D}\phi e^{iS[\phi]}} \,, \tag{3.6}$$

and the one particle irreducible (1PI) diagrams are obtained from functional derivatives of $\Gamma$ :

$$\langle \phi(x_1)...\phi(x_n) \rangle_{1PI} = i \frac{\delta^n \Gamma}{\delta\phi(x_1)...\phi(x_n)} \,. \tag{3.7}$$

Since $\langle \phi(x_1)\phi(x_2)\phi(x_3).. \rangle_{1PI}$ is constructed from the full correlator $\langle \phi(x_1)\phi(x_2)\phi(x_3).. \rangle$ the functional method and the diagrammatic one are both valid tools to perform the matching [58]. Since we are going to work with tree level (TL) processes we will mainly adopt the diagrammatic one for the scalar singlet model. If we had to match the theory at higher loop a functional matching would have been more convenient as we briefly mention in the colored scalar model.

## 3.2 Diagrammatic approach

As said in section 1.3 fields redefinitions, Integrations by parts and Fierz Identities connect different bases (operators) giving the same physical result, in other words a diagrammatic approach at the lagrangian level turns out to be field basis dependent. This problem is solved in diagrammatic approach where we directly compare $S$ matrix elements whose modulus squared is related to physical observable such as cross sections and decay rates. Because of the $S$ matrix equivalence theorem [59], the diagrammatic approach does not suffer from ambiguities due to field redefinition.[2]. This method is based on expanding Feynman diagrams in a Dyson series under the assumption of perturbativity.

Formally we impose an equation at the scattering amplitude level, also known as *on-shell matching*:

$$\boxed{\langle f| \, \hat{S}_{\text{UV}} \, |i\rangle \, |_{E \ll \Lambda} = \langle f| \, \hat{S}_{\text{EFT}} \, |i\rangle \, |_{E \ll \Lambda} \,.} \tag{3.8}$$

---

[2]Note that even in the diagramatic approach we have to reduce the lagrangian basis bu integration by parts as well as Fiertz identities

Here $\Lambda$ is a generic cutoff energy scale where the EFT breaks down. It is crucial to keep the condition $E \ll \Lambda$ otherwise the EFT formulation is not valid. Note that matching at 1 loop level requires to match at a fixed RG scale. Most of the times $\mu = M$ is considered and one needs to adopt a regularization and renormalization scheme.

Given our UV model (2.23) the matching to HEFT can be naturally be performed in the broken phase and the kinetic term is directly canonically normalized. Instead the matching in the SMEFT needs to be done in the unbroken phase and special attention to the canonical normalisation of the kinetic terms needs to be paid. Neglecting pre-factors and the delta ensuring momenta conservation in eq. (3.8) we get:

$$\mathcal{M}_{UV} + \mathcal{O}(\frac{1}{M^4}) = \mathcal{M}_{EFT} \,, \tag{3.9}$$

where the amplitude in the UV is truncated following a specific power counting scheme. Adopting an abuse of notation we equate the amplitude to its diagrammatic representation to point out clearly which process we are referring to.

For HEFT and SMEFT the particle content coincides with the SM one. In tab. 3.1 we match some the sub-graphs needed to compute the EFTs for the VBF process and to ggF di-Higgs production processes. While we fix the notation by considering $W^\pm$ as massive gauge bosons, the $Z$ boson case can be obtained by analogy. In the low energy regime the VBF channel reduces to four tree level diagrams:



$$\tag{3.15}$$

While the UV theory presents the same channels as EFT plus a tree level exchange diagram from the heavy new scalar field:



$$\tag{3.16}$$

Feynman rules of the UV model are summarized in Tab.(3.2). The analytic expression of the amplitude in VBF reads:

$$i\mathcal{M}_{UV}^{\lambda\lambda'}(W^+W^- \to h_1 h_1) = \epsilon_\mu^\lambda(p_1)\epsilon_\nu^{\lambda'}(p_2)\Big[\frac{m_W^2 g^{\mu\nu}}{v^2}\cos(\chi)^2 + \frac{2m_W^2 g^{\mu\nu}}{v}\cos(\chi)\frac{i}{s-m^2}(-i3!d_1)+$$

$$\frac{2m_W^2 g^{\mu\nu}}{v}\sin(\chi)\frac{i}{s-M^2}(-id_2) + \frac{2m_W^2 g^{\mu\sigma}}{v}\cos(\chi)\frac{-i}{t-M_W^2}\Big(g_{\sigma\rho} - \frac{(p_1-p_3)_\sigma(p_1-p_3)_\rho}{m_W^2}\Big)\frac{2m_W^2 g^{\rho\nu}}{v}\cos(\chi)+$$

$$+ \frac{2m_W^2 g^{\mu\sigma}}{v}\cos(\chi)\frac{-i}{u-M_W^2}\Big(g_{\sigma\rho} - \frac{(p_1-p_4)_\sigma(p_1-p_4)_\rho}{m_W^2}\Big)\frac{2m_W^2 g^{\rho\nu}}{v}\cos(\chi)\Big]. \qquad (3.17)$$

The first term stems from the contact interaction, the second term is the $s$ channel exhange of the light Higgs bosong, the third term the $s$ channel exchange of the new resonance and finally the $t$ and $u$ channels where the vector boson propagates.

$$i\mathcal{M}_{UV}(t\bar{t} \to h_1) = \quad \bar{t} \quad \overset{\bar{t}}{\diagdown}\!\!-\!\!-\!\!-\ h_1 \quad = -i\frac{Y_t}{\sqrt{2}}\cos(\chi)\bar{v}(p_1)u(p_2)\,, \tag{3.18}$$

$$i\mathcal{M}_{UV}(t\bar{t} \to h_2) = \quad \overset{\bar{t}}{\diagdown}\!\!-\!\!-\!\!-\ h_2 \quad = -i\frac{Y_t}{\sqrt{2}}\sin(\chi)\bar{v}(p_1)u(p_2)\,, \tag{3.19}$$

$$i\mathcal{M}_{UV}^{\lambda,\lambda'}(W^+W^- \to h_1) = \quad \overset{W^-}{\diagdown}\!\!-\!\!-\!\ h_1 \quad = \epsilon_\mu^\lambda(p_1)\epsilon_\nu^{\lambda'}(p_2)2i\frac{m_W^2 g^{\mu\nu}}{v}\cos(\chi)\,, \tag{3.20}$$

$$i\mathcal{M}_{UV}^{\lambda,\lambda'}(W^+W^- \to h_2) = \quad \overset{W^-}{\diagdown}\!\!-\!\!-\!\ h_2 \quad = \epsilon_\mu^\lambda(p_1)\epsilon_\nu^{\lambda'}(p_2)2i\frac{m_W^2 g^{\mu\nu}}{v}\sin(\chi)\,, \tag{3.21}$$

$$i\mathcal{M}_{UV}^{\lambda,\lambda'}(W^+W^- \to h_1 h_1) \supset \quad \overset{W^- \qquad h_1}{\diagdown\!\!\!\diagup} \quad = \epsilon_\mu^\lambda(p_1)\epsilon_\nu^{\lambda'}(p_2)i\frac{m_W^2 g^{\mu\nu}}{v^2}2!\cos(\chi)^2\,, \tag{3.22}$$

$$\mathcal{M}_{UV}(h_1 h_1 \to h_1) = \quad \overset{h_1}{\diagdown}\!\!-\!\!-\!\!-\ h_1 \quad = -i6d_1\,, \tag{3.23}$$

$$\mathcal{M}_{UV}(h_1 h_1 \to h_2) = \quad \overset{h_1}{\diagdown}\!\!-\!\!-\!\!-\ h_2 \quad = -i2d_2\,. \tag{3.24}$$

Table 3.2: relevant vertices in Di-Higgs production in the UV model

For the sake of completeness we also write down $\mathcal{M}_{UV}(\bar{t}t \to hh)$ as it enters the partonic

subprocess of gluon gluon fusion production channel.

$$i\mathcal{M}_{UV}(t\bar{t} \to h_1 h_1) = \quad\text{[diagram]}\quad + \quad\text{[diagram]}\quad + \quad\text{[diagram]}\quad + \text{(u-channel)}. \quad (3.25)$$



The analaytic expression for the scattering amplitude reads:

$$i\mathcal{M}_{UV}(\bar{t}t \to h_1 h_1) = \bar{v}_s(p_2) u_{s'}(p_1) \Big[ \frac{im_t}{v} \frac{3! d_1}{s - m^2} \cos(\chi) + \frac{i(\not{p}_1 - \not{p}_3 + m_t)}{(p_1 - p_3)^2 - m_t^2} \Big(-\frac{m_t}{v}\Big)^2$$

$$\cos(\chi)^2 + \frac{i(\not{p}_1 - \not{p}_4 + m_t)}{(p_1 - p_4)^2 - m_t^2} \Big(-\frac{m_t}{v}\Big)^2 \cos(\chi)^2 + \Big(-\frac{m_t}{v}\Big) \frac{2 d_2 \sin(\chi)}{s - M^2} \Big]. \quad (3.26)$$

The first term corresponds to an $s$ channel exchange of the light Higgs boson with mass $m$, the second and the third terms describes a fermion propagating respectively in the $t$ and $u$ channel while the last term describes $s$ channel exchange of the new heavy scalar particle.

## 3.3 Matching to HEFT

First, we address the matching of the UV model to the HEFT basis. This step seems very easy as both $\mathcal{L}_{UV}$ and $\mathcal{L}_{EFT}$ are written in the broken phase. In this EFT basis each term is given by a gauge invariant invariant part coupled with an integer power of the physical Higgs boson $h$.

$$\mathcal{L}_{HEFT} \supset \frac{v^2}{4} \text{Tr}\Big[(D_\mu U)^\dagger D^\mu U\Big]\Big(1 + 2a\frac{h}{v} + b\Big(\frac{h^2}{v^2}\Big) + \mathcal{O}\big(h^3\big)\Big)$$

$$- m_t \Big(C_t \frac{h}{v} + C_{tt}\Big(\frac{h^2}{v^2}\Big)\Big)\bar{t}t - \kappa_\lambda \frac{m_h^2}{2v} h^3 + \frac{\alpha_s}{\pi}\Big(C_{ggh}\frac{h}{v} + C_{gghh}\frac{h^2}{v^2}\Big) G^a_{\mu\nu} G^{a,\mu\nu}. \quad (3.27)$$

Proceeding via a diagrammatic approach, we compare tree level scattering amplitudes computed in the scalar singlet model and in the IR theory:[3]

$$\mathcal{M}^{\lambda\lambda'}_{HEFT}(W^+W^- \to h_1) = \mathcal{M}^{\lambda\lambda'}_{UV}(W^+W^- \to h_1),$$

$$\epsilon^\lambda_\mu(p_1)\epsilon^{\lambda'}_\nu(p_2) 2i \frac{m_W^2 g^{\mu\nu}}{v} a = \epsilon^\lambda_\mu(p_1)\epsilon^{\lambda'}_\nu(p_2) 2i \frac{m_W^2 g^{\mu\nu}}{v} \cos(\chi),$$

$$a = \cos(\chi). \quad (3.28)$$

---

[3]The tree level condition does not require to fix the RG scale where I perform the matching however it is needed for higher order matching. For our purposes a tree-level matching is sufficient. In some cases one-loop is important as for instance for the colored scalars.

Note that the same holds for the case of a single $h$ boson coupling to fermion-antifermion pair:

$$\mathcal{M}_{HEFT}(\bar{t}t \to h_1) = \mathcal{M}_{UV}(\bar{t}t \to h_1)\,,$$

$$-i\frac{Y_t}{\sqrt{2}}C_t\bar{v}(p_1)u(p_2) = -i\frac{m_t}{v}\bar{v}(p_1)u(p_2)\cos(\chi)\,,$$

$$C_t = \cos(\chi)\,. \tag{3.29}$$

The very same procedure give us the Higgs self coupling, note that in HEFT (as well as in SMEFT) triple and quartic Higgs coupling are different while in SM they are equal.

$$\mathcal{M}_{HEFT}(h_1 h_1 \to h_1) = \mathcal{M}_{UV}(h_1 h_1 \to h_1)\,,$$

$$-i3!\kappa_\lambda\frac{m_h^2}{2v} = -i3!d_1\,,$$

$$\kappa_\lambda^{HEFT} = \frac{2vd_1}{m_h^2}\,. \tag{3.30}$$

Proceeding with the diagrammatic approach we work out the coefficient $b$ appearing in eq. (3.27). Note that by considering $\mathcal{M}_{HEFT} = \mathcal{M}_{UV}$ we should match channels that are kinematically similar.[4] The $t$ channel and the $u$ channel of $\mathcal{M}_{HEFT}(WW \to h_1 h_1)$ can already be expressed in terms of UV quantities obtained by equating $\mathcal{M}_{HEFT}(W^+W^- \to h_1)$ and $\mathcal{M}_{UV}(W^+W^- \to h_1)$.

Analogous considerations allow us to not consider the $s$-channel where $h$ boson propagate because it essentially gives information on $C_t$ and $\kappa_\lambda$ that have already been found. We limit ourselves to match the contact term and the $s$-channel where the heavy d.o.f. propagates of the UV theory with the only one contact term in the low energy basis i.e.:

$$\mathcal{M}_{HEFT}^{\lambda\lambda'}(W^+W^- \to h_1 h_1) = \mathcal{M}_{UV}^{(s-chann,S)} + \mathcal{M}_{UV}^{(cont.)}\,,$$



$$\epsilon_\mu^\lambda(p_1)\epsilon_\nu^{\lambda'}(p_2)i\frac{m_W^2 g^{\mu\nu}}{v^2}b = \epsilon_\mu^\lambda(p_1)\epsilon_\nu^{\lambda'}(p_2)ig^{\mu\nu}\frac{m_W^2}{v^2}\left[\cos(\chi)^2 + 2v\sin(\chi)\frac{i}{s-M^2}(-id_2)\right]\,,$$

$$b = \cos(\chi)^2 + 2v\sin(\chi)\frac{d_2}{s-M^2}\,. \tag{3.31}$$

---

[4]Note that this is no longer true when we introduce derivatives in the field redefinitions as they introduce momentum dependence that could spoil this kinematic similarity between channels in the UV and in the EFT theory.

Since we are interested in the low energy limit we simplify the last step as [5]:

$$b \xrightarrow{s \ll M^2} \cos(\chi)^2 - \frac{d_2 v \sin(\chi)}{M^2}\left(1 + \frac{s}{M^2} + \frac{s^2}{M^4}\right) \simeq \cos(\chi)^2 - \frac{d_2 v \sin(\chi)}{M^2}.$$

(3.32)

Theoretical arguments lead to the expectation $b > 0$ [60]. Analogously $C_{2t}$ is computed equating the relevant scattering amplitudes in HEFT and UV. Note that such a coupling is not present in SM at tree level, it arise in the low energy limit of the chosen UV model.

$$\mathcal{M}_{HEFT}(\bar{t}t \to h_1 h_1) = \mathcal{M}_{UV}(\bar{t}t \to h_1 h_1)$$



$$-i\frac{m_t}{v^2}C_{2t}\bar{v}(p_2)u(p_1)2! = \left(-i\frac{m_t}{v}\sin(\chi)\right)\frac{i}{s - M^2}(-i2!d_2)\,\bar{v}(p_2)u(p_1).$$

$$C_{2t} = \frac{v\sin(\chi)d_2}{s - M^2},$$

$$C_{2t} \xrightarrow{s \ll M^2} -\frac{v\sin(\chi)d_2}{M^2}.$$

(3.33)

Let us comment on the SM limit of the above expressions: $a$ and $C_t$ recover their SM limit by taking $\chi \to 0$. Furthermore they are $M$ independent. A dependence on $M$ will arise when matching at the 1-loop level. The $b$ coefficient is SM like by taking $\sin(\chi) \to 0$. $C_{2t}$ recover its SM form by taking $M \to \infty$ or $\sin(\chi) \to 0$.

## 3.4 SMEFT matching

Matching the scalar singlet model to the SMEFT basis (1.39) is not as straightforward as in the HEFT case. In this section we are adopting a matching in the unbroken phase. We match to the Warsaw basis given in [21] at dimension 6. The first step is to integrate the heavy field $\Phi$ out. For our tree level analysis we solve the E.O.M. for $\Phi$, namely:

$$\frac{\partial \mathcal{L}_{UV}}{\partial \Phi} - \partial_\mu \frac{\mathcal{L}_{UV}}{\partial(\partial_\mu \Phi)} = 0,$$

$$\left(-\Box - \mu_2^2 - \lambda_3 H^\dagger H\right)\Phi = AH^\dagger H + \mu\Phi^2 + \lambda_2\Phi^3.$$

(3.34)

---

[5]In the $s \ll M^2$ limit we neglect scalar singlet width effects, however in the following numerical analysis where we compare the UV model and the HEFT, we could not guarantee an energy in the centre of mass always much below the scalar singlet physical mass, therefore we have included the contribution from the width, namely $\frac{1}{s - M^2 + i\Gamma_S M}$ where $\Gamma_S$ is the total width of the new particle.

The assumptions we make to solve the E.O.M. strongly affect the matching result we are going to obtain. In a SMEFT scenario where UV physics is not strongly coupled we consider a mixing regime that is negligible. Under the assumption of low mixing, perturbation theory and $\mu_2^2 \gg \lambda_3 |H|^2$ we solve eq. (3.34) iteratively getting:

$$\Phi \sim \frac{A}{\mu_2^2} H^\dagger H \,. \tag{3.35}$$

Note that solving eq. (3.34) without perturbative assumption means solving a cubic equation in $\Phi$. Then we have to substitute back (3.35) into $\mathcal{L}_{UV}$ that will be written only in terms of $H$. Finally we compare it with $\mathcal{L}_{SMEFT}$ that we know is made by independent operators.

In principle $\mathcal{L}_{UV}[\Phi[H], H]$ contains both effective operators in Warsaw basis and other non Warsaw operators. Applying Higgs E.O.M we can get rid of non-Warsaw effective operators [21]:

$$D_\mu D^\mu H = \lambda v H + 2\lambda(H^\dagger H)H - \bar{q}Y_u u \sigma_2 + \bar{d}Y_d q + \bar{e}Y_e l \,, \tag{3.36}$$

This step brings in a dependence on the $C_{uH}$. Since the resulting expression still contains non Warsaw operator as $H^\dagger H \left[(D_\mu H)^\dagger (D^\mu H)\right]$ we can exploit the formula (3.36) so that the latter operator is rewritten as a combination of $O_{H\Box}, C_H$ and $C_{uH}$ plus dimension 4 operator [61]:

$$H^\dagger H \left[(D_\mu H)^\dagger (D^\mu H)\right] = \frac{1}{2}(H^\dagger H)\Box(H^\dagger H) + (H^\dagger H)\bar{q}\tilde{H}u + (H^\dagger H)\bar{q}Hd + (H^\dagger H)\bar{l}He$$
$$+ (H^\dagger H)^3 + m^2(H^\dagger H)^2 + \text{E.O.M.}\,, \tag{3.37}$$

where E.O.M. stands for terms that vanish by substituting $H$ equations of motion. In this way the dependence on $C_{uH}$ vanishes. With this procedure we have also excluded the $O_{HD}$ operator. Note that $O_{HD}$ affects the two point functions of $W$ and $Z$ and thus contributes to the $\rho$ parameter. The constraints on $O_{HD}$ from the electroweak precision data imply that the coefficient of this operators to be extremely small. In our case we are safe though, since it vanishes by applying Higgs equations of motion and consequently $c_{H,kin} = C_{H\Box}$. Hence we find that at tree level the only two Wilson coefficients are generated:

$$C_{H\Box} = -\frac{A^2}{2\mu_2^2}\,, \tag{3.38}$$

$$C_H = -\frac{\lambda_3 A^2}{2\mu_2^2} + \frac{\mu A^3}{3\mu_2^4} = C_{H\Box}\left(\lambda_3 + \frac{4\mu}{3A}C_{H\Box}\right)\,. \tag{3.39}$$

In the $\mathbb{Z}_2$ symmetric limit we would have no Wilson coefficient generated at tree-level at dimension 6, but contributions matching at one loop level. These expression confirm the expectation traced in the $\hbar$ counting given in eq.(1.45),(1.46),(1.47). These quantities were checked by exploiting a Mathematica package that adopts a functional matching `Matchete` [62] and automatizes matching for NP models weakly coupled to SM up to 1-loop. We find agreement also with [63] that lists all effective operators generated at tree level for different UV models, and accordance with [64] as well.

In order to make differences between SMEFT and HEFT more evident we have to work on the SMEFT

lagrangian.

Two main issues are taken into account:

**v.e.v. redefinition:** with respect to SM we receive additional contribution from dimension 6. Those terms shift the vacuum state of the SM by $\frac{1}{M^2}$ suppressed terms.

**turn SMEFT in broken phase:** SMEFT is written in unbroken phase, i.e. in terms of $H$ doublet therefore it is still invariant under $\mathcal{G}_{\mathrm{SM}}$. A comparison with the HEFT basis can happen when turning to the broken phase.[6]

Because of higher dimensional operators the v.e.v. obtained from the SMEFT lagrangian is given by

$$v_T^2 = v^2\Big(1 + \frac{3C_H v^2}{4\lambda M^2}\Big)\,,$$

where $v$ has the usual SM expression in terms of the SM Lagrangian parameters. This means that the $H$ doublet is written as:

$$H = \frac{1}{\sqrt{2}}e^{\frac{i\pi_i\sigma_i}{v}}\begin{pmatrix} 0 \\ v_T + \hat{h} \end{pmatrix} = \frac{1}{\sqrt{2}}U(\pi)\begin{pmatrix} 0 \\ v_T + \hat{h} \end{pmatrix}\,, \tag{3.40}$$

and in the unitary gauge it further simplifies to:

$$H = \frac{1}{\sqrt{2}}\begin{pmatrix} 0 \\ v_T + \hat{h} \end{pmatrix}\,. \tag{3.41}$$

When the EW symmetry is broken additional contributions to the $h$ kinetic term appear and a shift is needed to restore a canonically normalized term.

Here we choose to perform a non-linear shift that is gauge-dependent (1.43). If we restrict ourselves to order $\frac{1}{\Lambda^2}$ then we get the SMEFT lagrangian in the broken phase contains the following pieces that are relevant for us:

$$\mathcal{L}_{SMEFT}^{\mathrm{broken}} \supset \frac{1}{2}(\partial_\mu h)(\partial^\mu h) + \frac{v^2}{4}\mathrm{Tr}\Big[(D_\mu U)^\dagger D^\mu U\Big]\Big(1 + 2\kappa_V^{\mathrm{SMEFT}}\frac{h}{v} + \kappa_{2V}^{\mathrm{SMEFT}}\frac{h^2}{v^2}\Big) - \kappa_\lambda^{SMEFT}\frac{m_h^2}{2v}h^3$$
$$- m_t\Big(C_t^{\mathrm{SMEFT}}\frac{h}{v} + C_{2t}^{\mathrm{SMEFT}}\frac{h^2}{v^2}\Big) \quad (\bar{t}t) \tag{3.42}$$

in particular VBF is related to $\kappa_V, \kappa_{2V}$ and $\kappa_\lambda$ coupling modifiers while ggF is mainly affected by the anomalous couplings $C_t$, $C_{2t}$ and $\kappa_\lambda$. If we rewrite the above lagrangian in terms of canonically

---

[6]We are not going to compare the two EFT at the lagrangian level, this would be incorrect as the two EFTs come from different assumptions on the Higgs.

normalized $h$ field we obtain:

$$\mathcal{L}_{\text{SMEFT}} \supset \frac{v_T^2}{4} \text{Tr}\Big[(D_\mu U)^\dagger D^\mu U\Big]\Big[1 + 2\Big(\frac{h}{v_T}\Big)\Big(1 + \frac{C_{H\square}v_T^2}{\Lambda^2}\Big) + \Big(\frac{h}{v_T}\Big)^2\Big(1 + 4\frac{C_{H\square}v_T^2}{\Lambda^2}\Big) + \Big(\frac{h}{v_T}\Big)^3$$
$$\Big(8\frac{C_{H\square}v_T^2}{3\Lambda^2}\Big) + \Big(\frac{h}{v_T}\Big)^4\Big(2\frac{C_{H\square}v_T^2}{3\Lambda^2}\Big)\Big] - \lambda v_T h^3\Big(1 - \frac{5}{2}\frac{2v_T^2}{m_h^2}\frac{C_H v_T^2}{\Lambda^2} + 3\frac{v_T^2}{\Lambda^2}C_{H\square}\Big). \qquad (3.43)$$

The Yukawa part of SMEFT lagrangian that can be used to describe the $t\bar{t} \to hh$ process is

$$\mathcal{L}_{\text{SMEFT}} \supset -m_t\Big[\Big(1 - \frac{3v_T^2}{2\sqrt{2}\Lambda^2}C_{uH}\frac{v_T}{m_t} + \frac{v_T^2}{\Lambda^2}C_{\square H}\Big)\frac{h}{v_T} + \Big(-\frac{3v_T^2}{2\sqrt{2}\Lambda^2}C_{uH}\frac{v_T}{m_t} + \frac{v_T^2}{\Lambda^2}C_{\square H}\Big)$$
$$\frac{h^2}{v_T^2}\Big] \quad (\bar{t}t). \qquad (3.44)$$

Since we are going to stay within the SMEFT framework in the following equations we just write $v$ and not $v_T$. The most relevant coupling modifiers of SMEFT formulation once the broken phase is explicitly written down are collected in the following table 3.3. A comprehensive paper about the Feynman rules in the SMEFT framework can be found in [65] however the latter reference adopts a linear field redefinition 1.42. Therefore our results cannot be checked with this reference. The same non-linear refedfinition was instead adopted by Ref. [30], with which our expressions were checked whenever possible.

For the gluon fusion process, also the couplings of the Higgs boson to gluons are relevant. Those are though not generated in the singlet model as long as the top quark is not integrated out as there are no new colored states. Later on, we will though come back to the couplings $c_{ggh}$ and $c_{gghh}$ when discussing the case of the colored scalar field with SM charges $\Phi_c \to (3, 1, -1/3)$.

The Lagrangian of eqs. (3.43) and (3.44) show how different couplings are correlated in a linear way in the SMEFT. In particular we note :

$$\kappa_{2V} = 4\kappa_V - 3, \qquad (3.45)$$

$$C_{2t} = 1 - C_t. \qquad (3.46)$$

These correlations hold only in SMEFT, this is because they are a remnants of the additional structure we consider for Higgs field, i.e. that it transforms as a doublet under the chiral SM group $SU(2)_L \otimes SU(2)_R$. This means such relations do not hold in general in HEFT that therefore is much less constrained from symmetry properties [66].

Since these correlation arise from a specific assumption on $H$ they can be seen in multi-Higgs interactions as was reported in [60]. In addition we emphasize these particular linear relations heavily depend on the field redefinition we have used for the $h$ field. Lagrangians and consequently couplings are subject to field redefinitions. This means concretely that for VBF adopting a different field redefinition than the one in eq. (1.43) changes $\kappa_{2V}$ and also $\kappa_\lambda$, whereas it leaves the total amplitude invariant. Hence, physical consideration on the difference between SMEFT and HEFT are better carried out at

the amplitude level. Analogously for the gluon gluon fusion process where the coupling modifiers $C_{2t}$ and $\kappa_\lambda$ change their form according to which $h$ field redefinition is choosen. In the singlet model case the $C_{2t}$ coupling is zero when $h$ is linearly redefined while it obtains a contribution which is non vanishing after (1.43). This contribution is re-obtained for the linear redefinition due to extra momentum-dependent terms in the trilinear Higgs self-coupling from the operator $O_{H\square}$. This reminds us that an analysis based solely on the coupling evaluation is not physical and we must compute quantities that are not affected by different definitions of the h field. Our aim in the next chapter will be to highlight differences between two EFT's in a way that is not affected by field redefinition, namely cross sections or amplitudes.

$$i\mathcal{M}_{EFT}(t\bar{t} \to h_1) = \quad = -i\frac{Y_t}{\sqrt{2}}C_t\bar{v}(p_1)u(p_2)\,, \tag{3.10}$$

$$i\mathcal{M}_{EFT}(t\bar{t} \to h_1 h_1) = \quad = -i2!\frac{Y_t}{\sqrt{2}}C_{2t}\bar{v}(p_1)u(p_2)\,, \tag{3.11}$$

$$i\mathcal{M}_{EFT}^{\lambda,\lambda'}(W^+W^- \to h_1) = \quad = \epsilon_\mu^\lambda(p_1)\epsilon_\nu^{\lambda'}(p_2)2i\frac{m_W^2 g^{\mu\nu}}{v}\kappa_V\,, \tag{3.12}$$

$$i\mathcal{M}_{EFT}^{\lambda,\lambda'}(W^+W^- \to h_1 h_1) \supset \quad = \epsilon_\mu^\lambda(p_1)\epsilon_\nu^{\lambda'}(p_2)i\frac{m_W^2 g^{\mu\nu}}{v^2}\kappa_{2V}2!\,, \tag{3.13}$$

$$\mathcal{M}_{EFT}(h_1 \to h_1 h_1) = \quad = -i\kappa_\lambda\frac{3m_h^2}{v}\,. \tag{3.14}$$

Table 3.1: relevant TL amplitudes in Di-Higgs production, $\kappa$'s expression will change according to the IR considered

|  | HEFT | SMEFT |
|---|---|---|
| $\kappa_V$ | $a_1$ | $1 + \frac{c_{H,\text{kin}} v^2}{\Lambda^2}$ |
| $\kappa_{2V}$ | $a_2$ | $1 + \frac{4 c_{H,\text{kin}} v^2}{\Lambda^2}$ |
| $\kappa_\lambda$ | $b_1$ | $1 - \frac{2v^2}{m_h^2} \frac{C_H v^2}{\Lambda^2} + 3 \frac{v_T^2}{\Lambda^2} c_{H,\text{kin}}$ |
| $\kappa_t$ | $C_t$ | $1 - \frac{3v_T^2}{2\sqrt{2}\Lambda^2} \frac{v}{m_t} C_{uH} + \frac{v^2}{\Lambda^2} c_{H,\text{kin}}$ |
| $\kappa_{2t}$ | $C_{2t}$ | $-\frac{3v_T^2}{2\sqrt{2}\Lambda^2} \frac{v}{m_t} C_{uH} + \frac{v^2}{\Lambda^2} c_{H,\text{kin}}$ |
| $\kappa_{hhg}$ | $c_{ggh}$ | $\frac{8\pi}{\alpha_s} \frac{v^2}{\Lambda^2} C_{HG}$ |
| $\kappa_{gghh}$ | $c_{gghh}$ | $\frac{4\pi}{\alpha_s} \frac{v^2}{\Lambda^2} C_{HG}$ |

Table 3.3: Relevant couplings in Higgs pair production, both in HEFT and in Warsaw basis. With respect to [30] we have added the coupling modifiers of the VBF process.

# Chapter 4

# Scalar singlet as Loryons

In the following we will concretely show for the scalar singlet model that the effective expansion does not converge if the new particle gets most of its mass from EWSB.

## 4.1 Scalar singlet

In this section we are showcasing the validity of the expansion for the $\mathbb{Z}_2$ symmetric scalar singlet model as it simplifies the computation while not changing the physics we want to highlight.

The model we are using in this section is given by eq. (2.1) where $A \to 0$, $\mu \to 0$:

$$
\begin{aligned}
\mathcal{L}_{UV} =& \mathcal{L}_{SM} + (D_\mu H)^\dagger (D^\mu H) + \frac{1}{2} \partial_\mu \Phi \partial^\mu \Phi - \mu_1^2 H^\dagger H \\
& - \frac{\mu_2^2}{2} \Phi^2 - \lambda_1 (H^\dagger H)^2 - \frac{\lambda_2}{4} \Phi^4 - \frac{\lambda_3}{2} \Phi^2 (H^\dagger H) \,.
\end{aligned}
\tag{4.1}
$$

Both $\Phi$ and $H$ acquire a v.e.v. according to $\langle \Phi \rangle = v_s$ and $\langle H \rangle = \frac{v}{\sqrt{2}}$. In order to highlight the difference between SMEFT and HEFT we are going to make only one crucial assumption on the EWSB. If we only assume a weakly coupled UV theory then the new heavy degree of freedom does not affect EWSB and consequently the mixing between $h$ and $S$ is a subleading effect. Thus we can identify $\Phi = v_s + S$ and $H = \frac{v+h}{\sqrt{2}} U(\pi)$ where $h$ and $S$ are the physical fields.

Under this assumptions we consider $\Phi$ takes a v.e.v. while the $H$ doublet is left invariant, in this way $\mathbb{Z}_2$ symmetry is spontaneously broken.

The UV model allows $\Phi$ to acquire a v.e.v. and the lagrangian reduces to:

$$
\begin{aligned}
\mathcal{L}_{UV} =& \mathcal{L}_{SM} + (D_\mu H)^\dagger (D^\mu H) + \frac{1}{2} \partial_\mu S \partial^\mu S - \mu_1^2 H^\dagger H - \frac{\mu_2^2}{2} S^2 - \frac{v_s \mu_2^2}{2} S - \lambda_1 (H^\dagger H)^2 \\
& - \frac{\lambda_3}{2} |H|^2 S^2 - \lambda_3 v_s |H|^2 S - \frac{\lambda_3}{2} v_s^2 |H|^2 - \frac{\lambda_2}{4} (S^4 + 4 v_s S^3 + 4 v_s^3 S + 2 v_s^2 S^2) \,.
\end{aligned}
\tag{4.2}
$$

From tadpole equations for the heavy field we get:

$$
\frac{\partial V(H, S)}{\partial S} = 0 \,, \longrightarrow v_s (\mu_2^2 + \lambda_2 v_s^2) = 0 \,,
$$

solving for cases where $S$ has a non vanishing v.e.v. means to choose $\mu_2^2 = -\lambda_2 v_s^2$.

Note we can define the field dependent mass for the singlet S:

$$m_S(H) = \mu_2^2 + \lambda_3 |H|^2 \,. \qquad (4.3)$$

We can integrate the heavy field $S$ out by means of the equations of motion, in the static limit it reduces to:

$$0 = \frac{\partial \mathcal{L}_{\mathrm{UV}}}{\partial S} = (v_s + S)(2\lambda_2 v_s S + \lambda_2 S^2 + 2\lambda_3 |H|^2) \,, \qquad (4.4)$$

$$S[H] = -v_s \pm \sqrt{v_s^2 - \frac{2\lambda_3 |H|^2}{\lambda_2}} \,. \qquad (4.5)$$

Substituting back in $\mathcal{L}_{\mathrm{UV}}$ I get an expression for the effective lagrangian, the latter include non analyticities in the vicinity of $|H| = 0$ which is the physical vacuum, i.e. the lowest energy configuration of the $H$ field. This is indeed problematic since the SMEFT expansion is usually a polynomial expansion in $|H|^2$ or $\partial |H|^2$ in other words SMEFT lagrangian does not contain any non analyticity in $|H|$. Therefore this might be the case where the low energy theory must be written in terms of HEFT. The effective lagrangian is rewritten only in terms of $H$:

$$\mathcal{L}_{\mathrm{Eff}} = |D_\mu H|^2 - \frac{\lambda_3}{8(\mu_2^2 + \lambda_3 |H|^2)} \left(\partial_\mu |H|^2\right)^2 + \mu_1^2 |H|^2 - \lambda_1 |H|^4 + \frac{1}{4\lambda_2}(\mu_2^2 + \lambda_3 |H|^2)^2 \,, \qquad (4.6)$$

which is clearly problematic around $|H| = 0$ in the limit $\mu_2^2 \to 0$. Most importantly this issue cannot be solved by any field redefinition and therefore is physical, in other words this non-analyticity is an intrinsic property of the model independent on the field basis that we employ.

This is the typical case where SMEFT expansion is not possible and we must rely on HEFT.

Note that if we solve the E.O.M. for $S$ assuming $\mu_2^2 \gg \lambda_3 |H|^2$ then the expression for the heavy field in eq. (4.4) would be expanded as :

$$S \sim v_s \pm \mu_2 \left[ 1 + \frac{1}{2} \frac{\lambda_3 |H|^2}{\mu_2^2} + \mathcal{O}\left(\frac{(\lambda_3 |H|^2)^2}{\mu_2^4}\right) \right] \,, \qquad (4.7)$$

and we would cut away any non analyticity around $|H| = 0$ at the lagrangrian level [32].

In the case of a singlet model where the $\mathbb{Z}_2$ symmetry is explicitly broken we can't solve the third order equation as we did above, namely factorizing a second order equation and a first order polynomial in $S$. In that case we have to solve:

$$S(\mu_2^2 + 2\mu v_s + \lambda_3 |H|^2 - S(\mu + 3v_s) + \lambda_2 S^2) = A|H|^2 + \lambda_3 |H|^2 v_s \,. \qquad (4.8)$$

The real solution of the latter equation is rather lengthy and crucially it contains terms non-analytic in $|H| = 0$. If we expand it for an infinite explicit mass $\mu_2^2$ we get:

$$S[H] \simeq -\frac{A|H|^2 + \lambda_3 v_s |H|^2}{\mu_2^2} + \frac{A|H|^2 + \lambda_3 v_s |H|^2}{\mu_2^4}(2\mu v_s + \lambda_3 |H|^2) - \frac{A|H|^2 + \lambda_3 v_s |H|^2}{\mu_2^6}$$
$$\left[(2\mu v_s + \lambda_3 |H|^2)^2 + (A|H|^2 + \lambda_3 v_s |H|^2)(\mu + 3v_s)\right] + \mathcal{O}\left(\frac{1}{\mu_2^8}\right). \tag{4.9}$$

As expected if we substitute back this equation in the UV model with explicitly broken $\mathbb{Z}_2$ symmetry we get no non-analyticities around the $O(4)$ invariant point $|H| = 0$. In eq. (4.9) we can identify the quantity $\frac{A|H|^2 + \lambda_3 v_s |H|^2}{\mu_2^2}$ as an expansion parameter [1] which reduced to $\frac{\lambda_3 v_s |H|^2}{\mu_2^2}$ for the $\mathbb{Z}_2$ symmetric case for $A \to 0$. These statements suggest the existence of a SMEFT expansion is related to the ratio $\frac{A|H|^2 + \lambda_3 v_s |H|^2}{\mu_2^2}$ since expanding the $S$ field in terms of that quantity leads to an effective lagrangian that is analytic in $|H|^2$ and $\partial H$ with terms suppressed by the inverse powers of the explicit mass. Hence the expansion parameter crucial in the scalar singlet model that appear either in the $\mathbb{Z}_2$ symmetric case and in the non $\mathbb{Z}_2$ symmetric case is:

$$r = \frac{\lambda_3 v^2}{\mu_2^2}, \tag{4.10}$$

which is the field independent part of the expansion parameter in eq. (4.7).

The extrema for r are given by an infinte explicit mass ($\mu_2 \to \infty$) which correspond to $r \to 0$ and a vanishing explicit mass ($\mu_2 \to 0$) leading to $r \to \infty$. If the latter is small we can expand solution for $S$ E.O.M. getting an effective lagrangian that is analytic in H, if instead this ratio is non negligible we cannot end up with an expansion in inverse powers of the explicit mass scale as in SMEFT. In this case the mass contribution from EWSB is comparable with the explicit mass source and at the lagrangian level $\mathcal{L}_{eff}$ may show up non-analytic terms in $|H|$ [31].

---

[1] An expansion parameter is indeed dimensionless.

# Chapter 5

# Results for the singlet model

In this chapter we collect all the meaningful results showing up evidence how different low energy theories for the Higgs boson may lead to different predictions. Our results mainly concern the scalar singlet model taking into account the two dominant production channels for Higgs pair production, i.e. ggF and VBF.

## 5.1  Scalar singlet results

First of all we will discuss the coupling modifiers in the singlet model focusing on $\kappa_{hhVV} = \kappa_{2V}$ ($\kappa_{hVV} = \kappa_{V}$) that enters in the VBF and $c_{tthh} = c_{2t}$ ($c_{tth} = c_{t}$) relevant for the ggF channel. A scan has been performed in these coupling modifier space.

The scan performed is shown in Fig. 5.1 for the Higgs couplings to vector bosons and in Fig. 5.2 for the Higgs couplings to top quarks. The orange line represents the linear correlation that arises in SMEFT while the points represent possible values in the coupling space according to HEFT. The red (blue) color stands for a physical mass of the heavy scalar below (above) 1TeV.

The other parameters vary as:

$$\sin(\chi) \in [-0.37, 0.37], \qquad v_s \in [0.01, 10v] \,.$$

We can already appreciate two main aspects from these plots:

- In SMEFT the linear transformation of the Higgs doublet under $O(4)$ allows for a linear relation between these couplings while HEFT is not necessarily following a linear relation due to the non linear realization of the EW symmetry.

- $c_{tthh} - c_{tth}$ points in the HEFT model provide strong deviation with respect to SMEFT prediction, in other words these EFT coincide only in the vicinity of the SM point.

The second point can be clarified by the expressions of $c_{tthh}$ and $c_{tth}$ resulting from matching and taking an appropriate limit where HEFT and SMEFT give the same analytic form. Given the results
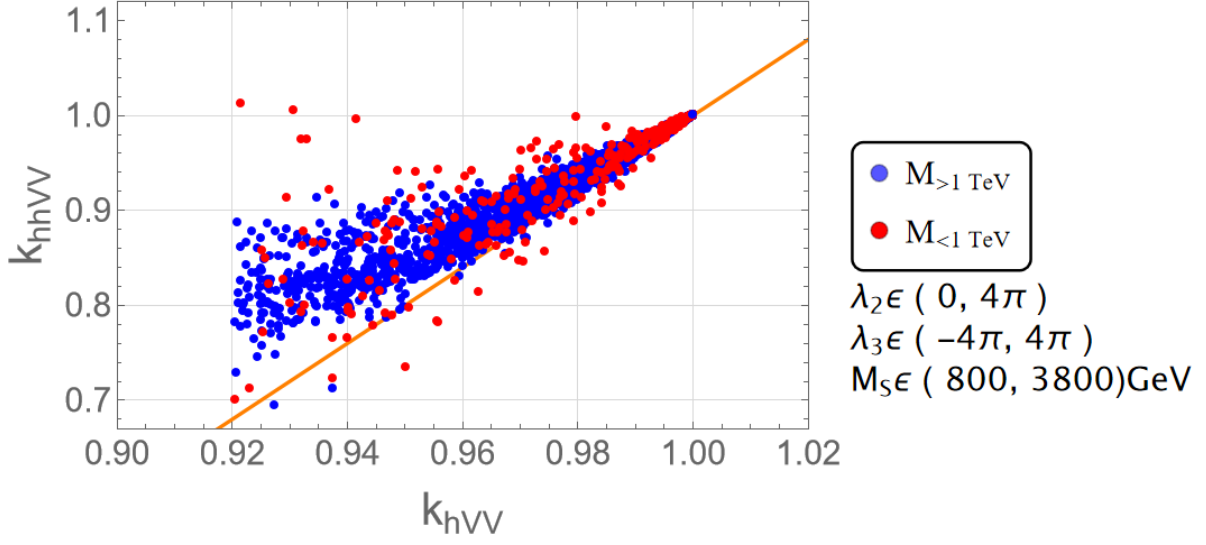
Figure 5.1: Behaviour of $\kappa_{hhVV}$ in function of $\kappa_{hhV}$. We find qualitative accordance with results of [67]. The SM limit is recovered in the point $[\kappa_{hhV}, \kappa_{hhVV}] = [1, 1]$.
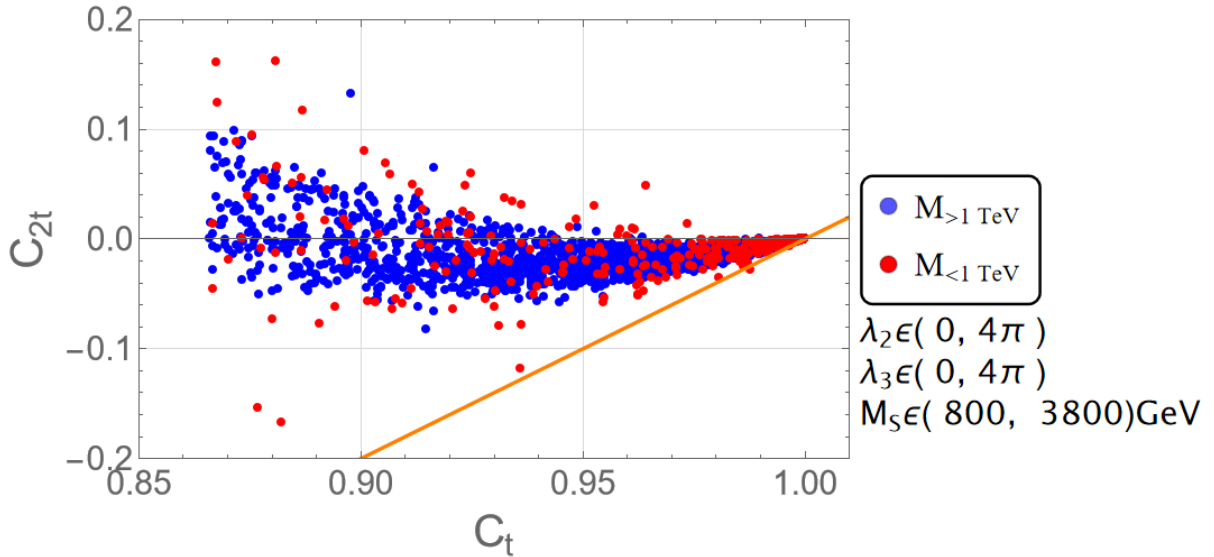


Figure 5.2: Behaviour of $c_{tthh}$ in function of $c_{tth}$. The SM limit is recovered in the point $[c_{tth}, c_{tthh}] = [1, 0]$.

from SMEFT we express the couplings in terms of our input parameters. We consider the coupling modifiers of the Higgs to fermion in the limit of vanishing mixing angle and infinite mass $M$:

$$
\begin{aligned}
c_{tth}^{\text{SMEFT}} =& 1 + \frac{v^2}{\mu_2^2}C_{H\Box} \xrightarrow{\chi \to 0, M \to \infty} 1 + \left(\frac{vv_s\lambda_3}{M^2}\right)\chi \\
& + \left(-\frac{1}{2} + \frac{2m^2 - 2v_s^2\lambda_2 - 5v^2\lambda_3}{2M^2}\right)\chi^2 + \left(\frac{v}{v_s} + \frac{8vv_s^2\lambda_3 + 27v^3\lambda_3 + 18vv_s^2\lambda_2 - 18m^2v}{6v_sM^2}\right)\chi^3 \\
& + \left(\frac{-9v^2 - 2v_s^2}{6v_s^2} + \frac{36m^2v^2 + 10m^2v_s^2 - 36v^2v_s^2\lambda_2 - 10v_s^4\lambda_2 - 42v^4\lambda_3 - 25v^2v_s^2\lambda_3}{6v_s^2M^2}\right)\chi^4 \\
& + \mathcal{O}\left(\frac{1}{M^4}, \chi^6\right),
\end{aligned}
\tag{5.1}
$$

$$
\begin{aligned}
c_{tthh}^{\text{SMEFT}} =& \frac{v^2}{\mu_2^2}C_{H\Box} \xrightarrow{\chi \to 0, M \to \infty} \frac{vv_s\lambda_3}{M^2}\chi + \left(-\frac{1}{2} + \frac{2m^2 - 2v_s^2\lambda_2 - 5v^2\lambda_3}{2M^2}\right)\chi^2 \\
& + \left(\frac{v}{v_s} + \frac{8vv_s^2\lambda_3 + 27v^3\lambda_3 + 18vv_s^2\lambda_2 - 18m^2v}{6v_sM^2}\right)\chi^3 + \\
& + \left(\frac{-9v^2 - 2v_s^2}{6v_s^2} + \frac{36m^2v^2 + 10m^2v_s^2 - 36v^2v_s^2\lambda_2 - 10v_s^4\lambda_2 - 42v^4\lambda_3 - 25v^2v_s^2\lambda_3}{6v_s^2M^2}\right)\chi^4 \\
& + \mathcal{O}\left(\frac{1}{M^4}, \chi^6\right).
\end{aligned}
\tag{5.2}
$$

We adopt the same procedure to the results obtained from HEFT:

$$
c_{tth}^{\text{HEFT}} = \cos(\chi) \xrightarrow{\chi \to 0, M \to \infty} 1 - \frac{\chi^2}{2} + \frac{1}{24}\chi^4 + \mathcal{O}\left(\chi^6\right),
\tag{5.3}
$$

$$
c_{tthh}^{\text{HEFT}} = -v\frac{d_2\sin(\chi)}{M^2} \xrightarrow{\chi \to 0, M \to \infty} \left(-\frac{1}{2} + \frac{2m^2}{M^2}\right)\chi^2 + \left(\frac{8}{3} - \frac{14m^2}{M^2}\right)\chi^4 + \mathcal{O}\left(\frac{1}{M^4} \cdot \chi^6\right).
\tag{5.4}
$$

These equations show HEFT and SMEFT couplings coincide only in the small mixing angle limit. Note that additional conditions have to satisfied:

- $c_{tthh}^{\text{HEFT}}$ and $c_{tth}^{\text{HEFT}}$ do not have any term at $\mathcal{O}(\chi)$ therefore $\frac{vv_s\lambda_3}{M^2}$ being small is also required if we want to recover equality between SMEFT and HEFT couplings.

- $\frac{-2v_s^2\lambda_2 - 5v^2\lambda_3}{M^2}$ must be small as well in order to to recover accordance at orderthe level of the couplings at $\mathcal{O}(\chi^2)$, note that $c_{tth}^{\text{HEFT}}$ does not involve any mass scale in its expansion therefore in $c_{tth}^{\text{SMEFT}}$ we must ensure a mass scale separation yielding a negligible $\frac{m^2}{M^2}$.

- $c_{tthh}^{\text{HEFT}}$ and $c_{tth}^{\text{HEFT}}$ do not have any term at $\mathcal{O}(\chi^3)$ therefore we require $\frac{v}{v_s}$ being negligible but this may enhance the other $\frac{3vv_s\lambda_2}{M^2}$ present at the same order in $\chi$. The choice of $v_s$ value is therefore non-trivial by this selection of the input parameters.

If these requirements are met we have an agreement between HEFT and SMEFT at least up to $\mathcal{O}(\chi^4)$. Given that we infer from the plot presented above (fig. 5.2) that the range of the mixing angle is not small enough to recover the agreement between SMEFT and HEFT.

These results do not have a clear physical relevance as they depend on the field basis that we are

adopting. As we have previously mentioned $\kappa_{hhVV}$ and $c_{tthh}$ depends on whether we use (1.42) or (1.43). We have adopted here the one of (1.43) since it does not lead to new Lorentz structures in the Higgs self-coupling. In this case, when writing down the amplitudes one can see the correspondence on the amplitude level between the SMEFT and HEFT couplings of two Higgs bosons to two vector bosons. We now turn to the computation of the amplitudes to provide also a comparison with the full UV model. Our results are based on the evaluation of unpolarized amplitudes squared, in particular we consider their ratio in an EFT framework with respect to the UV model.

$$R_{UV/EFT} = \frac{\sum_{\lambda,\lambda'} \mathcal{M}_{UV}^{\lambda} \mathcal{M}_{UV}^{*,\lambda'}}{\sum_{\lambda,\lambda'} \mathcal{M}_{EFT}^{\lambda} \mathcal{M}_{EFT}^{*\lambda'}} \,, \tag{5.5}$$

where EFT may be either SMEFT or HEFT and a sum over all the polarization in the initial state (VBF) and/or over color (ggF) is taken [1].

The $R_{EFT/UV}$ quantity describes how good the EFT limit is with respect to the full UV model. When $R \simeq 1$ our EFT is an appropriate description of the full model while $R$ values deviating from unity stands as a breakdown of the EFT prescription.

Our analysis consists in different scans of the above quantity taking into account all the constraints from the phenomenological analysis of the singlet model. Our main quest is to see how this quantity changes as the amount of mass that the new particle gets from EWSB grows. To do so we plot $R_{EFT}$ versus:

$$r_{\text{exp}} = \frac{\lambda_3 |H|^2}{\mu_2^2} \,,$$

more precisely we take its field independent part $\frac{\lambda_3 v^2}{\mu_2^2}$. Recalling $\lambda_{ex} = \frac{\mu_2^2}{2v^2}$ we can related our expansion parameter to the $f$ parameter defined in [34]:

$$f = \frac{\lambda_3}{\lambda_{ex} + \lambda_3} = \frac{\lambda_3}{\frac{\mu_2^2}{2v^2} + \lambda_3} = \frac{2r_{\text{exp}}}{1 + 2r_{\text{exp}}} \,, \tag{5.6}$$

therefore $r = 0.5$ corresponds to $f = 0.5$ which is the reference number above which HEFT is required. We focus on the partonic amplitudes and computed them at different centre of mass (c.o.m.) energies $s$ at fixed value of the scattering angle. Since no significant deviation has shown up at different values of $s$ we refrained to compute the full cross sections.

For the UV model we use eq. (3.17) and eq. (3.26). In our analysis the total width of the new scalar resonance is included :

$$\Gamma_{h_2,tot} = \sin(\chi)^2 \Gamma_{\text{SM}} + \Gamma_{h_2 \to h_1 h_1} \,, \tag{5.7}$$

---

[1]More precisely one averages over polarizations and color, for instance in ggF:

$$|\bar{\mathcal{M}}| = \frac{1}{2^2} \frac{1}{8^2} \sum_{\lambda,\lambda'} \sum_{a,b} \mathcal{M}_{ab,\text{EFT}}^{\lambda} \mathcal{M}_{ab,\text{EFT}}^{*,\lambda'} \,.$$

where $\Gamma_{\mathrm{SM}}$ the decay width of a SM Higgs boson $h_1$ with a mass $M$ computed with HDECAY [68] while $\Gamma_{h_2 \to h_1 h_1}$ is the decay of the new resonance in two SM Higgs bosons. The decay width $\Gamma_{h_2 \to h_1 h_1}$ is a two body decay in the kinematically allowed region i.e. when $M > 2m$ and given by

$$\Gamma_{h_2 \to h_1 h_1} = \frac{1}{2M} \frac{1}{2} \rho |\mathcal{M}(h_2 \to h_1 h_1)|^2 = \frac{1}{16\pi M} d_2^2 \sqrt{1 - \frac{4m^2}{M^2}} \, , \qquad (5.8)$$

where $\rho$ is the two body phase space and $\frac{1}{2}$ is due to identical particles in the final state.
For what concerns the SMEFT amplitude we consider $\mathcal{M}_{\mathrm{SMEFT}} = \mathcal{M}_{\mathrm{SM}} + \frac{c}{\Lambda^2} \mathcal{M}^{(6)}$ and keep the $\mathcal{O}\left(\frac{1}{\Lambda^4}\right)$ in the squared matrix element

$$|\mathcal{M}_{\mathrm{SMEFT}}|^2 = |\mathcal{M}_{\mathrm{SM}}|^2 + +2\frac{c}{\Lambda^2}\mathrm{Re}(\mathcal{M}_{\mathrm{SM}}\mathcal{M}^{(6)}) + \frac{c^2}{\Lambda^4}|\mathcal{M}^{(6)}|^2 \, . \qquad (5.9)$$

However the last term is formally of the order of dimension 8 for which we would have to include also dimension 8 operators leading to an interference with SM as $\frac{c'}{\Lambda^4}\mathrm{Re}(\mathcal{M}_{SM}\mathcal{M}^{(8)})$ [69]. HEFT relies on a different PC and these considerations are not needed in that case.

### 5.1.1  VBF

We consider the following truncated EFT amplitude for the VBF process:

$$\mathcal{M}_{VBF} \sim \epsilon\epsilon \Big[ \kappa_V \kappa_\lambda \frac{m^2}{s - m^2} \frac{m_W^2}{v^2} + \kappa_{2V} \frac{m_W^2}{v^2} + \kappa_v^2 \left(\frac{m_w^2}{v}\right)^2 \frac{1}{t - m_W^2}\left(-1 + \frac{(p_1 - p_3)^2}{m_W^2}\right)$$
$$+ \kappa_v^2 \left(\frac{m_w^2}{v}\right)^2 \frac{1}{u - m_W^2}\left(-1 + \frac{(p_1 - p_4)^2}{m_W^2}\right)\Big] \, , \qquad (5.10)$$

where $p_1$ is the momenta for gluon in the initial state while $p_3, p_4$ are the momenta of the higgses in the final state. We collect results for VBF at different centre of mass energies, namely $\sqrt{s} = 500$ GeV , $\sqrt{s} = 1000$ GeV and $\sqrt{s} = 1500$ GeV. For each energy scale we plot the following quantities with respect to the expansion parameter $r_{exp}$ : ratio between UV theory and the SMEFT limit, ratio between UV theory and the linearised SMEFT, ratio between full SMEFT prediction to the linearised one and finally the ratio between the UV model and the HEFT limit. The parameters are varying as:

$$\lambda_2 \in [0, 4\pi], \quad \lambda_3 \in [-4\pi, 4\pi], \quad \theta = \frac{\pi}{2}, \quad v_s \in [0, 10v], \quad \sin(\chi) \in [-0.37, 0.37] \, , \qquad (5.11)$$

where $\theta$ is the scattering angle in the partonic center of mass frame. For coefficients with mass dimension one we require that the 1-loop corrections to the trilinear Higgs self coupling are smaller than their tree level values in the SU(2) limit [70]. This leads to:

$$\frac{|A|}{\max\left(|\mu_2|, |\mu_1|\right)} \le 4\pi, \quad \wedge \quad \left|\frac{\mu}{\mu_2}\right| \le 4\pi \, . \qquad (5.12)$$

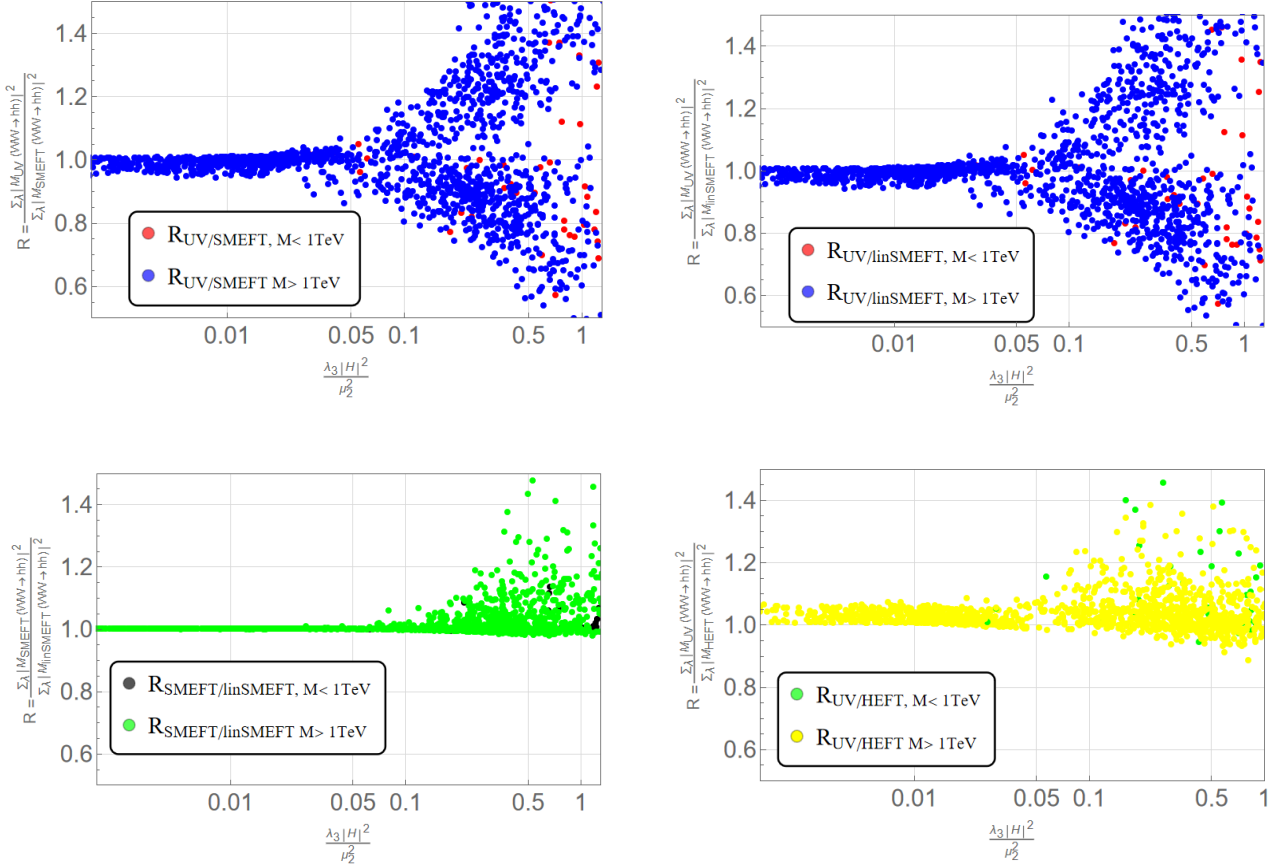The points displayed in each set of figures put together results collected from 2 scans of the

Figure 5.3: We display the UV model prediction divided by the SMEFT prediction (upper,left), the UV prediction divided by linearised SMEFT (upper,right), the full SMEFT prediction divided by the linearised SMEFT prediction (lower, left) and the UV prediction divided by and HEFT (lower,right). These plots refer to $s = 0.5\text{TeV}$ and $M \in [250, 3000]\text{GeV}$.
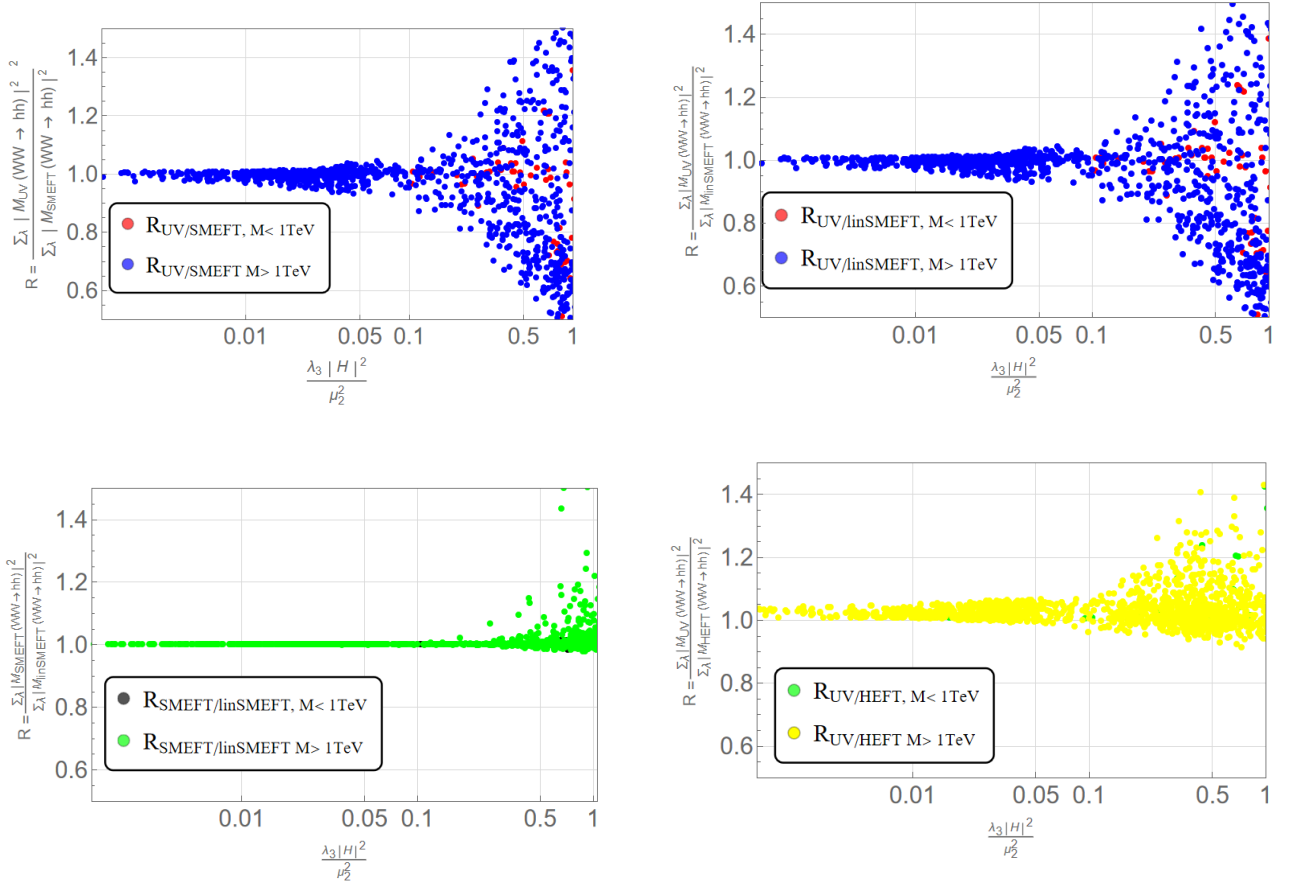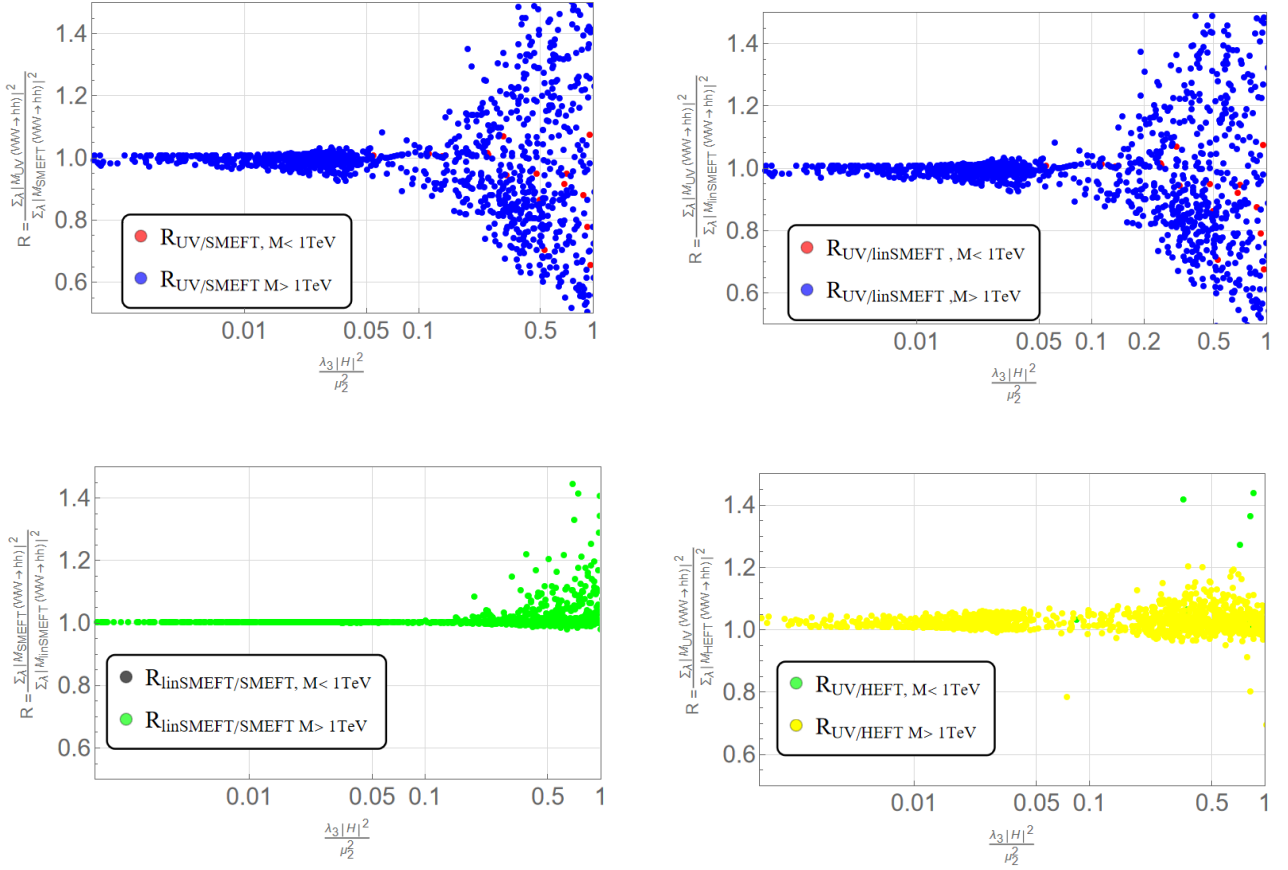
Figure 5.4: We display the UV model prediction divided by the SMEFT prediction (upper,left), the UV prediction divided by linearised SMEFT (upper,right), the full SMEFT prediction divided by the linearised SMEFT prediction (lower, left) and the UV prediction divided by and HEFT (lower,right). These plots refer to $s = 1\text{TeV}$ and $M \in [500, 3000]\text{GeV}$.

Figure 5.5: We display the UV model prediction divided by the SMEFT prediction (upper,left), the UV prediction divided by linearised SMEFT (upper,right), the full SMEFT prediction divided by the linearised SMEFT prediction (lower, left) and the UV prediction divided by and HEFT (lower,right). These plots refer to $s = 1.5\text{TeV}$ and $M \in [500, 3000]\text{GeV}$.
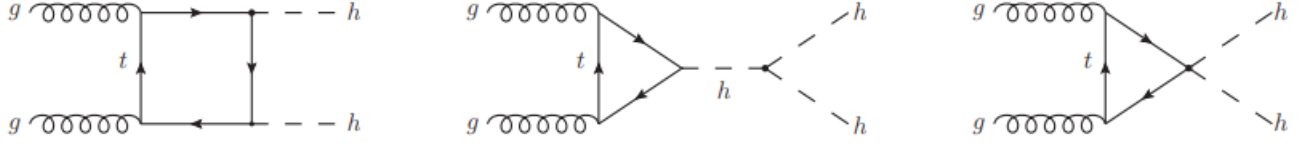
Figure 5.6: Feynman diagrams for double Higgs production via gluon fusion (an additional contribution comes from the crossing of the box diagram).

parameter space. For each value of s we consider the following ranges :

- scan 1: $\lambda_2 \in [0, 1]$, $\lambda_3 \in [-1, 1]$, $|\sin(\theta)| < 0.37$ and $v_S \in [0.02, 8v_H]$ with $M \in [250, 3000]$ GeV.

- scan 2: $\lambda_2 \in [0, 4\pi]$, $\lambda_3 \in [-4\pi, 4\pi]$, $|\sin(\theta)| < 0.37$ and $v_S \in [0.02, 8v_H]$ with $M \in [250, 3000]$ GeV.

We note that scan 1 populates only values of $r_{exp} < 0.1$ while scan 2 mostly populates the contrary regime. From these figures we interfere that while for $r_{exp} < 0.1$ SMEFT and HEFT do nearly equally well, for larger values of $r_{exp}$ HEFT seems to describe a little better the full UV model. As the energy in the centre of mass increases we observe in general terms a better convergence of the EFT. This is mainly due to vanishing dependence on the anomalous couplings, i.e. the term proportional to $\kappa_\lambda$ becomes irrelevant for large $s$. The process in the SM has destructive interference and the interference behavior dependence on the energy scale. Since the matrix element of VBF $\mathcal{M}_{VBF}(s)$ is maximal around $s \sim 4m^2$ it is no surprise that the plots at $s = 0.5$ TeV have a relative worse convergence with respect to other those at higher values of $s$ as there are more delicate cancellations due to the destructive interference. As the energy $s$ increases the contribution proportional to $\kappa_\lambda \kappa_V$ is suppressed and $\mathcal{M}_{VBF} \sim \frac{s}{m_W^2} \frac{m_W^2}{v^2} (\kappa_{2v} - 2\kappa_V^2)$ for large $s$.

## 5.1.2 ggF

In the effective field theory framework model we have three different diagrams contributing to ggF shown in fig.5.6. These processes are written in terms of anomalous coefficients of eq. (3.27), in particular the effective coupling $t\bar{t}hh$ is a new coupling that is not present in the SM. This parameter strongly affects the total cross section $\sigma(pp \to hh)$ with respect to the SM prediction, see [71, 72]. The EFT amplitudes of the diagrams in fig. 5.6 scale differently with the invariant masses $\sqrt{s}$, where $s$ is the Mandelstam variable. In the limit $s \gg m_t^2, m^2$ the scattering amplitudes reduce to [28]:

$$\mathcal{M}_\square \sim c_t^2 \alpha_s \frac{m_t^2}{v^2}, \tag{5.13}$$

$$\mathcal{M}_\triangle \sim c_t \kappa_\lambda \alpha_s \frac{m_t^2}{v^2} \frac{m_h^2}{s} \left[ \log\left(\frac{m_t^2}{s}\right) + i\pi \right]^2, \tag{5.14}$$

$$\mathcal{M}_\triangle^{new} \sim c_{2t} \alpha_s \frac{m_t^2}{v^2} \left[ \log\left(\frac{m_t^2}{s}\right) + i\pi \right]^2. \tag{5.15}$$

The matrix elements $\mathcal{M}_\square$, $\mathcal{M}_\triangle$ correspond to the first two diagrams in fig. 5.6 while $\mathcal{M}_\triangle^{new}$ is the amplitude with the new interaction. Triangle diagram $\mathcal{M}_\triangle$ is enhanced near threshold $s \sim m^2$ and is suppressed for higher energies $s \gg m^2, m_t^2$. If $c_{2t} \leq c_t^2$ and the centre of mass energies $s \gg m_t^2$ (which is the case we're focusing on) the contribution from new physics is comparable with the box diagram contribution leading to significant deviation from SM independent from the effective field theory framework we are going to use later. Therefore the squared amplitudes will be particularly sensitive to $c_{2t}$ (and consequently to new physics) unless $c_t^2 \gg c_{2t}$.

As a first step we focus on the process $t\bar{t} \to hh$. In principle this is enough to investigate the deviation from the SM prediction since all the anomalous couplings $c_t$, $c_{2t}$ and $\kappa_\lambda$ are already present in $t\bar{t} \to hh$. This has to be seen as a preliminary step that cannot reproduce physically meaningful features such as the destructive interference between the triangle and the box diagrams in ggF.

The scattering amplitude in the effective theory reads :

$$
\mathcal{M}_{tthh} \sim u(p_1)\bar{v}(p_2) \left[ c_{2t}\frac{m_t}{v^2} + c_t\kappa_\lambda\frac{m_t}{v^2}\frac{m_h^2}{s - m_h^2} + c_t^2\frac{m_t^2}{v^2}\frac{(\slashed{p}_1 - \slashed{p}_3 + m_t)}{t - m_t^2} + c_t^2\frac{m_t^2}{v^2}\frac{(\slashed{p}_1 - \slashed{p}_4 + m_t)}{u - m_t^2} \right] .
$$

$$(5.16)$$

A numerical analysis in complete analogy to the VBF case was performed, see fig. 5.7, 5.8 and 5.9. The UV parameters vary as:

$$
\lambda_2 \in [0, 4\pi], \quad \lambda_3 \in [-4\pi, 4\pi], \quad v_s \in [0.01, 10v], \quad \sin(\chi) \in [-0.024, 0.024] , \tag{5.17}
$$

while the condition (5.12) is left unchanged. As soon as $|\sin(\chi)| \geq 0.03$ SMEFT does not reproduce the UV model results, for graphical convenience we have chosen a mixing angle such that EFT agrees with the UV model for low values of the expansion parameter. HEFT instead provides a better convergence also in this case allowing a good accordance wit the UV model also for higher mixing angles. Given that agreement between HEFT and SMEFT is found only for small mixing angles, we have restricted the range for values of the mixing angle much more with respect to the VBF case. In addition to small mixing angles we have to take into account the separation of the mass scales that appear in the expressions of the couplings (5.1),(5.2),(5.3),(5.4). This is the reason why points referring to the physical mass scale below 1 TeV seem to be displaced with respect to the rest of the points.

At the squared amplitude level we agree with the statements made at the coupling level for Higgs-fermion interaction i.e. the SMEFT can reproduce UV model only for low values of the mixing angle while HEFT shows a better convergence. Therefore we conclude that SMEFT is a reliable EFT description only for low mixing angles.

Another effect that may be inferred from the plots: SMEFT departs from UV prediction at lower values of $r$ as the scale $s$ grows. This can be understood by looking at eq. (5.16) where in the limit $s \gg m_t^2, m^2$ the anomalous couplings $c_t$ and $\kappa_\lambda$ are suppressed and we get $\mathcal{M}_{tthh} \sim c_{2t}$ which can enhance significantly the cross section in ggF [28].
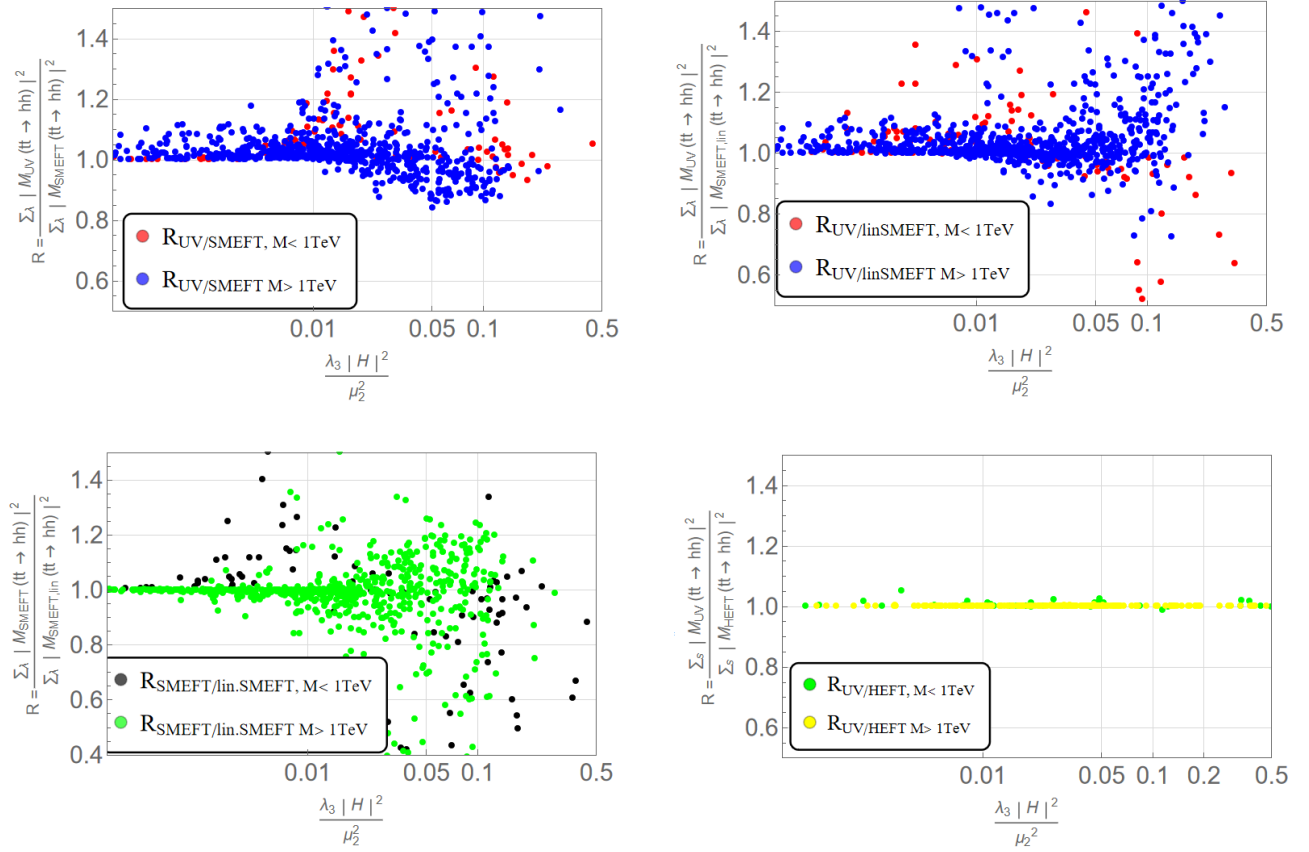
Figure 5.7: We display the UV model prediction divided by the SMEFT prediction (upper left), the UV prediction divided by linearised SMEFT (upper right), the full SMEFT prediction divided by the linearised SMEFT prediction (lower left) and the UV prediction divided by and HEFT (lower right). These plots refer to $s = 0.5$ TeV and $M \in [500, 3000]$ GeV.
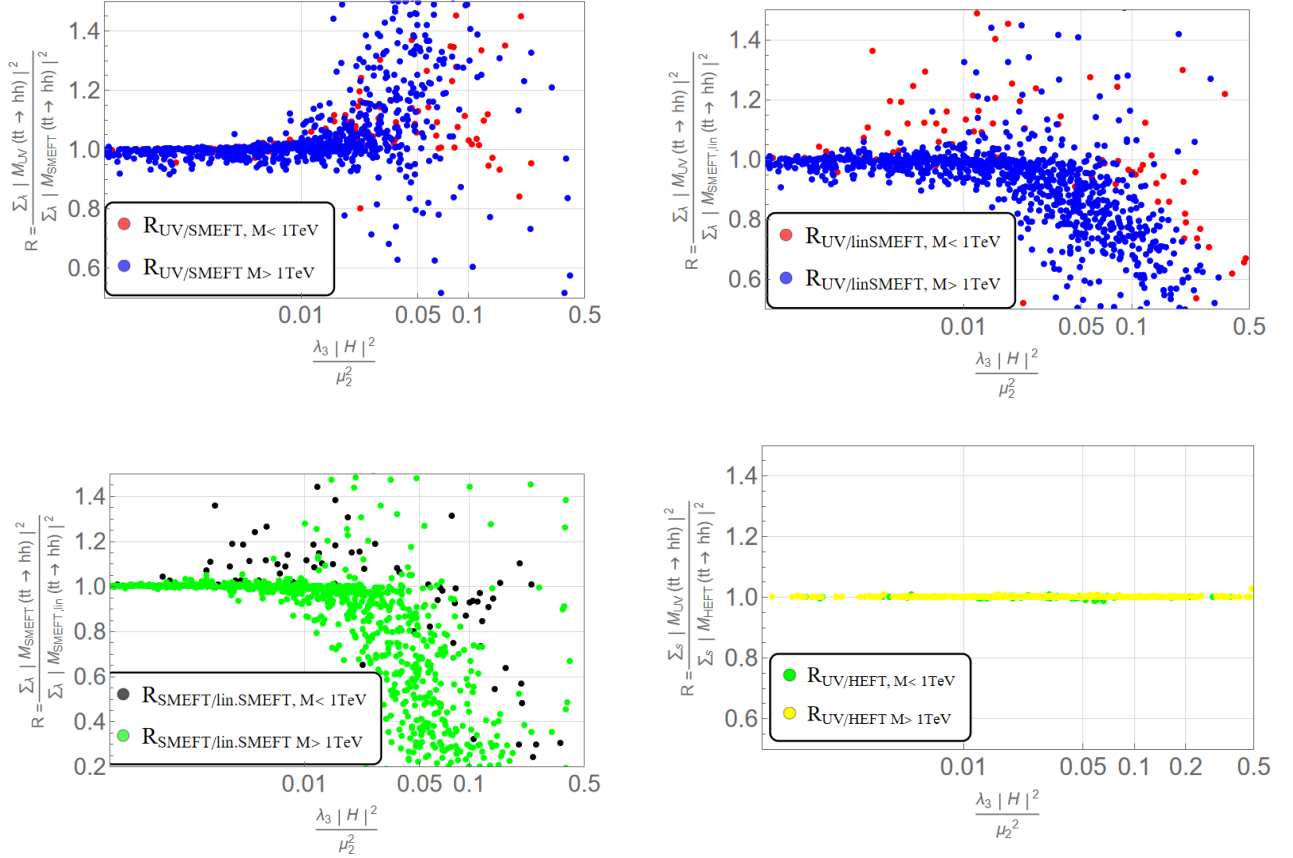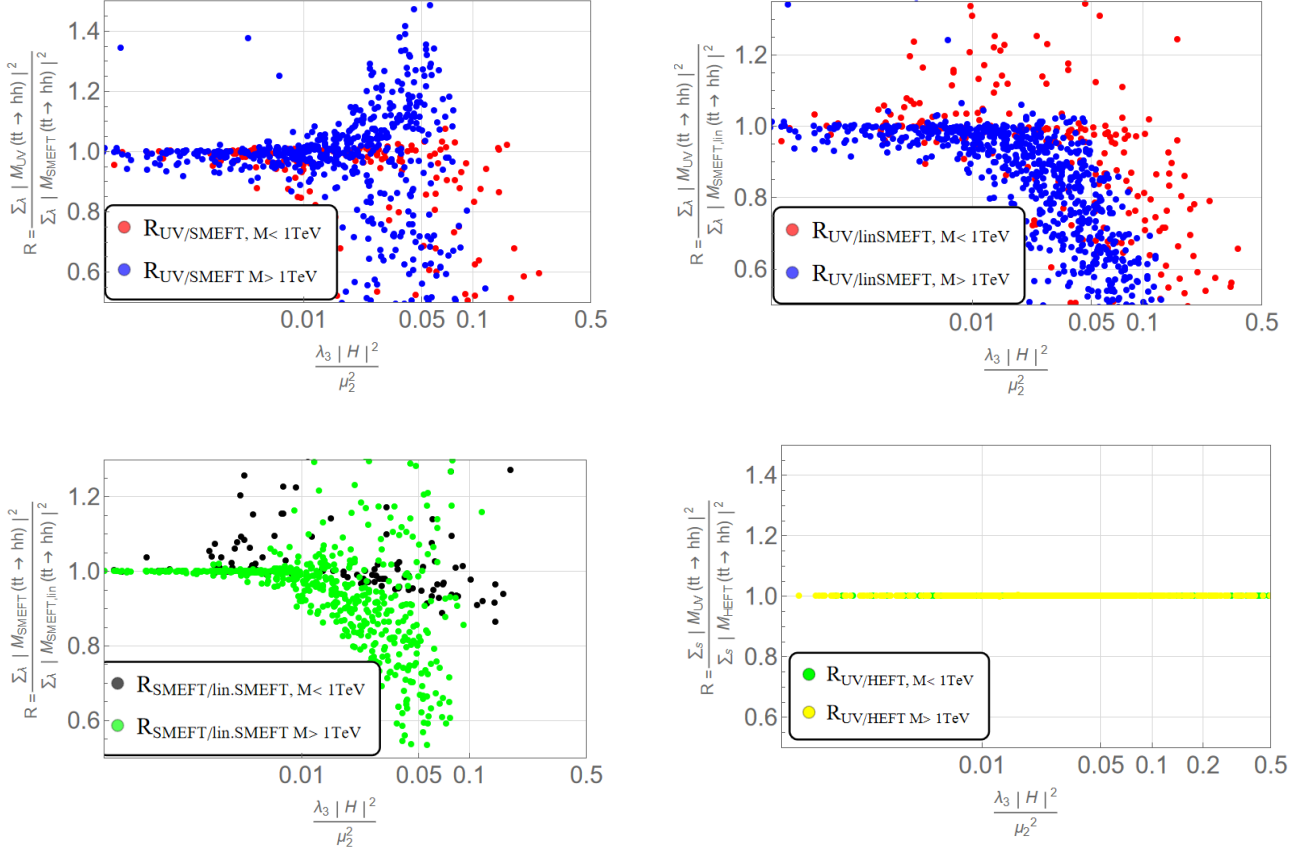
Figure 5.8: We display the UV model prediction divided by the SMEFT prediction (upper,left), the UV prediction divided by linearised SMEFT (upper,right), the full SMEFT prediction divided by the linearised SMEFT prediction (lower, left) and the UV prediction divided by and HEFT (lower,right). These plots refer to $s = 1\text{TeV}$ and $M \in [500, 3000]\text{GeV}$.

Figure 5.9: We display the UV model prediction divided by the SMEFT prediction (upper,left), the UV prediction divided by linearised SMEFT (upper,right), the full SMEFT prediction divided by the linearised SMEFT prediction (lower, left) and the UV prediction divided by and HEFT (lower,right). These plots refer to $s = 1.5\text{TeV}$ and $M \in [500, 3000]\text{GeV}$.

Note in addition the significant difference between the SMEFT prediction and the linear SMEFT while in the VBF their prediction were similar up to $r \simeq 1$.

# Chapter 6

# Colored scalar

So far we have been focusing only on the Higgs interactions with fermions or electroweak gauge bosons. In this chapter, we will focus instead on a colored state that can generate effetive vertices of the Higgs boson to gluon as those can modify the main Higsg pair production channel i.e. gluon gluon fusion (ggF).

There is yet another reason why we have selected this colored model: it appears in the list of Loryon particles [8], namely it is a good candidate to show different predictions between the two EFTs of the Higgs bosons we are considering throughout this work. In addition, this model will not produce a new resonance in di-Higgs production but rather indirectly affect the cross section which is hence qualitatively very different from the singlet model discussed before. With respect to the scalar singlet case now we deal with 1-loop amplitudes in the UV model. In the first section we define the model and the associated Feynman rules. After that we pass to the matching onto the HEFT and SMEFT lagrangian. A final comment on the effective couplings involved will show clearly under which additional conditions SMEFT can be derived from HEFT.

## 6.1   Model

In this section we enlarge the SM spectrum with a complex colored scalar $\omega_1$ whose charges under the SM group are $(3, 1)_{-1/3}$. This particle couples to the SM Higgs doublet and to gluons via the lagrangian :

$$\mathcal{L} \supset D_\mu \omega_1^\dagger D^\mu \omega_1 - M_{ex}^2 \omega_1^\dagger \omega_1 - \frac{c_{\lambda h}}{2} \omega_1^\dagger \omega_1 H^\dagger H, \tag{6.1}$$

$$D_\mu \omega_1 = \left( \partial_\mu - i g_3 G_\mu^a T^a - i g_1 Y B_\mu \right) \omega_1, \tag{6.2}$$

where $T^a = \frac{\lambda^a}{2}$ are the Gell-Mann matrices an $a = 1, 2, ..8$. In eq. (6.1), the first term contains the covariant derivative which couples $\omega_1$ to the gauge sector, the second piece is the explicit mass term and the last one represents a Higgs-portal interaction which provides another mass contribution to $\omega_1$

in the broken phase. In other words after EWSB the physical mass of the new particle is given by:

$$M_{ph}^2 = M_{ex}^2 + \frac{c_{\lambda h}}{4} v^2 \,. \tag{6.3}$$

The latter being a particular case of the general formula (1.67). The new field $\omega_1^i$ has an internal index $i = 1, 2, 3$ labeling the color state i.e. it is a triplet under color hence transforming in the fundamental representation of $SU(3)_C$. Let $U(x)$ be an element of $SU(3)_C$ gauge group, then the field and its covariant derivative transform as;

$$\omega_1 \to \omega_1' = U(x)\omega_1 \,, \quad \text{and} \quad (D_\mu \omega_1)' = U(x)(D_\mu \omega_1) \,. \tag{6.4}$$

In order to evaluate the scattering amplitudes of this NP model we should work out the relative Feynman rules. We note that $D_\mu \omega_1 (D^\mu \omega_1)^\dagger$ gives the Feynman Rules of scalar electrodynamics where the gauge group is not the photon field $A_\mu$ rather it's a non abelian-one yielding an internal structure that does matter in this particular coupling between $\omega_1$ and the gauge bosons $g$.



$$= ig_3(p_2 + p_1)^\mu (T^a)_{i,j}, \qquad = ig_3^2 g_{\mu\nu}(T^a)_{i,k}(T^b)_{k,j} \,. \tag{6.5}$$

The other Feynman rules of the model describe the interaction between $\omega_1$ and the Higgs boson:



$$= -i\frac{c_{\lambda h}}{2} v \delta^{i,j}, \qquad = -i\frac{c_{\lambda h}}{4} \delta^{i,j} 2!, \tag{6.6}$$

where $i, j$ are color indices of $\omega_1$ while $a, b = 1, ..., 8$ label different generators in $SU(3)_C$.// The relevant diagrams for Higgs pair production are given in tab.6.2. From a naive dimensional analysis one would expect logarithmic divergences to arise therefore a dimensional regularization prescription (DR) is adopted in order to regularise the loop integrals. We pass to dimension $d = 4 - \epsilon$ and rewrite the strong coupling $g_3 \to \mu^\epsilon g_3$ where $\mu$ is a renormalization group energy scale. Under the assumption of perturbation theory we can write the following scattering amplitude for single Higgs production:

$$i\mathcal{M}_{UV}(gg \to h) = \epsilon_\mu^a \epsilon_\nu^b \delta^{ab} \alpha_S \pi c_{\lambda h} \int \frac{d^d k}{(2\pi)^d} \frac{(2k + p_1)^\mu (2k - p_2)^\nu}{(k^2 - M_{ph}^2)((k + p_1)^2 - M_{ph}^2)((k - p_2)^2 - M_{ph}^2)}$$

$$- \epsilon_\mu^a \epsilon_\nu^b \delta^{ab} \alpha_S \pi c_{\lambda h} 2 g^{\mu\nu} \int \frac{d^d k}{(2\pi)^d} \frac{1}{(k^2 - M_{ph}^2)((k + p_1)^2 - M_{ph}^2)((k - p_2)^2 - M_{ph}^2)} \,. \tag{6.7}$$

Note this is a genuine 1-loop process, with no tree-level diagrams, thus the cross section will be at least of order $\alpha_S^2$. While in principle the model matches also to other Wilson coefficients such as the one modifying the trilinear Higgs self-coupling, those contributions are not relevant for our analysis as they enter at a higher-loop order since the SM contribution is already one-loop order. The effective coupling of the Higgs boson to gluons gives a tree-level contribution to the amplitude. So matching the Higgs gluon coupling at one-loop level in total gives the same loop order as the SM contribution. In our analysis of the double Higgs production we need $\mathcal{M}_{UV}(g(p_1)g(p_2) \to h(p_3)h(p_4))$. Following the literature [73] we write the scattering amplitude as a linear combination of two orthogonal Lorentz structures $T_1^{\mu\nu}$ and $T_2^{\mu\nu}$ satisfying the Ward identity:

$$\mathcal{M}_{UV}(gg \to hh) = -i\frac{G_F \alpha_S(\mu_R) Q^2}{2\sqrt{2}\pi}\epsilon_\mu^a \epsilon_\nu^b \left(F_1 T_1^{\mu\nu} + F_2 T_2^{\mu\nu}\right)\delta_{ab}\,, \tag{6.8}$$

$$F_1 = C_\triangle F_\triangle + F_\square, \qquad F_2 = G_\square\,. \tag{6.9}$$

where $Q = (p_1 + p_2)^2$ and $G_F$ is the Fermi constant. The momenta $p_1$ and $p_2$ refer to the gluons. The expressions for form factors $F_\triangle, F_\square, G_\square$ depend on the physical scales of the process such as $m, M_{ph}, s$. Their expressions in terms of Passarino Veltman integrals are quite lengthy and are given in [74]. We note that the form factors are finite. Hence there is no parameter in the new UV Lagrangian that needs to be renormalized.

Nevertheless we adopt a regularisation scheme as in intermediate steps there are divergencies. We find it convenient to express our results in the language of dimensional regularization fixing the renormalization scale $\mu_R$ appearing in $\alpha_S$ to a different scale depending on the required matching condition.

Note that $\alpha_S$ is a running parameter and its running effects give sensible contributions that can't be neglected.

## 6.2 HEFT matching

As far as the matching onto the HEFT lagrangian is concerned we exploit a diagrammatic approach where we impose an equivalence between the same matrix element computed both in the UV theory and in the EFT framework, which allows us to extract the form of $c_{ggh}$ and $c_{gghh}$ depending on the matrix element we consider. These effective vertices are parametrized in terms of $c_{ggh}$ and $c_{gghh}$. The corresponding scattering amplitudes written in the HEFT framework are:

$$i\mathcal{M}_{HEFT}(g(p_1)g(p_2) \to h(p_3)) = i\frac{\alpha_S}{\pi}\epsilon_\mu^a \epsilon_\nu^b \delta^{ab} \frac{1}{v} c_{ggh}\left(p_1^\nu p_2^\mu - p_1 \cdot p_2 g^{\mu\nu}\right) \tag{6.12}$$

$$i\mathcal{M}_{HEFT}(g(p_1)g(p_2) \to h(p_3)h(p_4)) = i\frac{\alpha_S}{\pi}\epsilon_\mu^a \epsilon_\nu^b \delta^{ab} \frac{1}{v^2}\left(c_{gghh} + \frac{3m_h^2}{s - m_h^2}c_{ggh}\kappa_\lambda\right)\left(p_1^\nu p_2^\mu - p_1 \cdot p_2 g^{\mu\nu}\right) \tag{6.13}$$

$$i\mathcal{M}_{HEFT}(g(p_1)g(p_2) \to h(p_3)) = \qquad\qquad \text{(6.10)}$$

$$i\mathcal{M}_{HEFT}(g(p_1)g(p_2) \to h(p_3)h(p_4)) = \qquad + \qquad \text{(6.11)}$$

Table 6.1: relevant vertices in the EFT formulation of ggF process.

We can proceed in the usual way equating amplitudes in HEFT with that in the UV model together with the assumption that $E \ll M$. We have collected the Feynman diagrams relevant in the matching procedure in tab. 6.2. The UV theory includes many others diagrams for the $\mathcal{M}_{UV}(gg \to hh)$ matrix element such as those with three and four gluon vertices however they are zero for color.

Even though the EFT limit requires to compute a tree level amplitude in terms of effective couplings, the UV side is a purely $1-$loop process. In the Appendix C we report the explicit calculation for a diagrammatic matching leading to:

$$c_{ggh} = \frac{1}{6} \frac{c_{\lambda h} v^2}{(4M_{ex}^2 + c_{\lambda h} v^2)} \,. \qquad \text{(6.16)}$$

The diagrammatic matching for $c_{gghh}$ is a bit more involved. We do not need all the diagrams in the $\mathcal{M}(gg \to hh)$ to come up with an expression for $c_{gghh}$ as many of them give contributions proportional to $c_{ggh}$ and/or $c_{hhh}$.

Therefore with respect to 6.15 we focus on the first four diagrams: the first and the second are simply obtained from those in $c_{ggh}$ replacing $\frac{c_{\lambda h}v}{2} \to \frac{c_{\lambda h}v}{4}$, the third and the fourth together with variants with external legs exchanged give a contribution only at $\mathcal{O}\left(\frac{1}{M_{ph}^4}\right)$ because the less suppressed terms $\mathcal{O}\left(\frac{1}{M_{ph}^2}\right)$ vanish once all the diagrams are considered. Thus if we stopped at $\mathcal{O}\left(\frac{1}{M_{ph}^2}\right)$ we would have the following relation:

$$c_{gghh}^{\text{HEFT}} = \frac{1}{2}c_{ggh}^{HEFT} + \mathcal{O}\left(\frac{1}{M_{ph}^4}\right) \,. \qquad \text{(6.17)}$$

In that case we would have no dependence on the momenta $p_3, p_4$ of the Higgs bosons in the final state and the associated Lorentz structure would have been given just by $p_1^\nu p_2^\mu - p_1 p_2 g^{\mu\nu}$ which satisfy the Ward Identity.

In the ggF literature [73, 75, 76] two Lorentz structures arise: one is recovered by our computation while the other is indeed proportional to $p_3$ and $p_4$, we are going to neglect the latter as it gives contributions that are higher order in $M_{ph}$.

$$i\mathcal{M}_{UV}(gg \to h) = \quad + \quad \tag{6.14}$$



$$i\mathcal{M}_{UV}(gg \to hh) \supset \quad + \quad + \tag{}$$



$$+ \quad + \quad +$$

$$+ \text{ (box diagrams exchanging final legs)} \tag{6.15}$$

Table 6.2: Relevant vertices for the matching of the colored UV model to the EFTs basis, note that diagrams with three gluon vertices are zero for color.

## 6.3 SMEFT

One of the assumption of SMEFT to be a predictive field theory is that BSM physics must be weakly coupled to SM.

This means that NP has a characteristic scale which is far from EW scale, from a top-down prospective this means $M_{ph}^2 = M_{ex}^2 + c_{\lambda h}v^2 \simeq M_{ex}^2$. In this scenario we integrate the new colored scalar out and subsequently we break the EW symmetry, thus the hypothetical new particle does not interfere with EWSB.

While the scalar singlet allows for a tree level the colored scalar gives pure 1-loop contribution to Higgs pair production and must integrated out using functional methods. The latter becomes clear when we solve the classical E.o.M. for $\omega_1$ from 6.1:

$$\left(D^2 + M_{ex}^2 + \frac{c_{\lambda h}}{4}|H|^2\right)\omega_1 = 0 \to \omega_1^C = 0\,. \tag{6.18}$$

Since $\omega_1^C$ vanishes at tree level, the contribution from NP to the effective lagrangian arises only at 1-loop.

### 6.3.1 Functional matching

We want to exploit the functional matching procedure which is easier to handle with respect to the diagrammatic approach. In the functional matching one imposes a relation at the level of the action and one does not need to enumerate all possible Feynman diagrams allowed in a specific model and consequently there's no need to work out the relative Feynman rules. It consists in the evaluation of one particle irreducible effective action $\Gamma_{1PI}$ (1PI) both in the UV theory and in the EFT. In particular we are interested in the $1PI$ actions where external states are only given by light fields, the so-called light particle irreducible action ($1LPI$). Under the assumption of perturbation theory the following relation holds for $\Gamma^l_{UV/EFT}$ at any order, where we indicate the loop counting by $l$ :

$$\Gamma^{(0)}_{L,EFT}[H,\Psi_{SM}] = \Gamma^{(0)}_{L,UV}[H,\Psi_{SM}], \tag{6.19}$$

$$\Gamma^{(1)}_{L,EFT}[H,\Psi_{SM}] = \Gamma^{(1)}_{L,UV}[H,\Psi_{SM}], \tag{6.20}$$

where $H$ denotes the Higgs field while $\Psi_{SM}$ stands for all the other SM fields. In general terms the 1PI effective action $\Gamma_{UV}[H]$ is a fucntional of both the light fields and the heavy one. $\Gamma_{UV}$ the tree level piece and the one loop level piece are respectively given by:

$$\Gamma^{(0)}_{UV}[H,\Psi_{SM},\omega_1] = S_{UV}[H,\Psi_{SM},\omega_1],$$

$$\Gamma^{(1)}_{UV}[H,\Psi_{SM},\omega_1] = i\log\det\left(-\frac{\delta^2 S_{UV}[H,\Psi_{SM},\omega_1]}{\delta(H,\Psi_{SM},\omega_1)^2}\right). \tag{6.21}$$

This functional is not the $\Gamma_{L,UV}$ yet as it still depends on the heavy field $\omega_1$, however the $\Gamma_{L,UV}$ can be easily obtained by exploiting the Equations of motion:

$$\Gamma^{(0)}_{L,UV}[H,\Psi_{SM}] = S_{UV}[H,\Psi_{SM},\omega_{1,C}],$$

$$\Gamma^{(1)}_{L,UV}[H,\Psi_{SM}] = i\log\det\left(-\frac{\delta^2 S_{UV}[H,\Psi_{SM},\omega_1]}{\delta(H,\Psi_{SM},\omega_1)^2}\bigg|_{\omega_1=\omega_{1,C}}\right). \tag{6.22}$$

We can proceed in a similar way for the EFT side where the 1PI effective action is already a $1LPI$ as there is no heavy field. The tree level part contains all the effective operators with their Wilson Coefficient, the one loop part contains in principle the same operators but their Wilson coefficients are 1-loop sized, i.e. they are suppressed by a loop factor:

$$\Gamma^{(0)}_{L,EFT}[H,\Psi_{SM}] = S^{(0)}_{EFT}[H,\Psi_{SM}],$$

$$\Gamma^{(1)}_{L,EFT}[H,\Psi_{SM}] = S^{(1)}_{EFT}[H,\Psi_{SM}] + i\log\det\left(-\frac{\delta^2 S^{(0)}_{EFT}[H,\Psi_{SM}]}{\delta(H,\Psi_{SM})}\right). \tag{6.23}$$

In our case we are considering the Warsaw basis as the EFT and it's written in terms of dimension 6 operators. Because of the fact that $\omega_1^C = 0$, the matching condition between $\Gamma^0_{L,UV}$ and $\Gamma^{(}_{EFT}0)$ does not give any result. This entails no effective operators of the Warsaw basis are generated at tree level. We must pass to the one loop contribution of $\Gamma_{L,UV}$ that in general is quite involved. In this model

we deal with loops where only heavy fields are circulating, in this case $\Gamma_{L,UV}^{(1)}$ can be easily computed. We can rewrite the functional determinant of $\Gamma_{L,UV}$ embedding all the SM fields into H:

$$\log \det \begin{pmatrix} \frac{\delta^2 S_{UV}[H,\Psi_{SM},\omega_1]}{\delta(\omega_1,\omega_1)} & \frac{\delta^2 S_{UV}[H,\omega_1]}{\delta(H,\omega_1)} \\ \frac{\delta^2 S_{UV}[H,\omega_1]}{\delta(H,\omega_1)} & \frac{\delta^2 S_{UV}[H,\omega_1]}{\delta(H,H)} \end{pmatrix} \Bigg|_{\omega_1 = \omega_1^C} = \log \det \left( \frac{\delta^2 S_{UV}[H,\omega_1]}{\delta(\omega_1,\omega_1)} \right) \Bigg|_{\omega_1 = \omega_1^C} + \log \det \left( \frac{\delta^2 S_{UV}[H,\omega_1]}{\delta(H,H)} \right) \Bigg|_{\omega_1 = \omega_1^C}.$$

$$(6.24)$$

Note that we impose $\omega_1 = \omega_1^C$ after the functional trace and the functional determinant are evaluated. We can then compute the functional determinant exploiting the fact that $\omega_1^C = 0$, thus $\Gamma_{L,UV}^{(1)}$ is diagonal, finally the basic properties of the logarithms leads to the expression above.

We keep the explicit expression of functional determinant as $H$ and $\omega_1$ could be multiplets that can be decomposed further. By imposing (6.20) we appreciate how the functional determinant of only the light fields simplifies and we are left with:

$$\Gamma_{L,UV}^{(1)} = \log \det \left( \frac{\delta^2 S_{UV}[H,\omega_1]}{\delta(\omega_1,\omega_1)} \right) = \Gamma_{L,EFT}^{(1)} = S_{EFT}^{(1)}[H] \,. \tag{6.25}$$

Equation 6.22 can be derived adopting the path integral formalism, in particular we integrate over the heavy field configurations:

$$e^{i\Gamma_{eff}(H)(\mu)} = \int \mathcal{D}\omega_1 e^{iS[H,\omega_1](\mu)} \,.$$

This relation defines the effective action at the scale $\mu = M_{ex}$ where we match the UV theory to the effective one. In these steps the SM fields are treated as a classical background [1].

A standard way to proceed is to express $\omega_1$ as $\omega_1 = \omega_1^c + \tilde{\omega}_1$ and expanding close to its minimum given by the classical field configuration:

$$S[\phi, \omega_1^c + \tilde{\omega}_1] = S[\omega_1^c] + \frac{1}{2} \frac{\delta^2 S}{(\delta\omega_1)^2} \bigg|_{\omega_1^c} + \mathcal{O}\left(\tilde{\omega}_1^3\right) \,. \tag{6.26}$$

By using method of steepest descendent, one loop contribution to the effective action boils down to the evaluation of a functional determinant:

$$i \log \det \left( D^2 + M_{ex}^2 + \frac{c_{\lambda h}}{2} |H|^2 \right) = i \text{Tr} \log \left( D^2 + M_{ex}^2 + \frac{c_{\lambda h}}{2} |H|^2 \right) \tag{6.27}$$

where Tr is a trace over internal and external degrees of freedom. It turns out that $(D^2 + M_{ex}^2 + \frac{c_{\lambda h}}{2}|H|^2)$ is an elliptic operator that can be always computed using a covariant derivative expansion (CDE) which is a way of performing one loop evaluations keeping gauge covariance of formulas at each step [58].

---

[1] $\Gamma_{eff}$ can be considered as a Wilsonian action where we have integrated out shell of momenta $\Lambda_0 < p < \Lambda$ where $M > \Lambda_0$. In this way non localities do not show up in $\Gamma_{eff}$ and an expansion in terms of local operators is possible.

Following [77] it is possible to rewrite the functional trace as:

$$\text{Tr}\Big[\frac{1}{-D^2 - M_{ex}^2}\frac{c_{\lambda h}}{2}|H|^2\Big] = \text{tr}\int d^4x \int \frac{d^4p}{(2\pi)^4}\sum_{n=0}^{\infty}\Big[\frac{1}{p^2 - M_{ex}^2}(2ip_\mu D^\mu + D^2)\Big]^n \frac{1}{p^2 - M_{ex}^2}\frac{c_{\lambda h}}{2}|H|^2,$$

$$(6.28)$$

where `tr` on the right hand side stands for trace over internal degrees of freedom. Recalling that odd powers of $p^\mu$ vanishes after integration and that crucially $G_{\mu\nu} \equiv [D_\mu, D_\nu]$ we obtain the following contributions for the functional trace [58] valid for a single mass scale in the loop:

$$\text{Tr}\Big[\frac{1}{-D^2 - M_{ex}^2}\frac{c_{\lambda h}}{2}|H|^2\Big] \supset \int d^4x \frac{-i}{(4\pi)^2}\text{tr}\Big\{M_{ex}^2\Big[\Big(-\log\Big(\frac{M_{ex}^2}{\mu^2}\Big)+1\Big)\frac{c_{\lambda h}}{2}|H|^2\Big]$$
$$+M_{ex}^0\Big[-\frac{1}{2}\log\Big(\frac{M_{ex}^2}{\mu^2}\Big)\Big(\frac{c_{\lambda h}}{2}|H|^2\Big)^2 - \frac{1}{12}\Big(\log\Big(\frac{M_{ex}^2}{\mu^2}\Big)-1\Big)G_{\mu\nu}G^{\mu\nu}\Big]$$
$$+\frac{1}{M_{ex}^2}\Big[\frac{-1}{6}\Big(\frac{c_{\lambda h}}{2}|H|^2\Big)^3 - \frac{c_{\lambda h}}{24}|H|^2 G_{\mu\nu}G^{\mu\nu} + \frac{c_{\lambda h}}{24}\big(D_\mu|H|^2\big)^2$$
$$+\frac{1}{60}\big(D_\mu G^{\mu\nu}\big)^2\Big]+\mathcal{O}\Big(\frac{1}{M_{ex}^4}\Big)\Big\}.$$

$$(6.29)$$

Already at this level we can see that integrating out $\omega_1$ generates one relevant operator that corrects the mass of the Higgs, as well as other irrelevant operators of dimension 6. The logarithmic divergences that show up can be removed by renormalization by a redefinition of the Higgs mass (1st line) and Higgs quartic coupling (2nd line).

As a first step we bring this lagrangian to the Warsaw basis such that it becomes clear we are generating $O_H$, $O_{H\square}$ and $O_{HG}$ at one loop level as they are suppressed by $\frac{1}{16\pi^2}$. Functional matching does not know anything about the set of operators of the EFT basis and does not give in general a minimal set of effective operators, in other words $\Gamma_{L,UV}$ may contain redundancies.

The same procedure can be automatically implemented through the `Matchete` program [62]. This tool is based on a functional matching routine and can be used to study weakly interacting BSM theories. As far as the scattering amplitudes in SMEFT framework are concerned, we note that they correspond to the expressions of $\mathcal{M}_{HEFT}$ with the additional constraint that $c_{gghh} = \frac{1}{2}c_{ggh}$ where $M_{phys}$ is replaced by $M_{ex}$, leading to :

$$c_{ggh}^{\text{SMEFT}} = \frac{c_{\lambda h}v^2}{24M_{ex}^2}, \qquad\qquad c_{gghh}^{\text{SMEFT}} = \frac{1}{2}\frac{c_{\lambda h}v^2}{(24M_{ex}^2)}.$$

This linear relation among the couplings is again a consequence of the symmetry constraints imposed in the SMEFT framework being $H$ a doublet under SU(2). A physically meaningful limit relate these expressions of $c_{ggh}$ and $c_{gghh}$: considering the case of $M_{ex} \gg c_{\lambda h}v^2$ and neglecting orders in $1/M_{ex}^4$ we explicitly find that HEFT and SMEFT coefficients coincide.

## 6.4 Low Energy Theorem

It is possible to recover the same results of the HEFT matching section adopting a low energy theorem (LET) [78, 79], which is an elegant way to get analytical structure of multi Higgs boson couplings. LET treats Higgs boson as a background field with a low momentum such that $H$ is very close to its vacuum configuration. Following [79] we can think of $gg \rightarrow hh$ process as the QCD vacuum polarization where two (or more) external Higgs bosons are attached to the heavy particle loop where the heavy particle loop can consist of BSM particles, the top quark or the massive gauge bosons.

In the LET, we assume that the Higgs boson momentum is vanishing, namely the Higgs field is kept to a constant value. In these conditions, interactions with Higgs field are formally equivalent to a redefinition of the heavy particle mass. At the lagrangian level we have [78]:
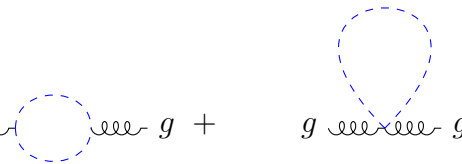
$$\mathcal{L}_{h^n gg} = \frac{g_3^2}{96\pi^2} G_{\mu\nu}^a G^{a\mu\nu} \left( A_1 h + \frac{1}{2} A_2 h^2 + ... \right) . \tag{6.30}$$

where we have defined :

$$A_n \equiv \left( \frac{\partial^n}{\partial v^n} \log \det \mathcal{M}_{mass}^2(v) \right) , \tag{6.31}$$

where $\mathcal{M}_{mass}^2 = \mathcal{M}_{mass}^\dagger \mathcal{M}_{mass}$ is mass matrix of the new heavy particles interacting with the higgs field. In our case we are interested in $A_1$ and $A_2$ standing for the effective couplings between the Higgs and gluons. In the following we are integrating out just the $\omega_1$ particle leaving the other particles as dynamical degrees of freedom, thus the determinant of the mass matrix reduces to $\mathcal{M}_{mass}^2 = M_{ex}^2 + \frac{c_{\lambda h} v^2}{4}$.

Diagrammatically these effective couplings can be obtained by a QCD vacuum diagram corrected by loops of $\omega_1$ where we attach n external legs of the higgs field h . The general form of QCD vacuum polarization in the case of the new colored scalar is:

$$i4\pi\alpha_S \Pi_{ab}^{\mu\nu} = \; g \;\text{〰〰}\bigcirc\text{〰〰}\; g \;+\; g \;\text{〰〰〰}\; g \;\;\; = i4\pi\alpha_S(p^\mu p^\nu - p^2 g^{\mu\nu})\Pi(p^2)\delta^{ab}, \tag{6.32}$$

where $p$ is the gluon momenta and $\alpha_S = \frac{g_3^2}{4\pi}$ . The second diagram is proportional to $\Pi^{\mu\nu} \simeq p^2 g^{\mu\nu} \Pi$, given that the Higgs boson in LET has vanishing momenta and that the Higgs boson momenta is equal to the gluon momenta by momentum conservation. It follows that this diagram does not contribute. So we take into account only the bubble diagram in our analysis. [2]

Factorizing out the tensorial part the explicit expression for the scalar quantity is given in dimensional

---

[2]For the sake of completeness a tadpole diagram should be considered in the QCD vacuum polarization however it vanishes due to color conservation.

regularization by[3] :

$$\Pi^{\omega_1}(p^2) = \frac{\Delta_\epsilon}{16\pi^2} - \frac{1}{16\pi^2} \int_0^1 dx(1-2x)^2 \log\left(\frac{M_{phys}^2(v) - p^2 x(1-x)}{\mu^2}\right). \qquad (6.33)$$

The first term contains the divergent part of the bubble diagram. The second terms is given by the the bubble diagram and contains the field dependent mass of the new particle. If we focus on the scalar part of the QCD vacuum polarization in the limit of vanishing momentum for the Higgs we can expand $\Pi[v+h](p=0)$ getting the coefficients corresponding to $c_{ggh}$ and to $c_{gghh}$. Thus we can Taylor expand around v:

$$\Pi[v+h](0) \simeq \Pi(0) + h\frac{\partial\Pi[v](0)}{\partial v} + \frac{h^2}{2}\frac{\partial^2\Pi[v](0)}{(\partial v)^2} + ..., \qquad (6.34)$$

inserting it back into (6.30) clearly gives us the explicit form of $c_{ggh}$ and $c_{gghh}$.

Note also that the same Lagrangian contains $gggh, ggggh$ as well as $ggghh, gggghh$ vertices due to the Non-Abelian nature of $G_{\mu\nu}$ field strength tensor. In other words we can say:

$$c_{ggh} = v\frac{\partial\Pi[v]}{\partial v} = \frac{1}{6}\frac{c_{\lambda h}v^2}{4M_{ex}^2 + c_{\lambda h}v^2}, \qquad (6.35)$$

$$c_{gghh} = \frac{v^2}{2}\frac{\partial^2\Pi[v](0)}{(\partial v)^2} = \frac{1}{12}\left[\frac{c_{\lambda h}v^2}{4M_{ex}^2 + c_{\lambda h}v^2} - 2\left(\frac{c_{\lambda h}v^2}{4M_{ex}^2 + c_{\lambda h}v^2}\right)^2\right]. \qquad (6.36)$$

The same result is recovered in the HEFT matching procedure where we have assumed the heavy (physical) mass limit of the colored scalar, namely the two procedures are explicitly shown to be equivalent at order $1/M_{phys}^2$.

## 6.5  HEFT and SMEFT at the level of the couplings

We comment on the relations between $c_{ggh}$ and $c_{gghh}$ worked out in the different EFTs frameworks. From the results obtained above one can interfere that under the assumption $M_{ex}^2 \gg c_{\lambda h}v^2$ the couplings found in the matching to the HEFT lagrangian reduce to those obtained in the matching to SMEFT. This can be seen in :

$$c_{ggh}^{\text{HEFT}} = \frac{1}{6}\frac{c_{\lambda h}v^2}{4M_{ex}^2 + c_{\lambda v^2}} \xrightarrow{M_{ex}^2 \gg c_{\lambda v^2}} \frac{c_{\lambda h}v^2}{24M_{ex}^2}\left[1 - \frac{c_{\lambda h}v^2}{4M_{ex}^2} + \mathcal{O}\left(\frac{1}{M_{ex}^4}\right)\right], \qquad (6.37)$$

where the first contribution is indeed the SMEFT result, and the second term is higher order in $1/M_{ex}^2$. Again this holds true only in the so called decoupling limit where we have the freedom to take the $M_{ex}$ parameter high enough such that it satisfies $M_{ex}^2 \gg c_{\lambda h}v^2$. If the Higgs dependent mass of $\omega_1$ is comparable with $M_{ex}$ then HEFT does not converge to SMEFT prediction because terms of higher

---

[3]In the case a hard cut off was used as a regulator we would have to add $\delta\mathcal{L} = \frac{\alpha_S}{24\pi}G_{a,\mu\nu}G^{a,\mu\nu}\ln\frac{\Lambda^2}{M_{ph}^2}$ for the one loop contribution, so this result is independent from the regularization scheme adopted.

order in $\frac{c_{\lambda h} v^2}{M_{ex}^2}$ cannot be neglected anymore.

This holds also for the $c_{gghh}$ coupling up to $\mathcal{O}\left(\frac{1}{M_{ex}^4}\right)$ corrections, assuming again that $M_{ex}$ is the dominant contribution of the physical mass:

$$c_{gghh}^{\text{HEFT}} = \frac{1}{12}\left[\frac{c_{\lambda h} v^2}{4M_{ex}^2 + c_{\lambda h} v^2} - 2\left(\frac{c_{\lambda h} v^2}{4M_{ex}^2 + c_{\lambda h} v^2}\right)^2\right] \xrightarrow{M_{ex}^2 \gg c_{\lambda h} v^2} \frac{c_{\lambda h} v^2}{48 M_{ex}^2}\left[1 - \frac{c_{\lambda h} v^2}{4M_{ex}^2} + \mathcal{O}\left(\frac{1}{M_{ex}^4}\right)\right].$$
(6.38)

Thus If we restrict $c_{gghh}^{\text{HEFT}}$ to its lowest order contribution in $\frac{1}{M_{ph}^2}$ and in addition to that we assume $M_{ex}^2 \gg c_{\lambda h} v^2$ then it coincides with $c_{gghh}^{\text{SMFET}}$. These considerations suggest that the expansion parameter that is suitable to show the differences between HEFT and SMEFT for the colored scalar model will be most likely related to $r = \frac{c_{\lambda h} v^2}{M_{ex}^2}$. Infact when this quantity is small the couplings in HEFT and SMEFT coincide while in the non decoupling limit $M_{ex}^2 \geq c_{\lambda h} v^2$ HEFT predicts different couplings than SMEFT. From the coupling point of view SMEFT is a local approximation of the more general HEFT framework. We note that Higgs field redefinitions should not spoil this analysis at the level of the couplings as $c_{gghh}$ and $c_{ggh}$ have no tree level contribution. In the VBF for the scalar singlet case it was necessary to work with amplitudes because of the ambiguity that $h$ field redefinition introduced at the level of the coupling. The colored scalar model does not suffer from this as any additional redefinition in $h$ is higher order in the mass suppression. If our aim is to highlight differences between SMEFT and HEFT we may restrict our analysis to the coupling level but including the UV model in the analysis necessarily requires to work at the (squared) amplitude level.

# Chapter 7

# Conclusions

The ultimate aim in the EFT context is to shed light on the scale of new physics that may lead for instance to a better understanding of the EWSB mechanism. With this idea we have analyzed the main differences between two EFT of the Higgs boson, namely SMEFT and HEFT. To do so we have considered processes with two Higgs bosons in the final state. Those processes allow to distinguish between the two EFTs as at dimension-6 in SMEFT single and double Higgs couplings are correlated whereas they are not in HEFT. This holds also true for triple or even more Higgs final states, but in this case the cross section is too small to be accessible at the HL-LHC. The goal of this thesis was to check whether differences in HEFT and SMEFT can be realised in concrete UV models and to investigate how large this differences are in Higsg pair production.

Adopting a Top-Down approach we have selected two models from the Loryon list [34]: a real scalar singlet and complex colored scalar. The UV models were matched to both SMEFT and HEFT, showing already at the level of the couplings that differences between the HEFT and SMEFT description can be realised. In particular, we found that in the singlet model only for small mixing angles the SMEFT matching is accurate.

In the next step, the amplitudes for $W^+W^- \to hh$ and $t\bar{t} \to hh$ were compared to the ones obtained in the UV model. This has shown clearly that SMEFT description of Higgs pair production cannot reproduce the UV model prediction when the new particle gets most of its mass from EWSB. We quantify this by introducing a quantity $r$ that measures the amount of mass that stems from EWSB. In particular when $r \geq 0.5$ in VBF or $r \geq 0.05$ in $t\bar{t} \to hh$ the SMEFT prediction is already 20% off from the UV prediction. HEFT instead is showing a better convergence to the UV model even for large $r$. Therefore we could conclude that SMEFT is not enough to describe di-Higgs production in the limit of high $r$, instead HEFT should be used. In practice we do not know what is the UV completion of the SM and we proceed with a bottom-up approach driven by data. In this sense HEFT stands as a proper EFT formulation even for Loryon-like new particles. In other words if we parametrize new physics in terms of a SMEFT we are cutting away the possibility that it is a Loryon particle while HEFT, being a more general framework can also cover the case of a Loryon particle. Our claim, in its strongest version, is that the upcoming di-Higgs data should be interpreted in HEFT as concrete UV models can realise HEFT even taking into account various constrains ranging from theoretical

ones like perturbative unitarity to experimental ones like Higgs data or electroweak precision tests. We did not investigate whether the differences that we see between the UV model and the SMEFT decrease when going to dimension-8 but leave this to future research. Besides the models discussed in this thesis, there may be more phenomenologically viable models showing differences between HEFT and SMEFT. Those will constitute an additional motivation to adopt an HEFT formulation in the data interpretation.

# Appendix A

# Numerical analysis of a $\mathbb{Z}_2$ symmetric singlet model

In the following we present numerical results of the renormalization group equations for the irrelevant couplings of the singlet model (2.1). Let us mention that the lack of including $A$ and $\mu$ in the analysis should not represent a problem as relevant operators usually vanish under the renormalization group evolution. The idea is to express $\lambda_1$ and $\lambda_2$ in terms of the other parameters of the model:

$$\lambda_1 = \lambda_1 \left( m, M\chi, v, \lambda_3 \right) ,$$
$$\lambda_2 = \lambda_2 \left( m, M\chi, v, \lambda_3 \right) . \tag{A.1}$$

Exploiting relations between $\tan(2\chi)$, $m^2$ and $M^2$ I can express $v_s$ in terms of the other parameters:

$$v_s = \frac{(M^2 - m^2)\sin(2\theta)}{2\lambda_3 v} \tag{A.2}$$

I can substitute it back into the expressions of the physical masses getting formulas for $\lambda_2$ and $\lambda_1$ which are valid at the electroweak scale:

$$\lambda_1 = \frac{m^2}{2v^2} + \sin(\chi)^2 \frac{M^2 - m^2}{2v^2} ,$$
$$\lambda_2 = \frac{2\lambda_3^2}{\sin(2\chi)^2} \frac{v^2}{M^2 - m^2} \left( \frac{M^2}{M^2 - m^2} - \sin(\chi)^2 \right) . \tag{A.3}$$

The next step is to solve numerically the coupled system of seven differential equations (2.49) in `Mathematica`. A major problem is the choice of $\lambda_3$ value at the electroweak scale, since we have no direct experimental measure of it we take a value which respects perturbativity at low energies. In the analysis we require that the perturbativity condition holds for every coupling up to the Planck scale and for negative values of $\lambda_3$ we impose the additional condition $4\lambda_1\lambda_2 > \lambda_3^2$ to ensure vacuum stability. From fig.A.1 we can only conclude that the $\sin(\chi)$ is decreasing by for higher values $M$ this is in accordance with 2.1 of the text.
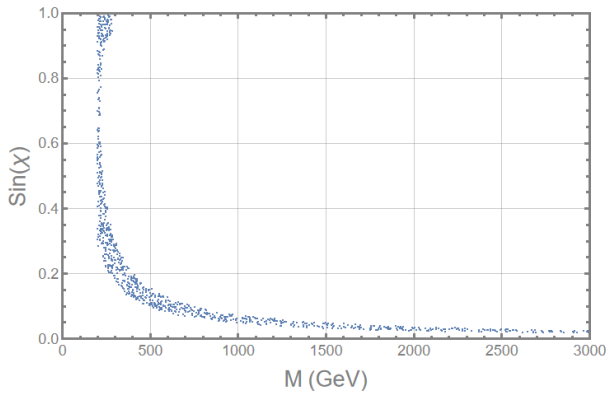
(a) Allowed $\sin(\chi)$ and relative $M$ values.
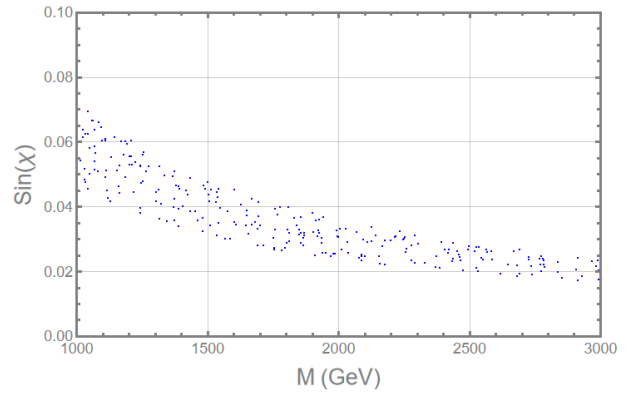
(b) Zoom into the mass range from 1TeV to 3 TeV

Figure A.1: A set of points allowed by RGE are presented in the $\sin(\chi) - M$ plane. In this run we have fixed $\lambda_3$ to have a value of $0.13$ at the electroweak scale.

# Appendix B

# Geometric formulation

Instead of considering the convergence of the effective theory expansion we can highlight the differences between SMEFT and HEFT adopting a geometric approach. The following discussion is largely taken from [9].

We have seen by a suitable change of coordinates that it is possible to pass from the SMEFT to the HEFT formulation, however, there are physical situations where this change of coordinates is not possible.

To address this point one can rely on geometric arguments. Given the fact that the $S$ matrix is invariant under field redefinitions, while the form of the Lagrangian generically is not, can be understood through the geometry of field space with the scalar fields as the coordinates.

If we restrict ourselves to the field redefinition $\tilde{\phi} \to \phi + F(\phi)$ such that $F(\phi) = \phi^N$, i.e. no derivatives involved in the redefinition, we can rewrite the same scattering amplitudes in terms of geometrical objects, see for instance [80]. As far as the scalar sector of the SM is concerned we can split the physical Higgs boson from the Goldstone bosons. Recalling (1.34) we can express the $\vec{\phi}$ field as:

$$\vec{\phi} = (v + h)\mathbf{n}(\pi), \qquad \text{where} \qquad \mathbf{n}(\pi) \in SU(2)_L \otimes SU(2)_R / SU(2)_V, \qquad \text{(B.1)}$$

where $h$ is the radial coordinate while $\mathbf{n}$ is a four-dimensional vector satisying $\mathbf{n} \cdot \mathbf{n} = v^2$ and containing 3 degrees of freedom, namely the Goldstone bosons:

$$\mathbf{n} = \begin{pmatrix} n_1 = \pi_1 \\ n_2 = \pi_2 \\ n_3 = \pi_3 \\ \sqrt{v^2 - \pi_1^2 - \pi_2^2 - \pi_3^2} \end{pmatrix}. \qquad \text{(B.2)}$$

Under the chiral group $\mathcal{G}$ they transform as:

$$h \xrightarrow{\mathcal{G}} h, \qquad \mathbf{n} \xrightarrow{\mathcal{G}} O\mathbf{n}, \qquad O \in \mathcal{G}. \qquad \text{(B.3)}$$

91

In this case $\mathbf{n}(\pi)$ transforms linearly while $h$ is a singlet. As far as the scalar part of the SM is concerned, we can build an HEFT like lagrangian:

$$\mathcal{L}_{\text{HEFT}} = K(h)\frac{1}{2}(\partial h)^2 + \frac{(vF(h))^2}{4}\text{Tr}\left[(D_\mu \mathbf{n})^\dagger D^\mu \mathbf{n}\right] - V(h), \tag{B.4}$$

since the covariant derivative does not play any role in this geometric formulation we can rewrite $D_\mu \mathbf{n}$ as:

$$(\partial\mathbf{n})^2 = \left(\delta_{a,b} + \frac{n_a n_b}{1-n^2}\right)(\partial n_a)(\partial n_b), \qquad \text{where} \qquad a,b = 1,2,3.$$

This means I can rewrite the HEFT lagrangian at the two derivative level as:

$$\mathcal{L}_{\text{HEFT}} = K(h)\frac{1}{2}(\partial h)^2 + \frac{(vF(h))^2}{2}\left(\delta_{a,b} + \frac{n_a n_b}{1-n^2}\right)(\partial n_a)(\partial n_b) - V(h). \tag{B.5}$$

The SMEFT/HEFT analysis should clarify whether and when this lagrangian form can be mapped into a SMEFT lagrangian, i.e. when it's possible to construct the doublet $H$ starting from $\{h, \pi^i\}$. The fundamental request for converting a HEFT into SMEFT are summarized in [9] as follows:

Leading Order (LO) Criteria: A physical HEFT can be converted to a SMEFT at the fixed point if and only if the following three conditions hold:

- The function $F(h)$ has a zero at some real value $h = h^*$. This $h^*$ is a candidate for an $O(4)$ invariant point.

- The functions $K(h), F(h), V(h)$ all have a convergent single argument Taylor expansion in $h$ at $h = h^*$.

- The scalar curvature $R(h)$ is finite at $h^*$.

We apply the above prescription to the scalar singlet model, in its $\mathbb{Z}_2$ symmetric form. Recall the effective lagrangian is given by:

$$\mathcal{L}_{Eff} = |\partial H|^2 - \frac{\lambda_3^2}{8\lambda_2(\mu_2^2 + \lambda_3|H|^2)}(\partial|H|^2)^2 - \mu_1^2|H|^2 - \lambda_H|H|^4 + \frac{1}{4\lambda_S}(\mu_2^2 + \lambda_3|H|^2)^2. \tag{B.6}$$

As we know SMEFT can be always expressed as an HEFT theory, in particular by making use of Eq. 1.34 we recover the broken phase expression:

$$\mathcal{L}_{Eff} = \frac{1}{2}\left[1 - \frac{\lambda_3^2(v+h)^2}{2\lambda_S(2\mu_2^2 + \lambda_3(v+h)^2)}\right](\partial h)^2 + \frac{1}{2}(v+h)^2\text{Tr}\left[(DU)^\dagger DU\right]$$
$$- \frac{1}{2}\mu_1^2(v+h)^2 - \frac{1}{4}\lambda_1(v+h)^4 + \frac{1}{16\lambda_2}\left[2\mu_2^2 + \lambda_3(v+h)^2\right]^2. \tag{B.7}$$

We identify the quantities relevant in the construction of geometrical objects:

$$K(h) = \sqrt{1 - \frac{\lambda_3^2(v+h)^2}{2\lambda_2(2\mu_2^2 + \kappa(v+h)^2)}} \,, \qquad (B.8)$$

$$vF(h) = v + h \,, \qquad (B.9)$$

$$V(h) = \frac{1}{2}\mu_1^2(v+h)^2 + \frac{1}{4}\lambda_1(v+h)^4 - \frac{1}{16\lambda_S}\left(2\mu_2^2 + \lambda_3(v+h)^2\right)^2 . \qquad (B.10)$$

These quantities have a convergent Taylor expansion around the $O(4)$ invariant point and therefore point 1 and 2 of the LO criteria hold. We identify the kinetic term of the HEFT lagrangian in terms of a metric in the scalar field manifold. In general terms we rely on:

$$\mathcal{L} = \frac{1}{2}g_{i,j}(\Phi)\left((D_\mu\Phi^i)^\dagger D^\mu\Phi^j\right) \,, \qquad (B.11)$$

where in this case $\Phi^i = \{\pi^a, h\}$ i.e. the Goldstone bosons and the radial scalar $h$ together define the spherical polar coordinates on the manifold. By looking at the HEFT lagrangian we note that our metric has no off diagonal terms and is given by:

$$g_{i,j}(\Phi) = \begin{pmatrix} K(h) & 0 \\ 0 & vF(h)g'(\pi^a) \end{pmatrix} . \qquad (B.12)$$

More in detail we have the following elements:

$$g_{hh} = K(h)^2 \,, \qquad g_{ab} = v^2F^2\left(\delta_{a,b} + \frac{n_a n_b}{1 - n^2}\right) \,, \qquad g_{ha} = 0 \,. \qquad (B.13)$$

Analogous definition of connections for Yukawa sector as well as for gauge boson sector can be constructed, here we are only interested in the scalar sector [81, 82]. Note that when we make a field redefinition to have a canonically normalized term for $h$ we are indeed setting $K \to 1$, in that case we would consider just the scalar manifold of Goldstone bosons.

Once the metric is defined we can compute Christoffel symbols taking derivatives of the metric with respect to $h$ or to the Goldstone bosons:

$$\Gamma^h_{hh} = \frac{1}{2}g^{hh}(\partial_h g_{hh}) = \frac{1}{K}(\partial_h K) \,, \qquad\qquad \Gamma^h_{ha} = \frac{1}{2}g^{hh}(\partial_a g_{hh}) = 0 \,,$$

$$\Gamma^h_{ab} = -\frac{1}{2}g^{hh}(\partial_h g_{ab}) = -\frac{v^2 F}{K^2}(\partial_h F)\left(\delta_{a,b} + \frac{n_a n_b}{1 - n^2}\right) \,, \qquad\qquad \Gamma^i_{hh} = -\frac{1}{2}g^{ab}(\partial_j g_{hh}) = 0 \,,$$

$$\Gamma^a_{hb} = \frac{1}{2}g^{ak}(\partial_h g_{kb}) = \frac{1}{F}(\partial_h F)\delta_{ab} \,, \qquad\qquad \Gamma^a_{bc} = n_a\left(\delta_{b,c} + \frac{n_b n_c}{1 - n^2}\right) \,.$$

From these quantities it is possible to construct a non zero Riemann-tensor.

What we are interested in here is really the Ricci scalar curvature $R$ in particular at the $O(4)$ invariant fixed point because it's the putative point where EWSB is restored.

For the $\mu_2^2 \neq 0$ the scalar curvature is finite at the candidate $O(4)$ invariant point by

$$R(h = -v) = -\frac{\lambda_3^2}{4\mu_2^2 \lambda_S} N_\phi(N_\phi + 1) \overset{N_\phi = 3}{=} -3\frac{\lambda_3^2}{\mu_2^2 \lambda_S} \tag{B.14}$$

where $N_\phi$ is the number of scalar fields embedded in $U$. In this subcase, a mapping to SMEFT is allowed according to the criteria stated above. Infact if we expand the Lagrangian $\mathcal{L}_{Eff}$ in powers of $\frac{1}{\mu_2^2}$ we recover an expression analytic in $H$ which is of the same form as the SMEFT expansion. Furthermore the decoupling limit is well defined, i.e. $R(h = h*) \xrightarrow[m^2 \to \infty]{} 0$ that is the SM case which is geometrically seen as a flat manifold.

When $\mu_2^2 = 0$ the singlet gets all its mass from EWSB, it would be an extreme Loryon particle. In this case $\mathcal{L}_{Eff}$ is not be analytic around $H = 0$. The point where we think EWSB is restored shows up a divergence in the scalar curvature:

$$R\big|_{\mu_2^2 = 0} = -\frac{\lambda_3}{(\lambda_3 - 2\lambda_S)(h + v)^2} N_\phi(N_\phi + 1) \xrightarrow[h \to h^*]{N_\phi = 3} \infty. \tag{B.15}$$

In this case the EFT cannot be mapped into SMEFT and HEFT is required.

# Appendix C

# Diagrammatic matching for $c_{ggh}$

In this Appendix we explicitly show how to perform a diagrammatic matching in the colored scalar model. In particular we look at the processes $gg \to h$ both in the UV theory and in the HEFT limit. Formally we are imposing the following matching condition:

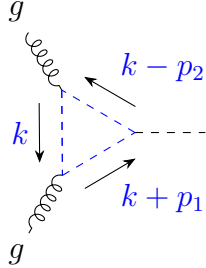$$\mathcal{M}_{UV}(g(p_1)g(p_2) \to h(p_3)) = \mathcal{M}_{HEFT}(g(p_1)g(p_2) \to h(p_3)) \,. \tag{C.1}$$

From the diagrammatic point of view we need to evaluate two diagrams in the UV theory whose low energy limit is given in terms of a single effective vertex:



$$\tag{C.2}$$

From the left we identify $\mathcal{M}_{UV}^{(1)}(gg \to h)$ and $\mathcal{M}_{UV}^{(2)}(gg \to h)$ as the two contributions from the UV theory. We start by writing down the amplitude in the HEFT framework:

$$i\mathcal{M}_{HEFT}(g(p_1)g(p_2) \to h(p3)) = i\frac{\alpha_S}{\pi}\epsilon_\mu^a \epsilon_\nu^b \delta^{ab} \frac{1}{v} c_{ggh} \left(p_1^\nu p_2^\mu - p_1 \cdot p_2 g^{\mu\nu}\right) \,. \tag{C.3}$$

In dimensional regularization we move to dimension $d = 4 - \epsilon$ and later and rewrite the strong coupling constant $g_3$ as $g_3 \mu^\epsilon$ to keep $g_3$ dimensionless. We start to evaluate the first diagram of the UV theory.



$$\epsilon_\mu^a \epsilon_\nu^b \mu^{2\epsilon} \int \frac{d^d k}{(2\pi^d)} \text{tr}\left[T^a T^b\right] (ig_3)^2 (2k + p_1)^\nu \frac{i}{(k + p_1)^2 - M_{ph}^2} \left(-i \frac{c_{\lambda h} v}{2}\right)$$

$$\frac{i}{(k - p_2)^2 - M_{ph}^2} (2k - p_2)^\mu \frac{i}{k^2 - M_{ph}^2} \,. \tag{C.4}$$

We evaluate the trace in color space $\text{tr}[T^a T^b] = \frac{\delta^{a,b}}{2}$ and rewrite $g_3^2 = 4\pi\alpha_s$. As a first step we implement the Feynman parametrization, then we shift the virtual momentum and we simplify terms that are linear in the virtual momentum $k$:

$$\frac{1}{(k + p_1)^2 - M_{ph}^2} \frac{1}{(k - p_2)^2 - M_{ph}^2} \frac{1}{k^2 - M_{ph}^2} = \Gamma(3) \int_0^1 dx \int_0^1 dy \int_0^1 dz$$
$$\frac{\delta(x + y + z - 1)}{\left[((k - p_2)^2 - M_{ph}^2)x + ((k + p_1)^2 - M_{ph}^2)y + (k^2 - M_{ph}^2)z\right]^3} \,, \tag{C.5}$$

after that we perform shifts in the variable $k \to k - p_1 y + p_2 z$ neglecting those terms that have an odd power of $k$.

$$4k^\mu k^\nu - p_1^\nu p_2^\mu + 2p_1^\nu k^\mu - 2p_2^\mu k^\nu \to 4(k - p_1 y + p_2 z)^\nu (k - p_1 y + p_2 z)^\mu - p_1^\nu p_2^\mu$$
$$+ 2p_1^\nu (k - p_1 y + p_2 z)^\mu - 2p_2^\mu (k - p_1 y + p_2 z)^\nu \,. \tag{C.6}$$

A further simplification comes from the on-shell condition for gluons $p_1^2 = 0$ and $p_2^2 = 0$, this means the numerator is reduced to:

$$4k^\mu k^\nu - p_1^\nu p_2^\mu (1 - 2y - 2z + yz) \,.$$

In this way our integral has been decomposed from a tensorial structure to a sum of scalar integrals that are tabulated for instance in Appendix B of [57]. This means we have to evaluate two types of $d$-dimensional integral for the first diagram:

$$I^{(1)} = \int \frac{d^d k}{(2\pi^d)} \frac{k^2}{(k^2 - \Delta^2 + i\epsilon)^3} = \frac{d}{4} \frac{i}{(4\pi)^{d/2}} \frac{1}{\Delta^{2 - \frac{d}{2}}} \Gamma\left(\frac{4 - d}{2}\right) \,,$$

$$I^{(2)} = \int \frac{d^d k}{(2\pi^d)} \frac{1}{(k^2 - \Delta^2 + i\epsilon)^3} = \frac{-i}{2(4\pi)^{d/2}} \frac{1}{\Delta^{3 - \frac{d}{2}}} \Gamma\left(\frac{6 - d}{2}\right) \,.$$

In the case at hand $\Delta^2 = -2p_1 p_2 yz + M_{ph}^2$ while $\Gamma$ stands for the Euler Gamma function. We have not made any assumption on the relative size of the masses involved in the process yet. Since we are assuming the physical mass of the new scalar to be much greater than the other particles in the process we are going to neglect the external momenta $p_1$ and $p_2$, in other words we perform the computation in the heavy loryon limit (HLM). When we solve $I^{(1)}$ substituting back $d = 4 - \epsilon$ we get in the limit of vanishing $\epsilon$ :

$$\mu^\epsilon \frac{(4\pi\mu^2)^\epsilon/2}{\Delta^{\epsilon/2}} \Gamma(\epsilon) = \mu^\epsilon \left[ 1 + \frac{\epsilon}{2} \log\left(4\pi^2\right) - \frac{\epsilon}{2} \log\left( \frac{M_{ph}^2 - 2p_1 p_2 yz}{\mu^2} \right) \right] \left( \frac{2}{\epsilon} - \gamma_E .. \right) . \quad \text{(C.7)}$$
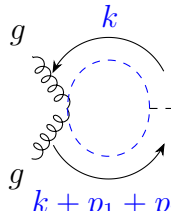
A few comments are in order now: we make use of the modified minimal subtraction scheme as a renormalization scheme ($\overline{\text{MS}}$), then we set the renormalization group scale $\mu = M_{ph}^2$ because this is the scale at which we are performing the matching. Finally we expand the logarithm as:

$$\int_0^1 dy \int_0^1 dz \log\left( 1 - \frac{2p_1 p_2 yz}{M_{ph}^2} \right) \simeq - \int_0^1 dy \int_0^1 dz \frac{2p_1 p_2 yz}{M_{ph}^2} + \mathcal{O}\left( \frac{1}{M_{ph}^4} \right) . \quad \text{(C.8)}$$

The final result from the first diagram is:

$$i\mathcal{M}_{UV}^{(1)}(g(p_1)g(p_2) \to h(p3)) = i\frac{\alpha_S}{\pi} \epsilon_\mu^a \epsilon_\nu^b \delta^{ab} \frac{1}{v} \frac{c_{\lambda h} v^2}{6(4M_{ex}^2 + c_{\lambda h} v^2)} \left( p_1^\nu p_2^\mu + p_1 p_2 g^{\mu\nu} \right) . \quad \text{(C.9)}$$

This diagram by itself does not provide the right Lorentz structure. In order to obtain it we need to take int account also the other diagram. We pass to the second diagram written as



$$= \epsilon_\mu^a \epsilon_\nu^b \mu^{2\epsilon} \int \frac{d^d k}{(2\pi)^d} \text{tr}\left[ T^a T^b \right] ig_3^2 g^{\mu\nu} \frac{i}{(k + p_1 + p_2)^2 - M_{ph}^2} \left( -i\frac{c_{\lambda h} v}{2} \right)$$

$$\frac{i}{(k^2 - M_{ph}^2)} . \quad \text{(C.10)}$$

The procedure to solve this loop integral is the same as for the last diagram and we do not repeat it. We just quote the final result:

$$i\mathcal{M}_{UV}^{(2)}(g(p_1)g(p_2) \to h(p_3)) = i\frac{\alpha_S}{\pi} \epsilon_\mu^a \epsilon_\nu^b \frac{1}{v} \frac{c_{\lambda h} v^2}{3(4M_{ex}^2 + c_{\lambda h} v^2)} (-p_1 p_2) g^{\mu\nu} . \quad \text{(C.11)}$$

This diagram contributes with a relative minus sign in the evaluation of $c_{ggh}$ yielding the right tensor structure:

$$i\mathcal{M}_{UV}^{(1+2)}(g(p_1)g(p_2) \to h(p3)) = i\frac{\alpha_S}{\pi}\epsilon_\mu^a\epsilon_\nu^b\delta^{ab}\frac{1}{v}\frac{c_{\lambda h}v^2}{6(4M_{ex}^2 + c_{\lambda h}v^2)}\left(p_1^\nu p_2^\mu - p_1p_2g^{\mu\nu}\right) . \quad (C.12)$$

We can now implement (C.1) to get the expression for the Wilson coefficient in HEFT basis:

$$i\frac{\alpha_S}{\pi}\epsilon_\mu^a\epsilon_\nu^b\delta^{ab}\frac{1}{v}c_{ggh}\left(p_1^\nu p_2^\mu - p_1p_2g^{\mu\nu}\right) = i\frac{\alpha_S}{\pi}\epsilon_\mu^a\epsilon_\nu^b\delta^{ab}\frac{1}{v}\frac{c_{\lambda h}v^2}{6(4M_{ex}^2 + c_{\lambda h}v^2)}\left(p_1^\nu p_2^\mu - p_1p_2g^{\mu\nu}\right) , \quad (C.13)$$

which finally leads to :

$$\boxed{c_{ggh} = \frac{c_{\lambda h}v^2}{6(4M_{ex}^2 + c_{\lambda h}v^2)} .}$$

# Bibliography

[1] **ATLAS** Collaboration, G. Aad *et al.*, "Observation of a new particle in the search for the Standard Model Higgs boson with the ATLAS detector at the LHC," *Phys. Lett. B* **716** (2012) 1–29, `arXiv:1207.7214 [hep-ex]`.

[2] **CMS** Collaboration, S. Chatrchyan *et al.*, "Observation of a New Boson at a Mass of 125 GeV with the CMS Experiment at the LHC," *Phys. Lett. B* **716** (2012) 30–61, `arXiv:1207.7235 [hep-ex]`.

[3] **CMS** Collaboration, "A portrait of the higgs boson by the cms experiment ten years after the discovery," *Nature* **607** (Jul, 2022) . `https://doi.org/10.1038/s41586-022-04892`.

[4] **ATLAS** Collaboration, "A detailed map of higgs boson interactions by the atlas experiment ten years after the discovery," *Nature* (Jul, 2022) . `https://doi.org/10.1038/s41586-022-04893`.

[5] G. Buchalla, O. Catá, and C. Krause, "On the Power Counting in Effective Field Theories," *Phys. Lett. B* **731** (2014) 80–86, `arXiv:1312.5624 [hep-ph]`.

[6] B. M. Gavela, E. E. Jenkins, A. V. Manohar, and L. Merlo, "Analysis of General Power Counting Rules in Effective Field Theory," *Eur. Phys. J. C* **76** no. 9, (2016) 485, `arXiv:1601.07551 [hep-ph]`.

[7] G. Buchalla, O. Cata, A. Celis, and C. Krause, "Comment on "Analysis of General Power Counting Rules in Effective Field Theory"," `arXiv:1603.03062 [hep-ph]`.

[8] I. Banta, T. Cohen, N. Craig, X. Lu, and D. Sutherland, "Non-decoupling new particles," *JHEP* **02** (2022) 029, `arXiv:2110.02967 [hep-ph]`.

[9] T. Cohen, N. Craig, X. Lu, and D. Sutherland, "Is SMEFT Enough?," *JHEP* **03** (2021) 237, `arXiv:2008.08597 [hep-ph]`.

[10] A. Salam, "Weak and Electromagnetic Interactions," *Conf. Proc. C* **680519** (1968) 367–377.

[11] S. Weinberg, "A Model of Leptons," *Phys. Rev. Lett.* **19** (1967) 1264–1266.

[12] S. L. Glashow, "Partial Symmetries of Weak Interactions," *Nucl. Phys.* **22** (1961) 579–588.

[13] P. W. Higgs, "Broken symmetries, massless particles and gauge fields," *Phys. Lett.* **12** (1964) 132–133.

[14] P. W. Higgs, "Broken Symmetries and the Masses of Gauge Bosons," *Phys. Rev. Lett.* **13** (1964) 508–509.

[15] F. Feruglio, "The Chiral approach to the electroweak interactions," *Int. J. Mod. Phys. A* **8** (1993) 4937–4972, `arXiv:hep-ph/9301281`.

[16] S. R. Coleman, J. Wess, and B. Zumino, "Structure of phenomenological Lagrangians. 1.," *Phys. Rev.* **177** (1969) 2239–2247.

[17] C. G. Callan, Jr., S. R. Coleman, J. Wess, and B. Zumino, "Structure of phenomenological Lagrangians. 2.," *Phys. Rev.* **177** (1969) 2247–2250.

[18] C. Hartmann and M. Trott, "Higgs decay to two photons at one loop in the standard model effective field theory," *Physical Review Letters* **115** no. 19, (Nov., 2015) . `http://dx.doi.org/10.1103/PhysRevLett.115.191801`.

[19] G. Isidori, F. Wilsch, and D. Wyler, "The standard model effective field theory at work," 2023.

[20] A. Falkowski, "Lectures on smeft," *The European Physical Journal* (2023) . `https://doi.org/10.1140/epjc/s10052-023-11821-3`.

[21] B. Grzadkowski, M. Iskrzynski, M. Misiak, and J. Rosiek, "Dimension-Six Terms in the Standard Model Lagrangian," *JHEP* **10** (2010) 085, `arXiv:1008.4884 [hep-ph]`.

[22] R. Alonso, "A primer on higgs effective field theory with geometry," 2023.

[23] I. Brivio, J. Gonzalez-Fraile, M. C. Gonzalez-Garcia, and L. Merlo, "The complete heft lagrangian after the lhc run i," *The European Physical Journal C* **76** no. 7, (July, 2016) . `http://dx.doi.org/10.1140/epjc/s10052-016-4211-9`.

[24] R. Alonso, E. E. Jenkins, and A. V. Manohar, "A geometric formulation of higgs effective field theory: Measuring the curvature of scalar field space," *Physics Letters B* **754** (Mar., 2016) 335–342. `http://dx.doi.org/10.1016/j.physletb.2016.01.041`.

[25] I. Brivio and M. Trott, "The standard model as an effective field theory," *Physics Reports* **793** (Feb., 2019) 1–98. `http://dx.doi.org/10.1016/j.physrep.2018.11.002`.

[26] I. Rosell, A. Pich, and J. J. Sanz-Cillero, "Heavy resonances and the oblique parameters s and t," 2023.

[27] R. Alonso, M. Gavela, L. Merlo, S. Rigolin, and J. Yepes, "The effective chiral lagrangian for a light dynamical "higgs particle"," *Physics Letters B* **722** no. 4–5, (May, 2013) 330–335. `http://dx.doi.org/10.1016/j.physletb.2013.04.037`.

[28] R. Contino, C. Grojean, M. Moretti, F. Piccinini, and R. Rattazzi, "Strong Double Higgs Production at the LHC," *JHEP* **05** (2010) 089, arXiv:1002.1011 [hep-ph].

[29] R. L. Delgado, R. Gómez-Ambrosio, J. Martínez-Martín, A. Salas-Bernárdez, and J. J. Sanz-Cillero, "Production of two, three, and four Higgs bosons: where SMEFT and HEFT depart," arXiv:2311.04280 [hep-ph].

[30] L. Alasfar, L. Cadamuro, C. Dimitriadi, A. Ferrari, R. Gröber, G. Heinrich, T. I. Carlson, J. Lang, S. Ördek, L. P. Sánchez, L. Scyboz, and J. Sjölin, "Effective field theory descriptions of higgs boson pair production," 2024.

[31] A. Falkowski and R. Rattazzi, "Which EFT," *JHEP* **10** (2019) 255, arXiv:1902.05936 [hep-ph].

[32] T. Cohen, N. Craig, X. Lu, and D. Sutherland, "Unitarity violation and the geometry of higgs efts," *Journal of High Energy Physics* **2021** no. 12, (Dec., 2021) . http://dx.doi.org/10.1007/JHEP12(2021)003.

[33] M. Alminawi, I. Brivio, and J. Davighi, "Jet Bundle Geometry of Scalar Field Theories," arXiv:2308.00017 [hep-ph].

[34] I. Banta, T. Cohen, N. Craig, X. Lu, and D. Sutherland, "Non-decoupling new particles," *Journal of High Energy Physics* **2022** no. 2, (Feb., 2022) . http://dx.doi.org/10.1007/JHEP02(2022)029.

[35] **ATLAS** Collaboration, G. Aad, B. Abbott, K. Abeling, S. H. Abidi, A. Aboulhorma, H. Abramowicz, H. Abreu, Y. Abulaiti, A. C. Abusleme Hoffman, B. S. Acharya, and A. B. et al., "Search for nonresonant pair production of higgs bosons in the $b\bar{b}b\bar{b}$ final state in $pp$ collisions at $\sqrt{s} = 13$ TeV with the atlas detector," *Phys. Rev. D* **108** (Sep, 2023) 052003. https://link.aps.org/doi/10.1103/PhysRevD.108.052003.

[36] R. Gröber, M. Mühlleitner, M. Spira, and J. Streicher, "Nlo qcd corrections to higgs pair production including dimension-6 operators," *Journal of High Energy Physics* **2015** no. 9, (Sept., 2015) . http://dx.doi.org/10.1007/JHEP09(2015)092.

[37] F. A. Dreyer and A. Karlberg, "Fully differential vector-boson fusion higgs pair production at next-to-next-to-leading order," *Physical Review D* **99** no. 7, (Apr., 2019) . http://dx.doi.org/10.1103/PhysRevD.99.074028.

[38] R. P. Feynman, "The behavior of hadron collisions at extreme energies," *Conf. Proc. C* **690905** (1969) 237–258.

[39] W.-L. Guo and Y.-L. Wu, "The real singlet scalar dark matter model," *Journal of High Energy Physics* **2010** no. 10, (Oct., 2010) . http://dx.doi.org/10.1007/JHEP10(2010)083.

[40] P. Athron, C. Balázs, T. Bringmann, A. Buckley, M. Chrząszcz, J. Conrad, J. M. Cornell, L. A. Dal, J. Edsjö, B. Farmer, P. Jackson, F. Kahlhoefer, A. Krislock, A. Kvellestad, J. McKay, F. Mahmoudi, G. D. Martinez, A. Putze, A. Raklev, C. Rogan, A. Saavedra, C. Savage, P. Scott, N. Serra, C. Weniger, and M. White, "Status of the scalar singlet dark matter model," *The European Physical Journal C* **77** no. 8, (Aug., 2017) . http://dx.doi.org/10.1140/epjc/s10052-017-5113-1.

[41] J. Espinosa, T. Konstandin, and F. Riva, "Strong electroweak phase transitions in the standard model with a singlet," *Nuclear Physics B* **854** no. 3, (Jan., 2012) 592–630. http://dx.doi.org/10.1016/j.nuclphysb.2011.09.010.

[42] S. Dawson, S. Homiller, and S. D. Lane, "Putting standard model eft fits to work," *Physical Review D* **102** no. 5, (Sept., 2020) . http://dx.doi.org/10.1103/PhysRevD.102.055012.

[43] C.-Y. Chen, S. Dawson, and I. Lewis, "Exploring resonant di-higgs boson production in the higgs singlet model," *Physical Review D* **91** no. 3, (Feb., 2015) . http://dx.doi.org/10.1103/PhysRevD.91.035015.

[44] S. Dawson and I. M. Lewis, "Singlet Model Interference Effects with High Scale UV Physics," *Phys. Rev. D* **95** no. 1, (2017) 015004, arXiv:1605.04944 [hep-ph].

[45] G. Chalons, D. Lopez-Val, T. Robens, and T. Stefaniak, "The Higgs singlet extension at LHC Run 2," *PoS* **ICHEP2016** (2016) 1180, arXiv:1611.03007 [hep-ph].

[46] S. Kanemura, M. Kikuchi, and K. Yagyu, "One-loop corrections to the Higgs self-couplings in the singlet extension," *Nucl. Phys. B* **917** (2017) 154–177, arXiv:1608.01582 [hep-ph].

[47] B. W. Lee, C. Quigg, and H. B. Thacker, "Weak Interactions at Very High-Energies: The Role of the Higgs Boson Mass," *Phys. Rev. D* **16** (1977) 1519.

[48] L. D. Luzio, J. F. Kamenik, and M. Nardecchia, "Implications of perturbative unitarity for scalar di-boson resonance searches at lhc," 2019.

[49] M. D. Goodsell and F. Staub, "Unitarity constraints on general scalar couplings with sarah," *The European Physical Journal C* **78** no. 8, (Aug., 2018) . http://dx.doi.org/10.1140/epjc/s10052-018-6127-z.

[50] T. Robens and T. Stefaniak, "Status of the higgs singlet extension of the standard model after lhc run 1," *The European Physical Journal C* **75** no. 3, (Mar., 2015) . http://dx.doi.org/10.1140/epjc/s10052-015-3323-y.

[51] G. Isidori, G. Ridolfi, and A. Strumia, "On the metastability of the standard model vacuum," *Nuclear Physics B* **609** no. 3, (Aug., 2001) 387–409. http://dx.doi.org/10.1016/S0550-3213(01)00302-9.

[52] J. Elias-Miró, J. R. Espinosa, G. F. Giudice, G. Isidori, A. Riotto, and A. Strumia, "Higgs mass implications on the stability of the electroweak vacuum," *Physics Letters B* **709** no. 3, (Mar., 2012) 222–228. `http://dx.doi.org/10.1016/j.physletb.2012.02.013`.

[53] D. López-Val and T. Robens, "$\delta r$ and the w-boson mass in the singlet extension of the standard model," *Physical Review D* **90** no. 11, (Dec., 2014) . `http://dx.doi.org/10.1103/PhysRevD.90.114018`.

[54] **CDF** Collaboration, T. Aaltonen *et al.*, "High-precision measurement of the $W$ boson mass with the CDF II detector," *Science* **376** no. 6589, (2022) 170–176.

[55] **ATLAS** Collaboration, G. Aad *et al.*, "Measurement of the W-boson mass and width with the ATLAS detector using proton-proton collisions at $\sqrt{s}$ = 7 TeV," `arXiv:2403.15085 [hep-ex]`.

[56] M. E. Peskin and T. Takeuchi, "Estimation of oblique electroweak corrections," *Phys. Rev. D* **46** (1992) 381–409.

[57] M. D. Schwartz, *Quantum Field Theory and the Standard Model*. Cambridge University Press, 3, 2014.

[58] B. Henning, X. Lu, and H. Murayama, "One-loop matching and running with covariant derivative expansion," 2016.

[59] B. W. Lee and J. Zinn-Justin, "Spontaneously Broken Gauge Symmetries Part 3: Equivalence," *Phys. Rev. D* **5** (1972) 3155–3160.

[60] R. Gómez-Ambrosio, F. J. Llanes-Estrada, A. Salas-Bernárdez, and J. J. Sanz-Cillero, "The falir of higgsflare: Distinguishing electroweak efts with $w_L w_L > hh$," *Physical Review D* **106** no. 5, (Sept., 2022) . `http://dx.doi.org/10.1103/PhysRevD.106.053004`.

[61] G. Passarino, "Field reparametrization in effective field theories," *Eur. Phys. J. Plus* **132** no. 1, (2017) 16, `arXiv:1610.09618 [hep-ph]`.

[62] J. Fuentes-Martín, M. König, J. Pagès, A. E. Thomsen, and F. Wilsch, "A proof of concept for matchete: an automated tool for matching effective theories," *Eur. Phys. J. C* **83** no. 7, (2023) 662, `arXiv:2212.04510 [hep-ph]`.

[63] J. de Blas, J. C. Criado, M. Pérez-Victoria, and J. Santiago, "Effective description of general extensions of the standard model: the complete tree-level dictionary," *Journal of High Energy Physics* **2018** no. 3, (Mar., 2018) . `http://dx.doi.org/10.1007/JHEP03(2018)109`.

[64] U. Haisch, M. Ruhdorfer, E. Salvioni, E. Venturini, and A. Weiler, "Singlet night in Feynman-ville: one-loop matching of a real scalar," *JHEP* **04** (2020) 164, `arXiv:2003.05936 [hep-ph]`. [Erratum: JHEP 07, 066 (2020)].

[65] A. Dedes, W. Materkowska, M. Paraskevas, J. Rosiek, and K. Suxho, "Feynman rules for the standard model effective field theory in r $\xi$ -gauges," *Journal of High Energy Physics* **2017** no. 6, (June, 2017) . `http://dx.doi.org/10.1007/JHEP06(2017)143`.

[66] R. Gómez-Ambrosio, F. J. Llanes-Estrada, A. Salas-Bernárdez, and J. J. Sanz-Cillero, "Smeft is falsifiable through multi-higgs measurements (even in the absence of new light particles)," *Communications in Theoretical Physics* **75** no. 9, (Sept., 2023) 095202. `http://dx.doi.org/10.1088/1572-9494/ace95e`.

[67] G. Buchalla, O. Cata, A. Celis, and C. Krause, "Standard Model Extended by a Heavy Singlet: Linear vs. Nonlinear EFT," *Nucl. Phys. B* **917** (2017) 209–233, `arXiv:1608.03564 [hep-ph]`.

[68] A. Djouadi, J. Kalinowski, M. Mühlleitner, and M. Spira, "Hdecay: Twenty++ years after," *Computer Physics Communications* **238** (May, 2019) 214–231. `http://dx.doi.org/10.1016/j.cpc.2018.12.010`.

[69] C. Degrande and H.-L. Li, "Impact of dimension-8 smeft operators on diboson productions," *Journal of High Energy Physics* **2023** no. 6, (June, 2023) . `http://dx.doi.org/10.1007/JHEP06(2023)149`.

[70] L. Di Luzio, R. Gröber, and M. Spannowsky, "Maxi-sizing the trilinear Higgs self-coupling: how large could it be?," *Eur. Phys. J. C* **77** no. 11, (2017) 788, `arXiv:1704.02311 [hep-ph]`.

[71] R. Grober and M. Muhlleitner, "Composite Higgs Boson Pair Production at the LHC," *JHEP* **06** (2011) 020, `arXiv:1012.1562 [hep-ph]`.

[72] R. Contino, M. Ghezzi, M. Moretti, G. Panico, F. Piccinini, and A. Wulzer, "Anomalous Couplings in Double Higgs Production," *JHEP* **08** (2012) 154, `arXiv:1205.5444 [hep-ph]`.

[73] T. Plehn, M. Spira, and P. Zerwas, "Pair production of neutral higgs particles in gluon-gluon collisions," *Nuclear Physics B* **479** no. 1–2, (Nov., 1996) 46–64. `http://dx.doi.org/10.1016/0550-3213(96)00418-X`.

[74] S. Dawson, A. Ismail, and I. Low, "What's in the loop? the anatomy of double higgs production," *Physical Review D* **91** no. 11, (June, 2015) . `http://dx.doi.org/10.1103/PhysRevD.91.115008`.

[75] J. Baglio, F. Campanario, S. Glaus, M. Mühlleitner, J. Ronca, M. Spira, and J. Streicher, "Higgs-pair production via gluon fusion at hadron colliders: Nlo qcd corrections," *Journal of High Energy Physics* **2020** no. 4, (Apr., 2020) . `http://dx.doi.org/10.1007/JHEP04(2020)181`.

[76] R. Gröber, M. Mühlleitner, and M. Spira, "Higgs pair production at nlo qcd for cp-violating higgs sectors," *Nuclear Physics B* **925** (Dec., 2017) 1–27. `http://dx.doi.org/10.1016/j.nuclphysb.2017.10.002`.

[77] B. Henning, X. Lu, and H. Murayama, "How to use the standard model effective field theory," 2015.

[78] M. Gillioz, R. Gröber, C. Grojean, M. Mühlleitner, and E. Salvioni, "Higgs low-energy theorem (and its corrections) in composite models," *Journal of High Energy Physics* **2012** no. 10, (Oct., 2012) . `http://dx.doi.org/10.1007/JHEP10(2012)004`.

[79] B. A. Kniehl and M. Spira, "Low-energy theorems in higgs physics," 1995.

[80] A. Helset, E. E. Jenkins, and A. V. Manohar, "Geometry in scattering amplitudes," *Physical Review D* **106** no. 11, (Dec., 2022) . `http://dx.doi.org/10.1103/PhysRevD.106.116018`.

[81] A. Helset, M. Paraskevas, and M. Trott, "Gauge fixing the Standard Model Effective Field Theory," *Phys. Rev. Lett.* **120** no. 25, (2018) 251801, `arXiv:1803.08001 [hep-ph]`.

[82] A. Helset, A. Martin, and M. Trott, "The Geometric Standard Model Effective Field Theory," *JHEP* **03** (2020) 163, `arXiv:2001.01453 [hep-ph]`.